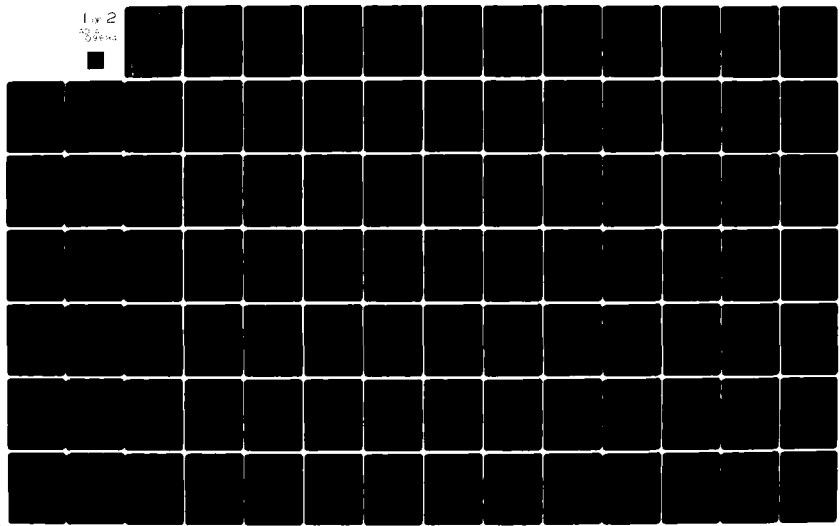
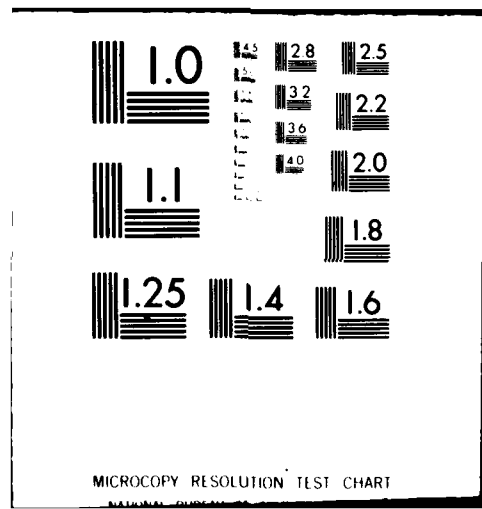


AD-A109 894 BOSTON COLL CHESTNUT HILL MA SPACE DATA ANALYSIS LAB F/G 20/6
ANALYSIS OF PROJECT EXCEDE II CIRCULAR VARIABLE FILTER SPECTROM--ETC(U)
JAN 81 W F GRIEDER, C I FOLEY F1962R-79-C-0139
UNCLASSIFIED BC-SDAL-80-3 AFGL-TR-81-0224 NL

For 2
3 copies





AFGL-TR-81-0224

LEVEL II

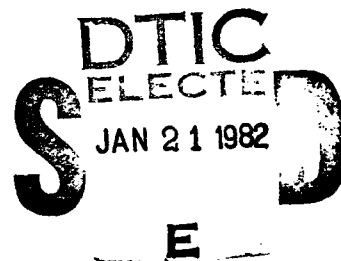
(11)

AD A109894

ANALYSIS OF PROJECT EXCEDE II CIRCULAR VARIABLE
FILTER SPECTROMETER DATA

William F. Grieder
Carol I. Foley

Space Data Analysis Laboratory
Boston College
885 Centre Street
Newton, MA 02159



Scientific Report No. 1
1 January 81

Approved for public release; distribution unlimited

Air Force Geophysics Laboratory
Air Force Systems Command
United States Air Force
Hanscom AFB, Massachusetts 01731

ONE FREE COPY

ws
403460
01 20 82 063

UNCLASSIFIED

SECURITY CLASSIFICATION OF THIS PAGE (When Data Entered)

| REPORT DOCUMENTATION PAGE | | READ INSTRUCTIONS BEFORE COMPLETING FORM |
|--|---|--|
| 1. REPORT NUMBER AFGL-TR-81-0224 | 2. GOVT ACCESSION NO. <i>PA-H109 694</i> | 3. RECIPIENT'S CATALOG NUMBER |
| 4. TITLE (and Subtitle) ANALYSIS OF PROJECT EXCEDE II CIRCULAR VARIABLE FILTER SPECTROMETER DATA | 5. TYPE OF REPORT & PERIOD COVERED Scientific Report No. 1 1 July 1979 - 30 Sept 1981 | |
| 7. AUTHOR(s) William F. Grieder Carol I. Foley | 6. PERFORMING ORG. REPORT NUMBER BC-SDAL-80-3 | |
| 9. PERFORMING ORGANIZATION NAME AND ADDRESS Space Data Analysis Laboratory Boston College 885 Centre Street Newton, MA 02159 | 10. PROGRAM ELEMENT, PROJECT, TASK AREA & WORK UNIT NUMBERS 62101F 767010AF | |
| 11. CONTROLLING OFFICE NAME AND ADDRESS Air Force Geophysics Laboratory Hanscom AFB, Massachusetts 01731 Contract Monitor: Mr. John A. Sandock/OPR 1 | 12. REPORT DATE 1 January 1981 | |
| 14. MONITORING AGENCY NAME & ADDRESS(if different from Controlling Office) | 13. NUMBER OF PAGES 149 | |
| | 15. SECURITY CLASS. (of this report) Unclassified | |
| | 15a. DECLASSIFICATION DOWNGRADING SCHEDULE | |
| 16. DISTRIBUTION STATEMENT (of this Report) Approved for public release; distribution unlimited | | |
| 17. DISTRIBUTION STATEMENT (the abstract entered in Block 20, if different from Report) | | |
| 18. SUPPLEMENTARY NOTES | | |
| 19. KEY WORDS (Continue on reverse side if necessary and identify by block number) Infrared Spectrometers Artificial Auroral Experiment Infrared Aurora Infrared Cryogenic Spectrometers Infrared Atmospheric Emissions | | |
| 20. ABSTRACT (Continue on reverse side if necessary and identify by block number) EXCEDE II is the fourth in a series of research experiments conducted by Air Force Geophysics Laboratory (AFGL) to study the infrared emission processes induced by rocketborne electron accelerators. The excitation of the upper atmosphere by the electron beam simulates aurora induced processes but provides the advantage that the dosing is more precisely quantified than in the natural auroral case. In addition, optical/infrared instruments carried | | |

(Cont.)

DD FORM 1 JAN 73 1473

UNCLASSIFIED

i SECURITY CLASSIFICATION OF THIS PAGE (When Data Entered)

20. Abstract (Cont.)

on-board the same payload with the accelerator provide controlled viewing geometry of the induced emissions and measurements do not suffer from long path atmospheric attenuation as would be the case for some ground based observations.

The EXCEDE II payload was launched from Pad 4, Poker Flat Research Range, Alaska on 25 October 1979 at 0546:40 UT hours. The payload reached a ~128 km apogee at ~187 seconds after launch. Although some difficulties were encountered with electron gun arcing the experiment was successful and data were obtained for gun on and off conditions throughout the flight (O'Neil 1980).

The primary purpose of this report is to describe in detail the techniques used to process and analyze the data measured with the two CVF spectrometers on the EXCEDE II payload. Part A of the report deals with the LN₂ CVF spectrometer (designated NS-6-4), Part B describes techniques employed with the LH CVF spectrometer (designated HS-3B-1) and Part C presents recommendations for final data processing of the HS-3B-1 CVF.

UNCLASSIFIED

PREFACE

EXCEDE II is an Air Force Geophysics (AFGL) research program to study auroral infrared emission processes using a rocketborne electron accelerator to generate artificial aurorae. The effort is sponsored by Defense Nuclear Agency (DNA). The EXCEDE concept was originally proposed by Dr. A. T. Stair of AFGL in 1971 and since that time four successful experiments have been conducted. These experiments have been directed by Mr. Robert O'Neil also of AFGL.

| | |
|---------------|-------|
| Accession For | |
| NTIS | GTAGI |
| DTIC | TAB |
| University | 111 |
| JSC | 111 |
| Pyro | |
| Dist | |
| Av | |
| Dist | |
| A | |

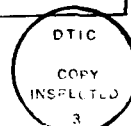


TABLE OF CONTENTS

| | <u>Page</u> |
|--|-------------|
| PREFACE | iii |
| LIST OF ILLUSTRATIONS | v |
| LIST OF TABLES | vi |
| 1.0 INTRODUCTION | 1 |
| Part A | |
| LN ₂ CVF Spectrometer | |
| 2.0 DESCRIPTION OF NITROGEN CVF (NS-6-4) | 3 |
| 2.1 NS-6-4 CVF Calibration Parameters | 5 |
| 2.1.1 Wavelength Calibration | 5 |
| 2.1.2 Radiance Calibration | 5 |
| 2.2 Telemetry Signal | 6 |
| 2.3 Data Processing | 8 |
| 2.3.1 Error Analysis | 9 |
| 2.3.2 Data Base | 11 |
| Part B | |
| LH _e CVF Spectrometer | |
| 3.0 DESCRIPTION OF HELIUM CVF (HS-3B-1) | 14 |
| 3.1 Calibration Parameters | 14 |
| 3.1.1 Wavelength Calibration | 16 |
| 3.1.2 Radiance Calibration | 16 |
| 3.2 Telemetry Signal | 17 |
| 3.3 Data Processing | 19 |
| 3.3.1 Data Reduction | 22 |
| 3.3.2 Data Base (HS-3B-1) | 29 |
| 3.4 Discussion | 30 |
| Part C | |
| 4.0 RECOMMENDATIONS | 32 |
| 5.0 ACKNOWLEDGEMENTS | 33 |
| 6.0 REFERENCES | 34 |
| Appendix A - NS-6-4 Spectral Scan Data | 48 |
| Appendix B - HS-3B-1 Spectral Scan Data | 58 |
| Appendix C - HS-3B-1 Phase Angle Data | 63 |
| Appendix D - Survey of NS-6-4 Data | 68 |
| Appendix E - Survey of HS-3B-1 Data | 99 |

LIST OF ILLUSTRATIONS

| <u>Figure</u> | | <u>Page</u> |
|---------------|--|-------------|
| 2.0-1 | Schematic of a typical circular variable filter (CVF) spectrometer | 35 |
| 2.1-1 | CVF brightness calibration (NS-6-4) | 36 |
| 2.3-1 | Sample spectra from EXCEDE short wavelength CVF spectrometer during electron gun operation | 37 |
| 3.1-1 | CVF brightness calibration (HS-3B-1) | 38 |
| 3.3-1 | Principles of optically chopped CVF signal production | 39 |
| 3.3-1a | Example of HS-3B-1 CVF telemetered data | 40 |
| 3.3-2 | Example of fit to chopper reference data | 41 |
| 3.3-3 | Demodulation of scan 1210 | 42 |
| 3.3-4 | Example of unfiltered spectral radiance profile | 43 |
| 3.3-5 | Smoothing filter frequency response characteristics | 44 |
| 3.3-6 | Example of smoothed spectral radiance profile | 45 |
| 3.4-1 | Frequency response of HS-3B-1 CVF electronic filter | 46 |
| 3.4-2 | Effects of chopper second harmonic and sampling | 47 |

LIST OF TABLES

| | | <u>Page</u> |
|-------|------------------------------------|-------------|
| 2.0-1 | NS-6-4 CVF Performance Parameters | 4 |
| 2.1-1 | NS-6-4 CVF Brightness Calibration | 7 |
| 2.3-1 | Accelerator Operation | 12 |
| 3.0-1 | HS-3B-1 CVF Performance Parameters | 15 |
| 3.1-1 | HS-3B-1 CVF Brightness Calibration | 18 |

INTRODUCTION

EXCEDE II is the fourth in a series of research experiments conducted by Air Force Geophysics Laboratory (AFGL) to study the infrared emission processes induced by rocketborne electron accelerators. The excitation of the upper atmosphere by the electron beam simulates aurora induced processes but provides the advantage that the dosing is more precisely quantified than in the natural auroral case. In addition, optical/infrared instruments carried on-board the same payload with the accelerator provide controlled viewing geometry of the induced emissions and measurements do not suffer from long path atmospheric attenuation as would be the case for some ground based observations. The other EXCEDE experiment programs were PRECEDE, EXCEDE II Test, and EXCEDE: SWIR (O'Neil 1976).

The EXCEDE II payload incorporated four electron guns programmed to function in different combinations and capable of producing a 10 ampere electron beam when activated simultaneously. The optical/infrared instruments on-board the payload were primarily for measuring spectral data and included; liquid nitrogen (LN_2) interferometer, LN_2 circular variable filter (CVF) spectrometer, liquid helium (LHe) CVF spectrometer, LN_2 radiometer, ultraviolet/visible spectrometer, a camera and five photometer units. In addition the payload contained several ionospheric probes and diagnostic sensors to measure ion and electron densities and fields. The optical/infrared instruments viewed the beam region throughout the flight at a stabilized zenith angle to local vertical of 45° .

The EXCEDE II payload was launched from Pad 4, Poker Flat Research Range, Alaska on 25 October 1979 at 0546:40 UT hours. The payload reached a ~ 128 km apogee at ~ 187 seconds after launch. Although some difficulties were encountered with electron gun arcing the experiment was successful and data were obtained for gun on and off conditions throughout the flight (O'Neil 1980).

The primary purpose of this report is to describe in detail the

techniques used to process and analyze the data measured with the two CVF spectrometers on the EXCEDE II payload. Part A of the report deals with the LN₂ CVF spectrometer (designated NS-6-4), Part B describes techniques employed with the LH CVF spectrometer (designated HS-3B-1) and Part C presents recommendations for final data processing of the HS-3B-1 CVF. Processed data for this instrument presented in this report is preliminary.

PART A
 LN_2 CVF SPECTROMETER

2.0 Description of Nitrogen CVF(NS-6-4).

Construction details and method of operation of the rocketborne CVF spectrometer have been reported by Rogers, 1976, and Wyatt, 1978. The CVF instruments were fabricated by the Electrodynamics Laboratory of Utah State University. In brief the monochromator portion of the sensor consists of two 180-degree circular variable (wedge) filters mounted so that the bandpass interference layers rotate just above the detector field stop which performs the function of a spectrometer slit (see Figure 2.0-1). The spectrometer scans a continuous wavelength region depending on which half of the filter is rotating over the detector. Spectral resolution ($\Delta\lambda$) depends on slit width and f number. Pertinent figures of merit for the EXCEDE NS-6-4 instrument are given in Table 2.0-1.

Two important parameters for CVF data processing are the start times of the beginning of each spectral scan and the speed of rotation of the CVF. Two assumptions made are that the speed of rotation is constant throughout the flight and that the wavelength of radiation being measured is linearly proportional to time (or filter position). One consequence of this CVF mode of operation is that since the payload is constantly changing altitude the spectra obtained are associated with different altitudes. Each part of a spectral scan is for a different altitude and thus altitude must be computed for every spectral data point.

Table 2.0-1

PERFORMANCE PARAMETERS

FOR CVF NS-6-4

| | |
|--|---|
| Wavelength Coverage (μm) | 2.1 to 3.5 , 3.25 to 5.4 |
| Spectral Resolution (μm) | 0.05 & 2.7 μm , 0.08 & 4.3 μm |
| Detector Type | InSb |
| NESR ($\text{w-cm}^{-2}\text{-sr}^{-1}\text{-}\mu\text{m}^{-1}$) | $2.4 \times 10^{-10}^*$ |
| Dynamic Range | 2×10^5 * |
| Half Angle Field of View (deg) | 1.871 |
| Spectral Scan Rate | -2/sec |

* reference 5

2.1 NS-6-4 Calibration Parameters

Radiance and wavelength calibrations for the NS-6-4 CVF were accomplished by both AFGL and Utah State University (Wyath 1978) prior to rocket launch. These calibrations showed good agreement so those of AFGL were used for this work.

2.1.1 Wavelength Calibration

The NS-6-4 CVF had two halves designated long (subscript l) and short (designated s) which refers to long wavelength and short wavelength. The AFGL calibration equations were adjusted using the data and known emission features such as the CO₂ (ν_3) peak at 4.28 μm . The appropriate equations are

$$\lambda_n(s) = 1.693 + (3.916 \times 10^{-2}) p_n \quad (2-1)$$

$$6.79 < p_n < 46.37 ,$$

$$p_n = \frac{n}{N} \times 100 \quad (2-2)$$

Where n = number of the data point in the scan

N = Total number of data points in the scan

P_n = percentage of n data point of total scan

For the long half of the filter.

$$\lambda_n(l) = -0.292 + (5.860 \times 10^{-2}) p_n \quad (2-3)$$

$$59.42 < p_n < 97.82$$

In the NS-6-4 the short half of the filter was scanned first.

2.1.2 Radiance Calibration

Radiance computations were done in units of megarayleighs per micron (MR/ μm) or brightness (B) since these units were used in calibration and permit direct physical interpretation of the results. In some cases the term "existence" is also used (Wyath 1978). To convert telemetry volts (V_{TM}) contained in the data channels the following calibration equations apply

$$B = M_{(\text{col})N} F_{V_{TM}} / \Delta\lambda \text{ megarayleighs/micron} \quad (2.4)$$

where the resolution ($\Delta\lambda$) is given by

$$\Delta\lambda_s = 0.013 + (1.4875 \times 10^{-2}) \lambda$$

$$\Delta\lambda_{\ell} = 0.0256 + (1.20 \times 10^{-2})\lambda$$

and

$$\text{HIGH GAIN } F(V_{TM}) = 6.5 \times 10^{-3} V_{TM}, V_{TM} \leq 10 \text{ volts} \quad (2.6)$$

$$\text{LOW GAIN } \begin{cases} F(V_{TM}) = 0.556 V_{TM} & , V_{TM} \leq 1.8 \text{ volts} \\ F(V_{TM}) = 0.5199^{1.11277} V_{TM} & , 1.8 < V_{TM} \leq 10 \text{ volts} \end{cases} \quad (2.7)$$

The values of $M_{(col)N}$ depends upon wavelength and are given in Table 2.1-1. $M_{(col)N}$ are set to zero for values of λ outside the tabled limits. The AFGL calibration was truncated based on data at 2.10, 3.50 and 3.25, 5.40 microns. These data are plotted in Figure 2.1-1 and show the wavelength overlap around 3.25 microns. This fact provided a convenient region to check consistency in calibration between the long and short wavelength filter halves. Notice the brightness scale on Figure 2.1-1 is $10^3 \text{ MR}/\mu\text{m}$. Thus the calibration peak at $2.95 \mu\text{m}$ is $8228 \text{ MR}/\mu\text{m}$.

2.2 Telemetry Signal

The EXCEDE II employed four telemetry (TM) links with ground receiving and recording systems. All data for the CVF instruments was contained in TM Link 3 tape (recorder 2 original) track 5 of the range tape. IRIG B time code to be used with these data was on track 3 station MUX (the normal 13 IRIG B track was reported to be spotty.) The data was pulse code modulated (PCM) which is described by Space Data Corporation (1979). Data for each instrument coded in several PCM words was "read", reformatted and recorded on separate digital tapes along with time in a format compatible with the AFGL CDC 6600 computer.

Flight data was digitized from T+40 sec (0457:20 UT hours) to T+340 sec (0553:50 UT) which was loss of signal. Data for the NS-6-4 CVF instrument were in words 2 and 26, 3 and 27, and 4 and 28 of all frames. Words 2 and 26 are high gain, 3 and 27 are low gain and 4 and 28 are the reference. The high and low gain contain the spectra and the reference contains the start pulse of each spectral scan, in addition to other wavelength reference pulses (of lower amplitude than the

TABLE 2.1-1
 $M(\text{col})_N$ vs. Wavelength NS 6-4

| λ μm | $M(\text{col})_N$ MR | λ μm | $M(\text{col})_N$ MR | λ μm | $M(\text{col})_N$ MR |
|------------------------------|-------------------------|----------------------------|-----------------------------|----------------------------|-------------------------|
| <u>Short Wavelength Half</u> | | | <u>Long Wavelength Half</u> | | |
| 2.10 | 3.03×10^2 | 3.25 | 3.01×10^2 | 4.85 | 2.44×10^2 |
| 2.15 | 3.03 | 3.30 | 2.93 | 4.90 | 2.38 |
| 2.20 | 2.95 | 3.35 | 2.91 | 4.95 | 2.35 |
| 2.25 | 2.77 | 3.40 | 2.95 | 5.00 | 2.32 |
| 2.30 | 2.56 | 3.45 | 2.88 | 5.05 | 2.31 |
| 2.35 | 2.40 | 3.50 | 2.84 | 5.10 | 2.29 |
| 2.40 | 2.28 | 3.55 | 2.81 | 5.15 | 2.28 |
| 2.45 | 2.24 | 3.60 | 2.83 | 5.20 | 2.28 |
| 2.50 | 2.27 | 3.65 | 2.85 | 5.25 | 2.30 |
| 2.55 | 2.38 | 3.70 | 2.88 | 5.30 | 2.35 |
| 2.60 | 2.51 | 3.75 | 2.93 | 5.35 | 2.48 |
| 2.65 | 2.60 | 3.80 | 2.98 | 5.40 | 2.83 |
| 2.70 | 2.94 | 3.85 | 3.00 | | |
| 2.75 | 3.60 | 3.90 | 3.01 | | |
| 2.80 | 4.01 | 3.95 | 3.03 | | |
| 2.85 | 4.30 | 4.00 | 3.05 | | |
| 2.90 | 4.57 | 4.05 | 3.05 | | |
| 2.95 | 4.68 | 4.10 | 3.03 | | |
| 3.00 | 4.43 | 4.15 | 3.09 | | |
| 3.05 | 4.15 | 4.20 | 3.14 | | |
| 3.10 | 3.81 | 4.25 | 3.08 | | |
| 3.15 | 3.42 | 4.30 | 2.97 | | |
| 3.20 | 3.16 | 4.35 | 2.91 | | |
| 3.25 | 2.91 | 4.40 | 2.85 | | |
| 3.30 | 2.74 | 4.45 | 2.83 | | |
| 3.35 | 2.66 | 4.50 | 2.76 | | |
| 3.40 | 2.69 | 4.55 | 2.74 | | |
| 3.45 | 2.72 | 4.60 | 2.72 | | |
| 3.50 | 2.79 | 4.65 | 2.70 | | |
| | | 4.70 | 2.63 | | |
| | | 4.75 | 2.57 | | |
| | | 4.80 | 2.51×10^2 | | |

start pulse) that were not used in the data processing. A review of these words showed a one data point lag in the start pulses between words 4 and 27. To avoid this confusion only word 4 was used to locate the scan start times.

Criteria for scan start was the first data point of value 20 counts or less following the peak (>900 counts) of the start pulse. A listing of these start times (with other parameters is given in Appendix A).

The high and low gain spectral data were contained in words 2 +26 and 3+27 were converted to TM volts using the equation

$$V_{TM} = \frac{C-12}{100} \quad (2-8)$$

Where C = number of counts (Space Data Corp. 1979).

2.5 Data Processing

The CDC digital tapes described in section 2.2 were processed using the scan start times (Appendix A) and the calibration equations to form a data base of one record per spectral scan. The seven parameters per data sample are

| <u>Parameter</u> | <u>Content</u> |
|------------------|------------------------------------|
| 1 | wavelength - microns |
| 2 | time after launch - seconds |
| 3 | altitude - km |
| 4 | high gain TM voltage - volts |
| 5 | high gain brightness - MR/ μ m |
| 6 | low gain TM voltage - volts |
| 7 | low gain brightness - MR/ μ m |

These parameters were computed for every data point. Payload altitude was computed with an eighth order fit to radar range data and utilized time after launch as the independent variable. The trajectory equation and coefficients are

$$h = a_0 + \sum_{i=1}^{i=8} a_i T^i$$

| | |
|--------------------------|--------------------------|
| $a_0 = -.539640506E+02$ | $a_5 = .1480695146E-07$ |
| $a_1 = .2741505348E+01$ | $a_6 = -.4493696965E-10$ |
| $a_2 = -.2947169205E-01$ | $a_7 = .7464427803E-13$ |
| $a_3 = .3475921337E-03$ | $a_8 = -.5216526696E-16$ |
| $a_4 = -.2907943273E-05$ | |

where

h = payload altitude - km

T = time after launch - seconds

The brightness data was plotted on semilog scale for each gain as a function of wavelength and altitude. All scans were plotted. The data was also plotted on a linear scale but otherwise in the same format. A sample brightness spectra is shown in Figure 2.3-1. The data shows Wu Benesch spectra between 2 and 3 microns and the prominent 4.28 micron CO₂. In the 3.4 micron region the filter short and long half responses overlap and indicates good agreement in the absolute brightness calibration. Notice that every spectral data point occurs at a different altitude because of payload motion as reported previously. Below 250 MR/ μm the presence of noise equivalent to 1 count in the onboard digitization process is evident. This effect is described in the next section of this report.

2.3-1 Error Analysis

For the NS-6 CVF the uncertainty in establishing counts is 1 count, therefore from Equation (2-8)

$$\min \Delta V = 0.01 \text{ volts}$$

Thus for high and low gain $F(V_{TM})$ is 6.5×10^{-5} and 5.56×10^{-3} respectively see Equations (2-6) and (2-7). For the short half the worst case uncertainty occurs at 2.95 microns (see Figure 2.1-1) and the uncertainty for high gain is 0.53 MR/ μm . For the long half the worst case high and low gain uncertainty occur at 3.25 microns and are .03 MR/ μm and 24.7 MR/ μm respectively. These values represent error bars (+ and -) of the measured data and in general are given by

$$\Delta B = \pm \frac{M(\text{col})}{\Delta \lambda} F(.01) \quad (2-10)$$

where

$F_{(.01)}$ = factor for $V_{TM} = 0.01$ volts

$\frac{M_{(col)}}{\Delta\lambda}$ = Figure 2.1-1.

The percentage error represented by the one error count depends only on the number of counts measured, viz,

$$\epsilon = \frac{\Delta B}{B} \times 100 = \frac{1}{C-12} \times 100\% \quad (2-11)$$

It is desirable to merge the low gain data with the high gain data when the high gain saturates. However as will be shown below problems of accuracy are incurred. High and low gain volts are related through the electrons gain factor G as follows

$$V_H = GV_L \quad (2-12)$$

where

G = gain factor

V_H = high gain volts

V_L = low gain volts

From Equation (1) the high gain counts (C_H) and low gain counts (C_L) are substituted in Equation (10).

$$C_L = \frac{C_H + 12(G-1)}{G} \approx \frac{C_H}{G} + 12 \quad (2-13)$$

If the switch from high gain to low gain is done using equation (11) the error due to 1 count at the switch over to low gain is found by substituting (11) in (9) which yields

$$\epsilon_{switch} = \frac{G}{C_H} \times 100 \quad (2-14)$$

If we choose to switch at $C_H = 900$ the error after the switch due to 1 count uncertainty is 8.3% assuming $G = 75$ where just prior to the switch the error is only 0.11% due to 1 count uncertainty. This discrepancy at the switchover point is undesirable and consequently the high and low gain data was not merged but treated separately.

2.3.2 Data Bases

In view of the incompatibility of high gain low gain data merge described above, no attempt was made to merge the two channels. Instead high and low gain channels were used to generate individual data bases. Samples from these data bases are given in Appendix D. High gain channels show the effects of one count digitization noise when the guns (accelerators) are not in operation, superimposed on a background signal caused by a small offset voltage in the system (see scan 116, 119, 121, etc.). The spectral structure of the background mirrors the system responsivity characteristic (see Figure 2.1-1). In the region of 100 km (scans 139, 153, 159) there appears to be a substantial signal enhancement probably due to instrument covers floating through the CVF field of view.

Periods for gun-on operation are given in Table 2.3-1. The correlation of signal enhancement with periods of gun-on operation can be observed by inspecting scans 237, 276, etc.

Table 2.3-1
ACCELERATOR OPERATION

| <u>Gun On Time*</u> <u>(seconds)</u> | <u>Gun Off Time*</u> <u>(seconds)</u> | <u>Gun Number</u> |
|---|--|-----------------------|
| 115.495 | 116.052 | 1 |
| 135.845 | 136.104 | 4 |
| 138.651 | 139.695 | 4 |
| 141.636 | 144.148 | 4 |
| 153.254 | 156.745 | 4 |
| 159.277 | 161.547 | 4 |
| 173.220 | 174.538 | 4 |
| 176.485 | 176.728 | 4 |
| 179.274 | 100.335 | 4 |
| 188.113 | 191.242 | 4 |
| 193.916 | 197.811 | 4 |
| 208.083 | 209.383 | 4 |
| 211.335 | 212.549 | 4 |
| 213.885 | 214.625 | 3 |
| 222.984 | 226.814 | 4 |
| 228.779 | 232.681 | 4 |
| 240.424 | 240.325 | 3 |
| 243.302 | 244.273 | 3 |
| 243.032 | 244.285 | 4 |
| 248.724 | 248.928 | 3 |
| 246.246 | 250.139 | 4 |
| 257.881 | 281.735 | 3 |
| 257.885 | 261.743 | 4 |
| 283.607 | 263.925 | 1 |
| 263.704 | 264.331 | 4 |
| 263.704 | 266.7 | 3 |
| 266.859 | 267.620 | 4 |
| 277.882 | 279.193 | 1 |
| 275.363 | 279.224 | 3 |

Table 2.3-1 (Cont.)

| <u>Gun On Time*</u> <u>(seconds)</u> | <u>Gun Off Time*</u> <u>(seconds)</u> | <u>Gun Number</u> |
|---|--|-----------------------|
| 275.367 | 279.228 | 4 |
| 281.083 | 282.047 | 1 |
| 281.189 | 282.750 | 4 |
| 234.525 | 235.032 | 1 |
| 283.684 | 285.088 | 3 |
| 286.929 | 290.859 | 1 |
| 292.863 | 293.236 | 4 |
| 292.759 | 244.156 | 1 |
| 298.149 | 296.72 | 2 |
| 292.863 | 296.723 | 3 |
| 298.581 | 298.795 | 1 |

PART B

H_e CVF SPECTROMETER

3.0 Description of Helium CVF (HS-3B-1)

The HS-3B-1 CVF (see specifications Table 3.0-1) is basically similar to the nitrogen CVF except a tuning fork optical chopper was added that periodically interrupted the incoming radiation to the sensor at a frequency of approximately 106 Hz. The sensor electrical output was filtered with an electronic filter centered at 100 Hz and passband approximately 50 Hz wide. This technique produced an amplitude modulated waveform whose envelope contained the observed spectral radiance information. Both a high and low gain channel were included for the modulated signal. The basic problem in processing the Helium CVF data was to demodulate and rectify the output signal then apply calibration factors to deduce the observed spectra in MR/ μ m.

Also unlike the Nitrogen CVF the long half of the HS-3B-1 CVF consisted of two filter segments in order to achieve the long wavelength response. However since the long half wavelength calibration applied throughout the spectral region the brightness calibrations at the joint wavelengths was simply set to zero and the long half of the CVF was treated as if it were continu .

3.1 Calibration Parameters

Radiance and wavelength calibrations were accomplished by both AFGL (Condron and Austin, private communications) and USU (Wyatt, 1979). Agreement of these data was adequate however the AFGL calibration data were used because the information was more detailed. In addition the AFGL wavelength data was also slightly modified (shifted) to agree with certain known emission features in the data such as CO_2 14.97 μ m. However the shift was less than a wavelength

Table 3.0-1
PERFORMANCE PARAMETERS FOR CVF HS-3B-1

| | |
|---|---|
| Wavelength Coverage (μm) | 3.9 to 6.8 , 12.7 to 22.3 |
| Spectral Resolution (μm) | 0.16 @ 5.3 μm , 0.4 @ 15 μm |
| Detector Type | Si : (As) |
| NESR ($\text{w}\cdot\text{cm}^{-2}\cdot\text{sr}^{-1}\mu\text{m}^{-1}$) | $1.08 \times 10^{-11^*}$ |
| Dynamic Range | $8 \times 10^4^*$ |
| Half Angle Field of View (deg) | 1.973 |
| Spectral Scan Rate | -0.8/sec |

* reference 7

resolution element of the instrument.

3.1.1 Wavelength Calibration

The HS-3B-1 filter halves are designated long wavelength (subscript ℓ) and short wavelength (subscript δ). The short half was scanned first (in time). The adjusted calibration equations for wavelength for each half are given by

$$\lambda_{\ell} = (2.388 \text{ E-1}) P_n - 1.097 \mu\text{m} \quad (3-1)$$

$$55 \leq P_n \leq 97\%$$

$$\lambda_{\delta} = (7.38 \text{ E-2}) P_n + 3.333 \mu\text{m} \quad (3-2)$$

$$4.0 \leq P_n \leq 44.4\%$$

where P_n is the percentage into the scan ($P_n = 100 n/N$).

The wavelength resolution elements at any wavelength determined by the CVF filter are given for each filter half by,

$$\Delta\lambda_{\delta} = (1.8667 \text{ E-2}) \lambda + 6.21\text{E-2} \mu\text{m} \quad (3-3)$$

$$\Delta\lambda_{\ell} = (5.482 \text{ E-3}) \lambda + 3.12\text{E-1} \mu\text{m}$$

3.1.2 Radiance Calibration

During actual radiance (brightness) calibration of the HS-3B-1 CVF the sensor output was a continuous analog signal and demodulation and rectification of the signal was accomplished using a phase sensitive amplifier (PAR). Since the telemetry signal was PCM this technique was not possible so a computerized demodulation and rectification scheme had to be formulated to accomplish these tasks which included the laboratory calibration data. This formulation is derived in section 3.3.1 of this report. However, the

final result to convert demodulated rectified telemetry volts V_{TM} to spectral radiance is given here

$$B_n = G_i M_{(col)} V_{TM} / \Delta\lambda \text{ MR}/\mu\text{m} \quad (3-4)$$

where B_n = brightness (radiance) of data point n

G_i = channel gain (high gain = 1, low gain = 100)

$M_{(col)}$ = calibration factor in MR/volt (see Table 2.1-1)

$\Delta\lambda$ = resolution (see equation (3-3))

The adjusted laboratory calibration data for $M_{(col)}$ is given in Table 3.1-1 in units of MR/volt. Notice that the values are zero at 17.50 and 17.70 μm where the long wavelength filter point occurs. Other values in the original data near the mask regions are located have also been adjusted to eliminate the tendency to "spike" when the mask passes over the sensor. A plot of the final calibration is shown in Figure 3.1-1 in units of MR/ μm - volt and derived using the data in Table 3.1-1 and equation (3-3).

3.2 Telemetry Signal

All aspects of the HS-3B-1 PCM telemetry were identical with CVF NS-6-4 (see section 2.2 of this report) except that since the HS-3B-1 CVF was optically chopped one additional channel of data was required (compared to the NS CVF) for the chopping frequency. The spectral data was contained in PCM words 5 + 29 (low gain) and words 6 + 30 (high gain). The spectral reference (start pulse) was on words 7 + 31 and the chopper sequel on word 46. Spectral scan start times are determined in the same manner as the NS instrument, see Appendix B for the listing of HS-3B-1 start times.

TABLE 3.1-1
 $M(\text{col})_N$ vs. Wavelength HS 3B-1

| λ μm | $M(\text{col})_N$ MR/volt | λ μm | $M(\text{col})_N$ MR/volt | λ μm | $M(\text{col})_N$ MR/volt |
|------------------------------|------------------------------|----------------------------|------------------------------|----------------------------|------------------------------|
| <u>Short Wavelength Half</u> | | | <u>Long Wavelength Half</u> | | |
| 3.70 | 0 | 11.90 | 0 | 18.50 | .8375 |
| 3.80 | 0 | 12.10 | 0 | 18.70 | .8225 |
| 3.90 | 7.91 | 12.30 | 0 | 18.90 | .821 |
| 4.00 | 4.54 | 12.50 | 0 | 19.10 | .843 |
| 4.10 | 4.355 | 12.70 | 1.53 | 19.30 | .869 |
| 4.20 | 4.20 | 12.90 | 1.26 | 19.50 | .8825 |
| 4.30 | 4.155 | 13.10 | 1.16 | 19.70 | .902 |
| 4.40 | 3.885 | 13.30 | 1.15 | 19.90 | .9235 |
| 4.50 | 3.61 | 13.50 | 1.09 | 20.10 | .8985 |
| 4.60 | 3.41 | 13.70 | 1.05 | 20.30 | .875 |
| 4.70 | 3.255 | 13.90 | 1.025 | 20.50 | .8935 |
| 4.80 | 3.14 | 14.10 | .9635 | 20.70 | .920 |
| 4.90 | 3.08 | 14.30 | .8545 | 20.90 | .9405 |
| 5.00 | 2.97 | 14.50 | .836 | 21.10 | .951 |
| 5.10 | 2.85 | 14.70 | .8855 | 21.30 | .964 |
| 5.20 | 2.75 | 14.90 | .8905 | 21.50 | .9805 |
| 5.30 | 2.70 | 15.10 | .835 | 21.70 | .9805 |
| 5.40 | 2.625 | 15.30 | .7925 | 21.90 | .9805 |
| 5.50 | 2.57 | 15.50 | .7665 | 22.10 | .9805 |
| 5.60 | 2.50 | 15.70 | .763 | 22.30 | .9805 |
| 5.70 | 2.50 | 15.90 | .804 | 22.50 | 0 |
| 5.80 | 2.51 | 16.10 | .853 | 22.70 | 0 |
| 5.90 | 2.49 | 16.30 | .8765 | 22.90 | 0 |
| 6.00 | 2.475 | 16.50 | .8205 | | |
| 6.10 | 2.42 | 16.70 | .716 | | |
| 6.20 | 2.33 | 16.90 | .735 | | |
| 6.30 | 2.265 | 17.10 | .7545 | | |
| 6.40 | 2.285 | 17.30 | .8725 | | |
| 6.50 | 2.30 | 17.50 | 0 | | |
| 6.60 | 2.215 | 17.70 | 0 | | |
| 6.70 | 2.14 | 17.90 | .9005 | | |
| 6.80 | 2.125 | 18.10 | .813 | | |
| 6.90 | 0 | 18.30 | .8765 | | |

3.3 Data Processing

The idea of chopped systems accompanied by phase sensitive demodulation and detection to reduce DC drift and improve signal to noise is well known (Schwartz, 1959) and widely used by electronic engineers. However for actual digital CVF data such as that of NS-3B-1 some special problems occur and so a brief review of the fundamentals will be presented prior to describing the actual data reduction techniques used for CVF HS-3B-1.

Figure 3.3-1 illustrates how the HS-3B-1 CVF modulated signal was produced. Since the CVF selectively passes the incident spectral radiance as it rotates at a constant rate the incident spectral radiance can be represented as a function of time instead of wavelength. This is shown in the top plate of Figure 3.3-1. The incident spectral radiance is periodically interrupted by a mechanical chopper which itself radiates some lower level since it is cooled. The chopped signal as seen by the CVF sensor is shown in the second plate of Figure 3.3-1. The sensor output is assumed proportional to this incident radiance. If we assume for the moment that the chopper radiance is negligible and that the frequency bandwidth of the incident spectral radiance is small compared to the chopper frequency then the sensor output can be estimated by the Fourier series

$$s(t) = \frac{1}{2} S(\lambda) \left[1 + 2 \sum_{n=1}^{\infty} \frac{\sin n\pi/2}{n\pi/2} \cos n\omega_c t \right] \quad (3-5)$$

where $s(t)$ = chopped spectra signal

$S(\lambda)$ = infrared spectra (unchopped)

ω_c = radian chopping frequency

If we now assume that there is no incident spectral signal and the chopper radiance is not negligible then the signal output from the chopper

radiance alone can be written in a similar manner except that there will be a 180° phase difference

$$b(t) = \frac{1}{2} R(\lambda) \left[1 + 2 \sum_{n=1}^{\infty} \frac{\sin n\pi/2}{n\pi/2} \cos(n\omega_c t + \pi) \right]$$

where $b(t)$ = chopped chopper signal

$R(\lambda)$ = chopper unchopped radiance

ω_c = radian chopper frequency

Clearly the phase angle π can be omitted simply by changing the + sign in front of the summation to -.

For the case of both incident spectral radiance and non zero chopper radiance the total sensor output signal is the sum of $s(t)$ and $b(t)$

$$g(t) = s(t) + b(t) = \frac{1}{2}(S(\lambda) + R(\lambda)) + (S(\lambda) - R(\lambda)) \left[\sum_{n=1}^{\infty} \frac{\sin n\pi/2}{n\pi/2} \cos n\omega_c t \right] \quad (3-6)$$

If we now A.C. Couple this output signal to remove the DC term $\frac{1}{2}(S(\lambda) + R(\lambda))$ then filter with a narrow bandpass filter centered at the fundamental chopping frequency ω_c we get for $n=1$

$$g(t) = \frac{2}{\pi} (S(\lambda) - R(\lambda)) \cos \omega_c t \quad (3-7)$$

This result is the modulated waveform of the EXCEDE sensor output shown in plate 3 of Figure 3.3-1. This sensor output was digitized on the payload and telemetered and recorded in PCM format. Actual data is shown in Figure 3.3-1A.

The sinusoidal waveform of the chopper reference (also digitized and telemetered) in plate 4 of Figure 3.3-1 is simply expressed as

$$h(t) = A \cos(\omega_c t + \Delta\theta) \quad (3-8)$$

where $h(t)$ = A.C. Component of the chopper signal.

$\Delta\theta$ = phase difference between data and chopper signals.

A = amplitude of the chopper signal.

The phase difference $\Delta\theta$ is included in this equation to account for such things as mechanical lag in sensing chopper position which would produce a phase difference between the sensor signal and the chopper reference.

In principle the demodulation and extraction of the spectra $S(\lambda)$ from equation (3-7) is done by forming the product of $h(t)$ and $g(t)$, which expanded and simplified yields

$$\begin{aligned} P = g(t)h(t) &= \frac{2A(S(\lambda) - R(\lambda))}{\pi} \cos \omega_c t \cos(\omega_c t + \Delta\theta) \\ &= \frac{A(S(\lambda) - R(\lambda))}{\pi} [\cos \Delta\theta + \cos(2\omega_c t + \Delta\theta)] . \end{aligned} \quad (3-9)$$

We now filter the product P with a low pass filter with cutoff frequency less than $2\omega_c$ and greater than the highest data frequency in the spectral radiance. Solving for $S(\lambda)$, yields

$$S(\lambda) = R(\lambda) + \frac{\pi P'}{A \cos \Delta\theta} \quad (3-10)$$

where P' represents the low pass filtered product of $h(t)$ and $g(t)$.

Equation 3-10 shows that the chopper radiance background is added to the incident signal and clarifies why it is necessary to keep the chopper radiance small (cold). Also if either the chopper amplitude A or the phase angle difference $\Delta\theta$ between spectral data and chopper reference are modulated with time in any manner false components will be introduced into the reduced spectra.

Notice from Equation 3-7 that if the incoming radiation $S(\lambda)$ is less than the chopper radiation $R(\lambda)$ then $g(t)$ is negative and the product term

in Equation (3-10) will also be negative resulting in a quantity of radiation being subtracted from $R(\lambda)$ to give $S(\lambda)$ just as it should be. If one attempted to retrieve the spectra $S(\lambda)$ by simply reconstructing the envelope of $g(t)$ this possibility would not be detected and an error in $S(\lambda)$ would result. On the other hand multiplying by chopper signal and filtering as explained, preserves all the phase properties of the signal. It is crucial however, to derive an accurate representation of the chopper data characteristics.

3.3.1 Data Reduction

Several problems arise in attempting to apply the principles derived above to the EXCEDE chopped CVF PCM data. For one thing all the data channels were sampled (on the payload) serially so that the chopper reference data points were not time coincident with the spectral data points. In addition the chopper was sampled at 512 Hz - just half the spectral data sample rate. Thus forming the correct product P (Equation (3-9)) of the chopper and spectral data needed for demodulation was not possible. Consequently it was elected to fit the digital chopper data for each spectral scan with a least squares technique to derive an analog equation to be used in forming the product term in Equation (3-3). The mean value of the chopper reference signal data was found and subtracted from the data set. An estimated frequency (f_c) of the signal was found by counting zero crossings during each scan and dividing by two times the product of the total number of data points and the sampling interval, viz.

$$f_c = \frac{N_0}{2N_{TOT}\Delta t} = \frac{N_0 f_s}{2N_{TOT}} \quad (3-11)$$

where f_c = chopper frequency - Hz

N_0 = number of zero crossing in the scan

N_{TOT} = total number of data points in the scan (1/2 number spectral data samples)

Δt = sampling interval

$f_s = 1/\Delta t$ = sampling frequency = 512 Hz.

Since the total number of chopper data points N_{TOT} is known precisely (1/2 the number of spectral data points) for each scan and the sampling frequency is considered invariant the error Δf_c in determining f_c is at most due to the error of missing one zero crossing and thus

$$\Delta f_c = \frac{(1)512}{2(616)} = 0.42 \text{ Hz}$$

(The value 616 for N_{TOT} was estimated based on 1232 data points in a typical spectral data scan - see Appendix A).

Knowing the frequency the assumed chopper sinusoidal signal equation derived below was least squares fitted to the data in each spectral scan.

$$h(t) = A \cos(\omega_c t - \theta_c) = A \cos \omega_c t \cos \theta_c + A \sin \omega_c t \sin \theta_c \quad (3-12)$$

$$h(t) = b \cos \omega_c t + c \sin \omega_c t$$

where $h(t)$ = chopper signal

A = amplitude

θ_c = phase angle relative to the scan start

$b = A \cos \theta_c$

$c = A \sin \theta_c$

As a result of the fit the constants b and c are found and the phase angle is determined by (see Figure 3.3-2 for typical data fit)

$$\theta_c = \tan^{-1} \left(\frac{c}{b} \right) \quad (3-13)$$

Finally setting the amplitude A=1 the chopper signal equation in digital form is

$$h(n) = \cos [2\pi f_c (n-1)\Delta t - \theta_c] \quad (3-14)$$
$$n = 1, 2, 3, \dots, N_{TOT}$$

where $h(n)$ = chopper equation

f_c = chopper frequency - Hz

n = data point number

Δt = sample interval = $\frac{1}{1024}$ sec. for the spectral data

θ_c = phase angle relative to the scan start

N_{TOT} = total data points in the scan.

In actual practice the frequency f_c was computed by the fit. Appendix C contains a tabulation of the phase angle and f_c for the actual data derived as discussed above for each spectral scan. Included in this tabulation is the "goodness of fit" parameter chi squared. The lower the number the better the fit. A typical example of the calculated chopper reference (solid line) using Equation 3-14 compared to the actual chopper data (points) is shown in Figure 3.3-2. As long as the chopper reference data amplitude was relatively constant (which was not always the case) the fit with Equation 3-14 was excellent.

Clearly Equation 3-14 permits calculating the necessary value of the chopper reference for any spectral data point n and thus satisfies the requirements needed for evaluating the product P in Equation 3-9 (which implied $\theta_s = 0$). When there is a phase difference between the spectral data and the chopper defined by $\theta_c - \theta_s = \Delta\theta$ where θ_s and θ_c are the phase differences from the start of scan for spectra and chopper respectively, Equation (3-7) becomes

$$g(t) = \frac{2}{\pi} (S(\lambda) - R(\lambda)) \cos(\omega_c t - \theta_s)$$

It was found by inspection of the data that the chopper lagged the spectral data by 1/3 a spectral data point (12°) so that $\Delta\theta = -12^\circ$.

An example of the product P for scan 1211 formed by multiplying each spectral data point in the scan by a numerical value computed for the chopper using Equation 3-14 for the same n (constant $A=1$ and the appropriate phase angle θ_c taken from Appendix C) is shown in Figure 3.3-3, both the high and low gain channels are shown. The product was evaluated in telemetry units of counts for the spectral data $g(t)$ while $h(t)$ is dimensionless. Prior to forming the product the mean of the modulated spectral data was determined and subtracted from each data value of $g(t)$. Theoretically the mean of the modulated wave should be zero. Note that all prominent count values, in Figure 3.3-3, are positive except for a few spurious data points in the high gain channel where the signal was saturated. In addition the noise values oscillate about zero as it should. The envelope of the data in Figure 3.3-3 contains the desired spectral information. All that is required to derive the spectrum is to extract the envelope and apply calibrations for wavelength and brightness. Ripple on the high gain is explained later.

Typically envelope detection is done by smoothing or filtering. Clearly the only useful data points of the waveforms shown in Figure 3.3-3 are the peak values since only they represent the observed spectrum. Since filtering of digital data is a somewhat complicated process especially with large data bases and when Fourier transforms are involved it was decided to attempt to derive the envelope data by a decimation technique prior to filtering.

Using the concept of referring phase angles of both the chopper reference and spectral data to the beginning of the scan and acknowledging that these phase angles could be different the product term of Equation 3-9 can be rewritten as

$$P = \frac{A}{\pi} (S_{(\lambda)} - R_{(\lambda)}) \left\{ \cos(\theta_s - \theta_c) + \cos[2\omega_c t - (\theta_c + \theta_s)] \right\} \quad (3-15)$$

since $\theta_c - \theta_s = \Delta\theta$ is constant the maximum value of the product P occurs when the $\cos[2\omega_c t - (\theta_c + \theta_s)] = +1$. Thus the data point number n_p defining the maximum value is

$$2[2\pi(n_p - 1) f_c \Delta t] - (\theta_c + \theta_s) = 2(i-1) \pi \\ i=1, 2, 3, \dots, N_{TOT}$$

Therefore solving for n_p yields

$$n_p = 1 + \frac{(i-1) \pi + (\theta_c + \theta_s)/2}{2\pi f_c \Delta t}. \quad (3-16)$$

Since θ_c is arbitrary it is clear that values of n_p computed with Equation (3-16) could take on non-integer values which do not exist in the digital data base, viz. data points are numbered in integer steps from 1 at scan start to N_{TOT} at the end of the scan. Assuming the sampling rate f_s is invariant (1024 samples/sec) and equal to the reciprocal of the sample interval time Δt Equation (3-1) is rewritten as follows

$$n_o = \text{round off integer value} \left[1 + \frac{(i-1) \pi + (\theta_c + \theta_s)/2}{2\pi f_c / f_s} \right] \quad (3-17)$$

$$i = 1, 2, 3, \dots, N_{TOT}$$

The envelope data base was determined for each scan by choosing only data points defined with Equation (3-17). The data point difference $\Delta n_o = 5$ and thus the data base was reduced by a factor of 5 by this decimation process and contained only the estimated envelope data.

Once the envelope data base was generated in this manner the spectral data in counts was converted to volts using the relationship

$$V_{TM} = \frac{C}{100} = \frac{P}{100} \quad (3-18)$$

where V_{TM} = telemetry volts

C = counts

This equation differs slightly from that used for the NS instrument (Equation (2-8)) because the A.C. coupling of the HS sensor output removes the 12 count D.C. offset. The decimated envelope data base derived by Equation (3-16) was units of counts. These data were converted to volts simply by dividing by 100 in accordance with Equation (3-18).

Returning to the basic relationship for deriving the product p in Equation (3-19), we must recall in subsequent discussion that we have already assumed the amplitude A of the chopper reference signal to be constant and equal to 1 and also that the phase difference $\Delta\phi$ between chopper reference and spectral data to be $+12^\circ$. Finally we make the assumption that chopper radiance $R_{(\lambda)}$ is negligible compared to the spectrum since it is cooled. In addition we have used n_o in choosing the envelope instead of n_p so solving for the spectrum $S_{(\lambda)}$ yields

$$S_{(\lambda)} = \frac{\pi p}{\cos\Delta\phi + \cos 2[2\pi f_c(n_o - 1)\Delta t - (\tau_c - \tau_s)/2]} \quad (3-19)$$

The units of $S_{(\lambda)}$ are counts. Notice the denominator -2 for small $\Delta\phi$. It was decided to first generate a data base where the spectra was not filtered but in the correct units of $MR/\mu m$ then filter the data set in units of radiance. This precaution was taken in the event the voltage calibration was not linear. The unfiltered spectral radiance was thus calculated from the unfiltered

$$\text{decimated data base where } V_{TM} = \frac{S_{(\lambda)}}{100}$$

$$B_{(\lambda)} = G_i M_{(col)} V_{TM}/\Delta\lambda \quad (3-20)$$

where $B_{(\lambda)}$ = unfiltered spectral radiance $MR/\mu m$

P = decimated product term (unfiltered) in units of

$M_{(col)}$ = calibration term - $MR/volt$

$\Delta\lambda$ = calibration term - μm (see Equation (3-3))

V_{TM} = decimated spectra term expressed in volts

G_i = gain factor (high gain = 1, low gain = 100)

Equation 6-21) was given previously in Equation 6-4 of this report.

Figure 3.3-4 shows a sample unfiltered spectral radiance profile derived by the techniques described above. The ripple on the spectra is caused by a chopping feed-through effect (viz $\cos 2\omega_c t$ term in Equation 6-9)) which was intentionally not filtered before initial examination of the spectral data. The spectral data shows the emission features of CO₂ at 4.28 and 14.97 μm and NO in the 5 to 6 μm region. However the need of filtering to remove the chopper effect is evident.

As a first approach a simple nonrecursive filter was used for initial data smoothing. The filtered brightness B'_n at point n is computed as follows

$$B'_n = [aB_{n-2} + bB_{n-1} + cB_n + bB_{n+1} + aB_{n+2}] \quad (3-21)$$

The transfer function of this filter is (Hamming, 1979)

$$H(\omega) = 2a \cos 2\omega + 2b \cos \omega + c \quad (3-22)$$

where $\omega = \pi f/f_N$

$f_N = 1/2 \Delta t = fs/2$ Nyquist frequency

fs = sampling frequency after decimating = 205 Hz

f = physical frequency

For this case we desire good low pass characteristics, so using the conditions

$$H(0) = 1$$

$$\frac{dH(0)}{d\omega} = 0 \quad (3-23)$$

$$\frac{d^2H(0)}{d\omega^2} = 0$$

leads to the following values

$$\begin{aligned}a &= -1/16 \\b &= +1/4 \\c &= +5/8\end{aligned}\quad (3-24)$$

A plot of the frequency response of this filter is shown in Figure 3.3-5.

The decimated data base was processed using Equation (3-21) to produce initial smoothed data. Spectral scan 1210 (Figure 3.3-6) illustrates the effect of the smoothing and the improvement of spectral radiance features are shown in Figure 3.3-6 as compared to Figure 3.3-4.

3.3.2 Data Base (HS-3B-1)

An "abridged" data base was generated for selected spectral scans from the HS-3B-1 CVF using the procedures outlined above. These data are given in Appendix E. In general the spectra show emission enhancement during periods of "gun" (accelerator) on times but in addition there seems to be a background enhancement (scan 1067) at times when the guns are off. This is attributed to the possibility of instrument covers floating through the CVF field of view. The fine structure in some of the enhanced emissions (see 5.8 μm of scan 1204) is due in part to the effects of chopper second harmonic and sampling which is explained in more detail in the next section of this report.

It should be noted that the spectral data shown in Appendix E consist of merged results from both the high and low gain channels. A signal voltage of 4.2 volts was used as the criterion for merging the two gain channels.

3.4 Discussion

The ripple (~40 Hz) superimposed on the demodulated waveform in Figure 3.3-3 is clearly an error source since it falls within the digital filter passband (see Figure 3.3-5). Power spectral density analyses of these signals do not indicate the presence of the 40 Hz ripple, however, the chopper second harmonic (212 Hz) is evident in the PSDs of both the spectral and chopper data. This indicates that the chopper second harmonic is leaking into the signals due to poor frequency cutoff characteristics of the system electronic filter on-board the payload. Inspection of the electronic characteristic in Figure 3.4-1 confirms this possibility. A simple trigonometric exercise demonstrates the point. Assume the chopper fundamental waveform is added to the second harmonic waveform approximately 90° out of phase and with reduced amplitude "a".

$$h(t) = \cos\omega_c t + a \sin(2\omega_c t - \phi) \quad (3-35)$$

where ϕ = small phase angle $\sim 9^\circ$

$h(t)$ = chopper waveform

f_c = chopper frequency 106 Hz

$\omega_c = 2\pi(n-1) f_c/f_s$

f_s = sampling frequency 512 Hz

n = data point number

a = amplitude <1

Setting a = 0.2 and evaluating Equation (3-35) for n=54 to 154 we produce the simulated chopper waveform in Figure 3.4-2 (scale factors have been introduced for ease of comparison). Comparing this to a portion of the actual waveform indicates obvious similarity. Note that the ripple frequency in the chopper is only ~20 Hz (rather than 40 Hz as it is in the data) because sampling of the

chopper was only 512 Hz compared to 1024 Hz in the case of the spectral data. As pointed out the ripple cannot be removed from the data without more sophisticated filtering techniques which are beyond the scope of this preliminary work.

There is also an inherent error in the spectral data due to a one count uncertainty due to digitization. One count is equivalent to 10 millivolts by Equation 3-18. From Equation 3-20 the noise radiance for this voltage in high gain ($G=1$) is

$$B_{\min} = 0.01 M_{(\text{col})} / \Delta\lambda \quad (3-36)$$

where $M_{(\text{col})} / \Delta\lambda$ is the calibration factor in MR/volt (see Figure 3.1-1) and $\Delta\lambda$ is the resolution. From the figure the calibration factor depends on wavelength showing values of 2.23 MR/ μm -volt at $\sim 15 \mu\text{m}$ and 16.9 MR/ μm -volt at $\sim 5.3 \mu\text{m}$. This produces a noise of

$$B_{\text{noise}} = 0.02 \text{ MR}/\mu\text{m} \text{ at } 15 \mu\text{m}$$

$$B_{\text{noise}} = 1.7 \text{ MR}/\mu\text{m} \text{ at } 5.3 \mu\text{m}$$

These values are well below the signal levels encountered (see Appendix E).

An additional error is introduced by the decimation process because of the necessity to round off the computed peak value data point number to the integer value. This causes a cyclical error every 5 data points of about 10%.

PART C

4.0 RECOMMENDATIONS

Data processing techniques of Circular Variable Filter Spectrometers have developed in the past 5 years to a point where spectral results can be accepted with good confidence. However, limitations in interpreting processed spectra are imposed by a variety of design parameters. For instance leakage due to imperfect out-of-band rejection of the CVF can contaminate low spectral signals. The best blocking possible with a CVF is probably four orders of magnitude. Non-constant CVF rotation can cause wavelength errors comparable with the spectral resolution of the CVF. In the case of the EXCEDE HS-3B-1 poor rejection properties of the electronic filter caused chopper second harmonic to contaminate the data.

Specifically we recommend that the EXCEDE data and techniques presented here be considered preliminary and reviewed for adequacy in terms of the physics involved. The helium instrument (HS-3B-1) data should be reprocessed by more sophisticated techniques to reduce as much as possible the effects of second harmonic contamination.

5.0 ACKNOWLEDGEMENTS

We wish to acknowledge the many helpful suggestions made by Robert O'Neil of AFGL and the Principal Investigator, Dr. E. Richard Hegblom of Boston College. We also thank Mary Kelly for typing this manuscript.

6.0 REFERENCES

1. O'Neil, R.R., Lee, E.T.P., Stair, A.T., Ulwick, J.C., (1976) EXCEDE II, AFGL-TR-76-0308.
2. O'Neil R.R., Stair, A.T., Bart, D., Kemp, J., Frogsham, G.T., Shepherd, R.E., EXCEDE Spectral; Artificial Auroral Experiment, EOS Vol. 61, No. 17, April 1980, p. 325.
3. O'Neil, R.R., August 1980 "Preliminary Results of EXCEDE experiment" AFGL-TM-41.
4. Rogers, J.W., (1976) LWIR (7-24 μm) Measurements From the Launch of A Rocketborne Spectrometer Into an Aurora (1973), AFGL-TR-76-0274, ERP No. 583, HAES Report No. 51.
5. Wyatt, C.L., (1978) Circular Variable Filter Spectrometer NS-6-4, Utah State University Report (unpublished).
6. Space Data Corporation (1979) EXCEDE II A51.970 Flight Results SDC TM-1686.
7. Wyatt, C.L., (1979) Circular Variable Filter Spectrometer Model HS-3B-1 Utah State University Report (unpublished).
8. Scwantz, M., (1959) Information Transmission, Modulation, and Noise McGraw Hill, p. 159.
9. Hamming, R. W. (1977) Digital Filters, Prentice Hall, p. 49.

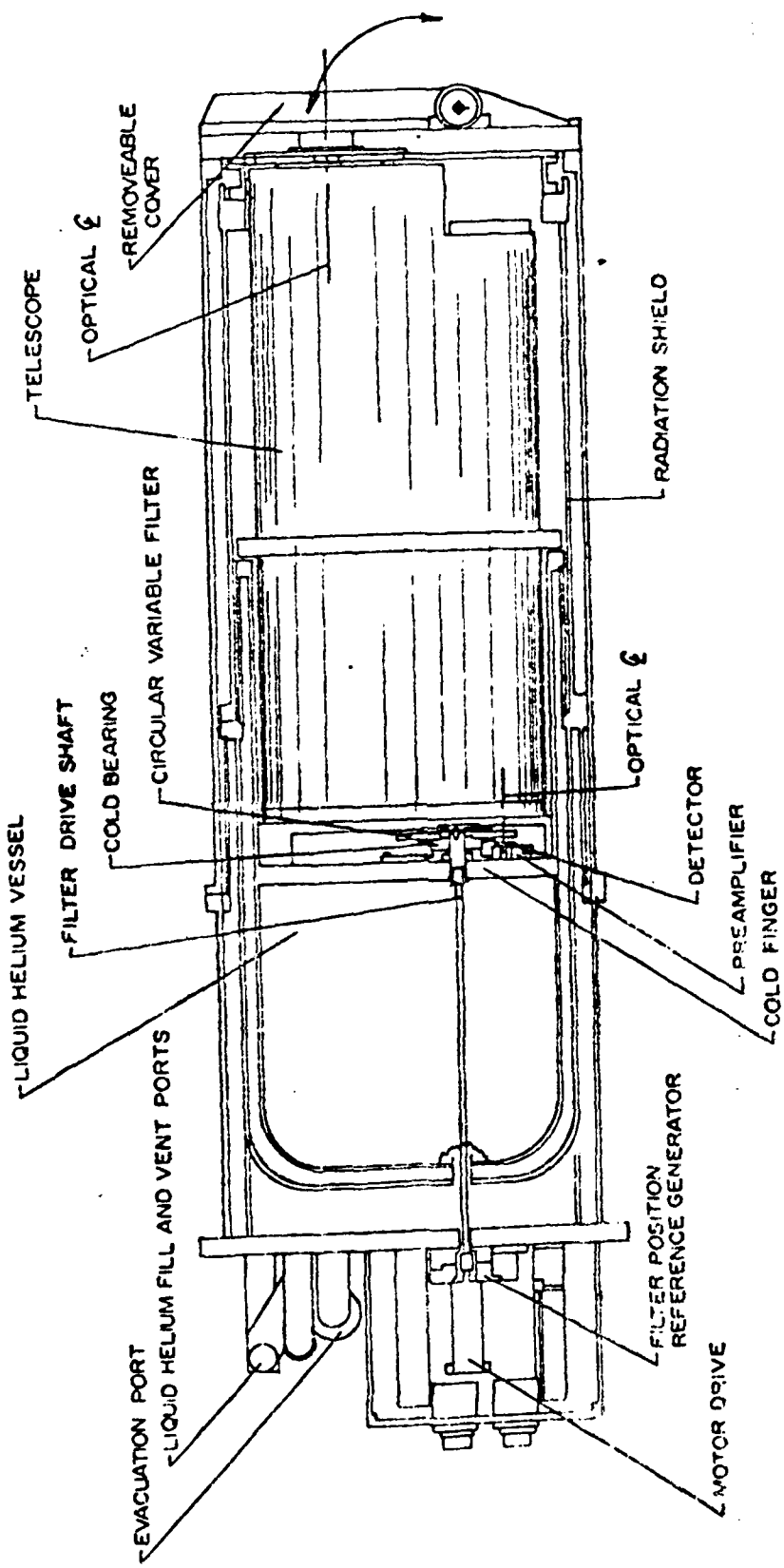


Figure: 2.0-1 Schematic of a typical circular variable filter (CVF) spectrometer.

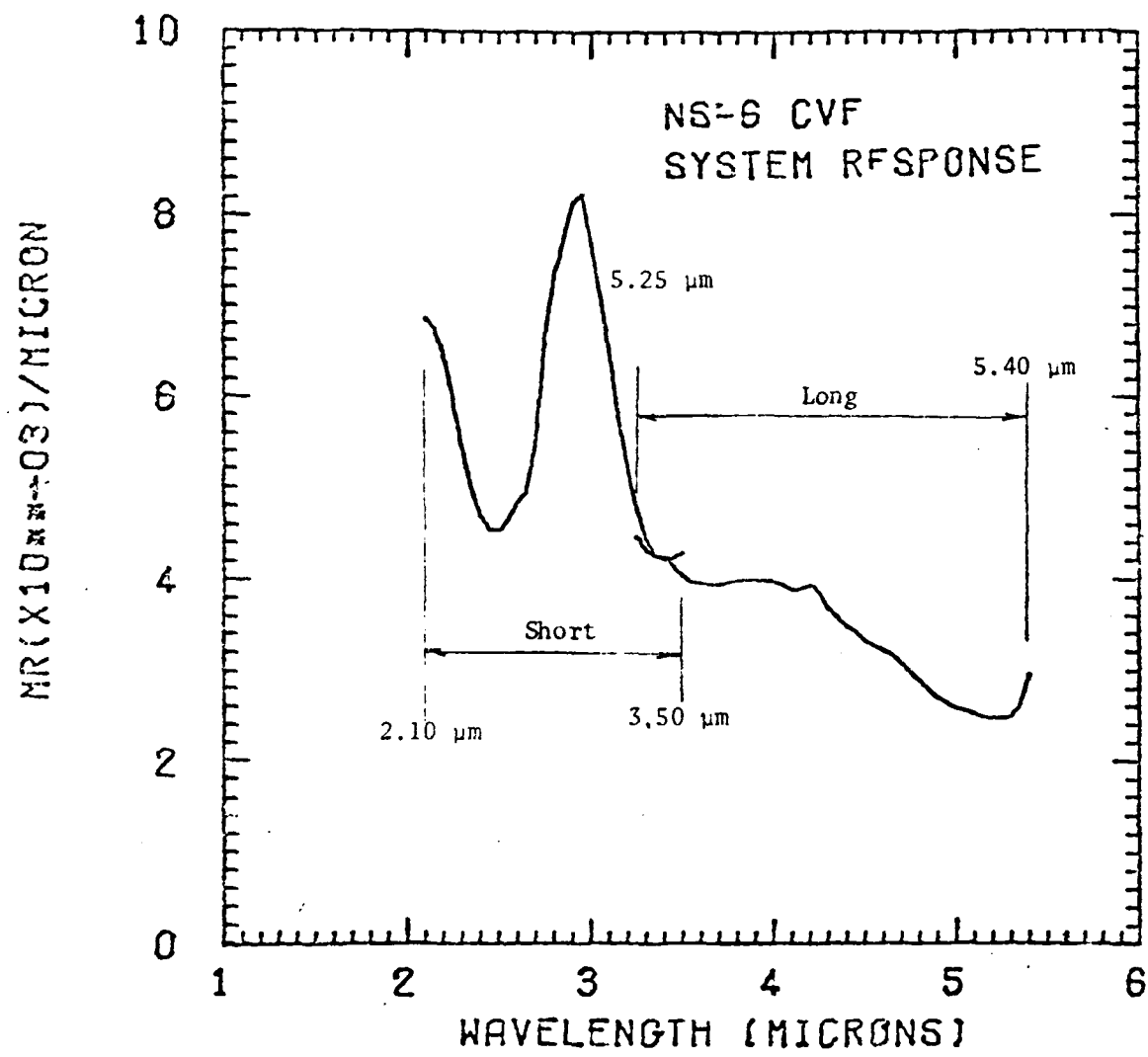


Figure 2,1-1. CVF brightness calibration (NS-6-4)

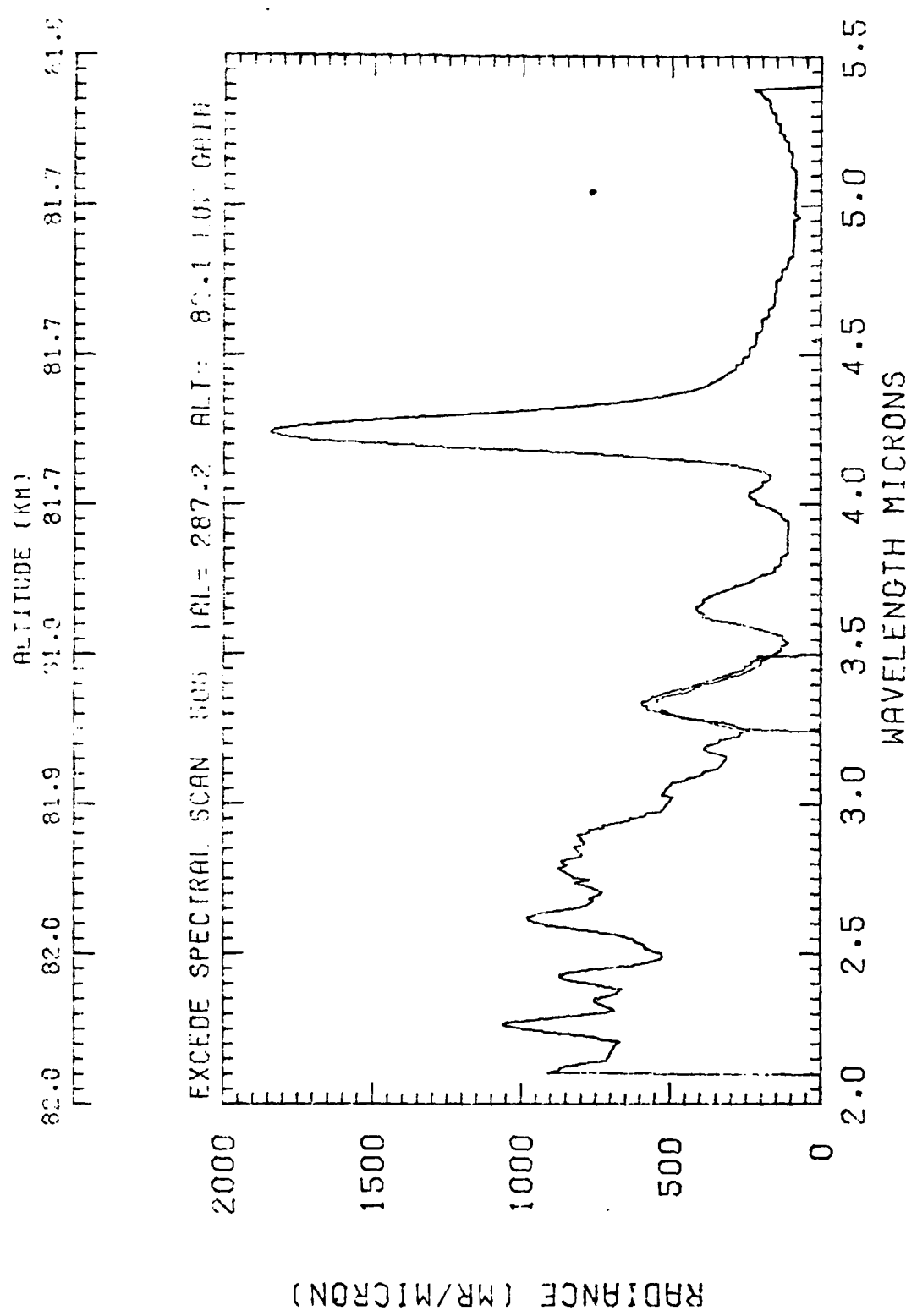


Figure 2.3-1. Sample spectra from EXCDE short wavelength CVF spectrometer during electron gun operation.

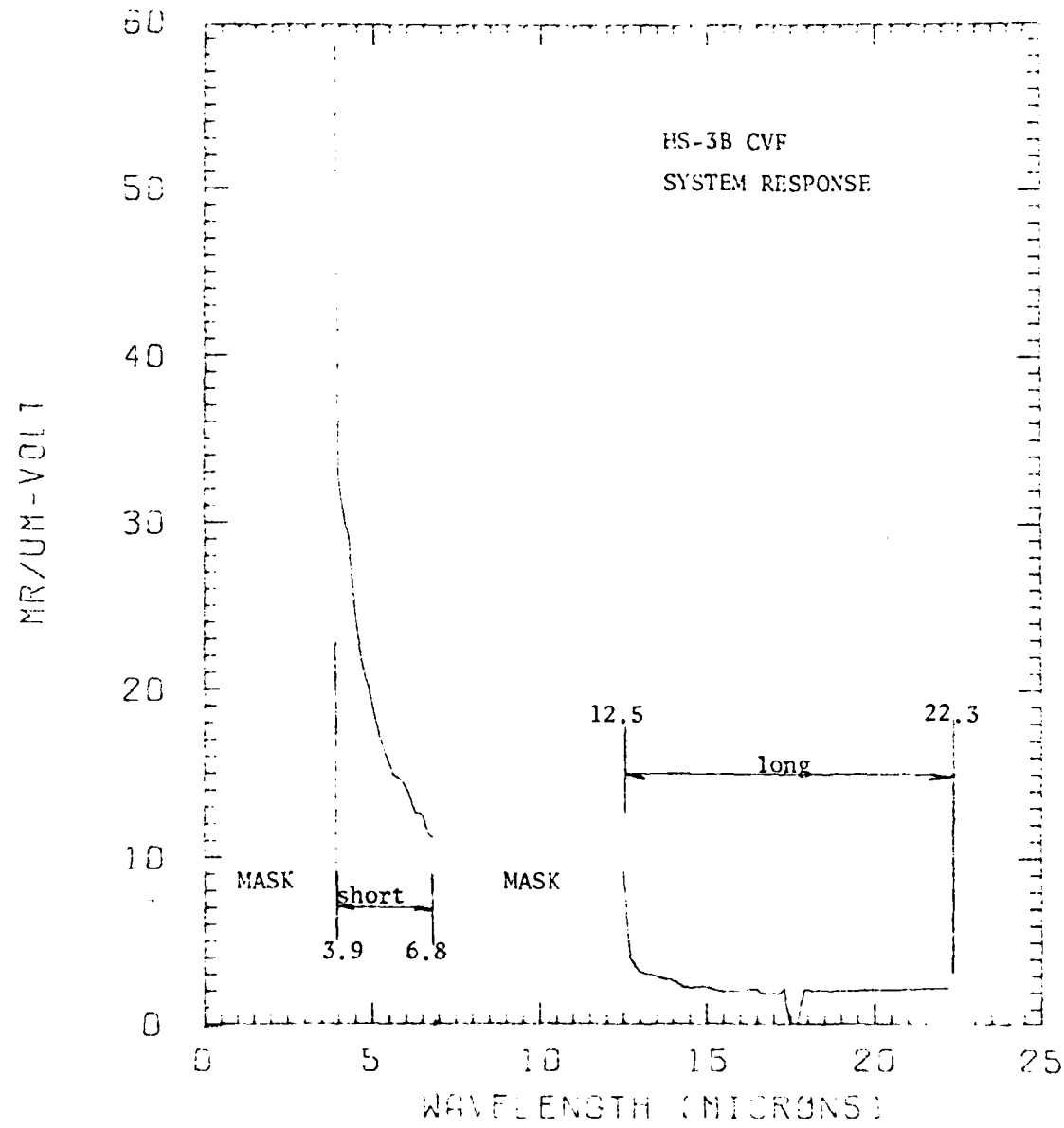


Figure 3.1-1 CVF Brightness Calibration (HS-3B-1)

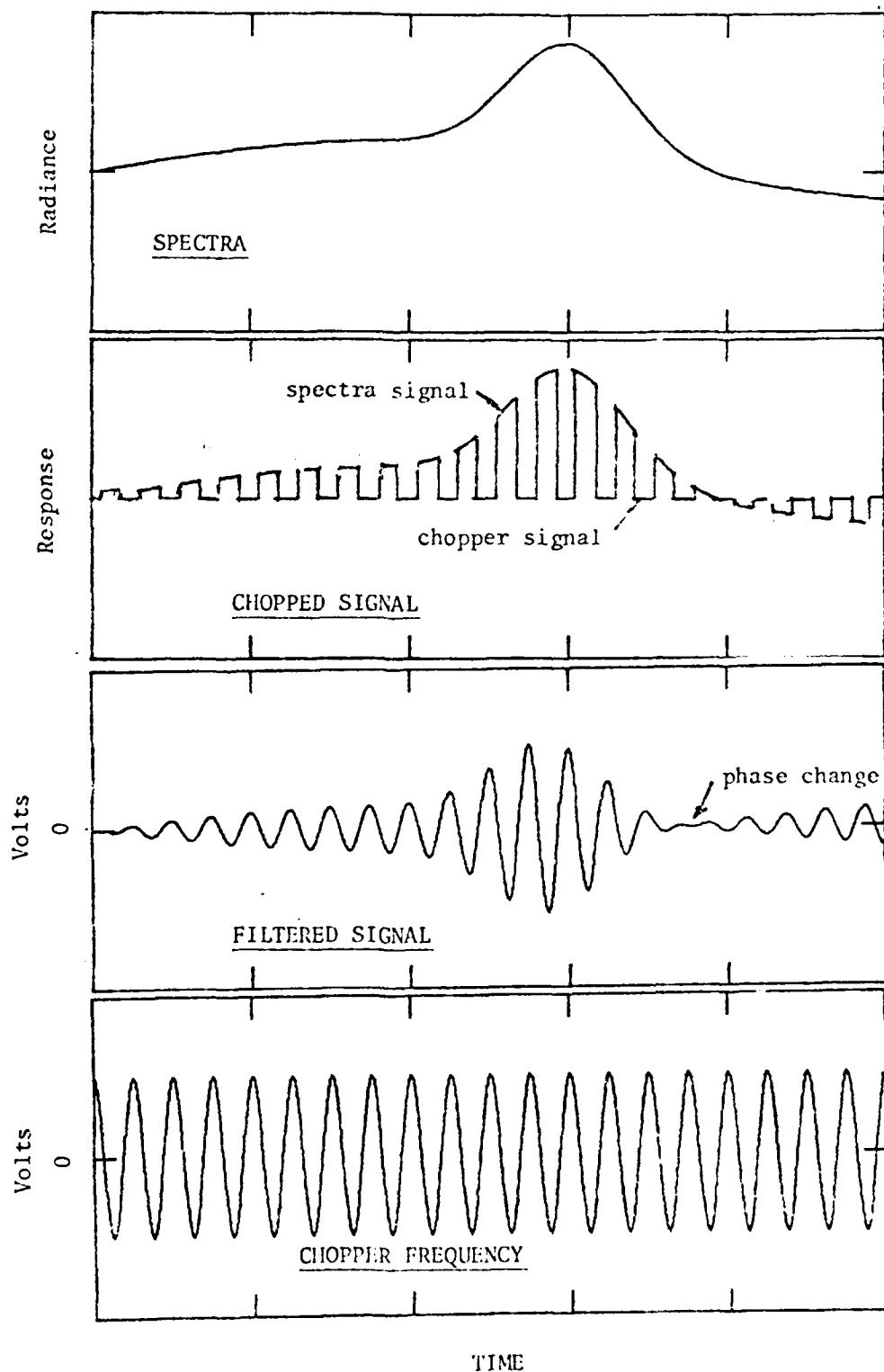


Figure 3.3-1. Principle of optically chopped CVF observation showing phase reversal when source radiance is less than copper radiance.

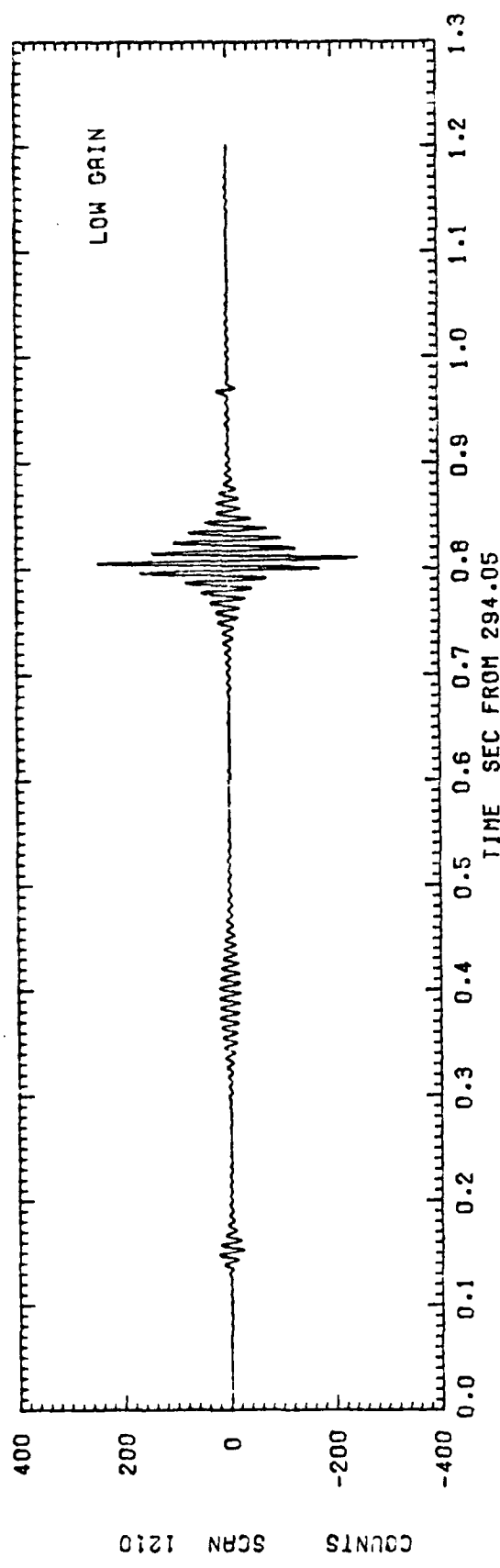


Figure 3, 3-1a. A portion of telemetered data from the EXCIDE HS-3B-1 CVF spectrometer.

CHOPPER FIT

B= 194.0954

C= -144.2404

FREQ 106.555

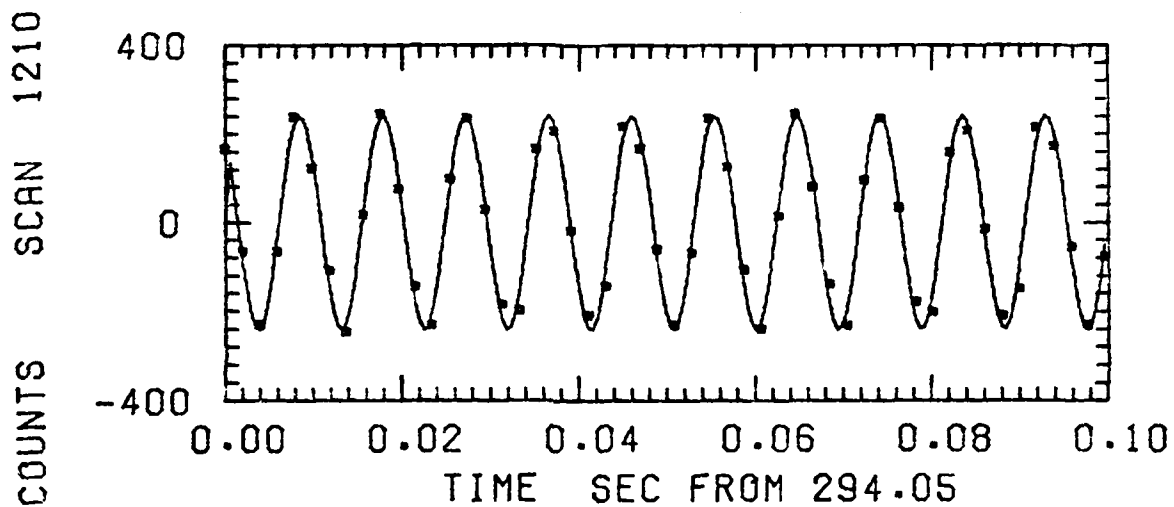


Figure 3.3-2. Example of least squares fit (sinusoid) to chopper signal (solid squares) for spectral scan 1210. Also shown are frequency and constants determined as a result of the best fit.

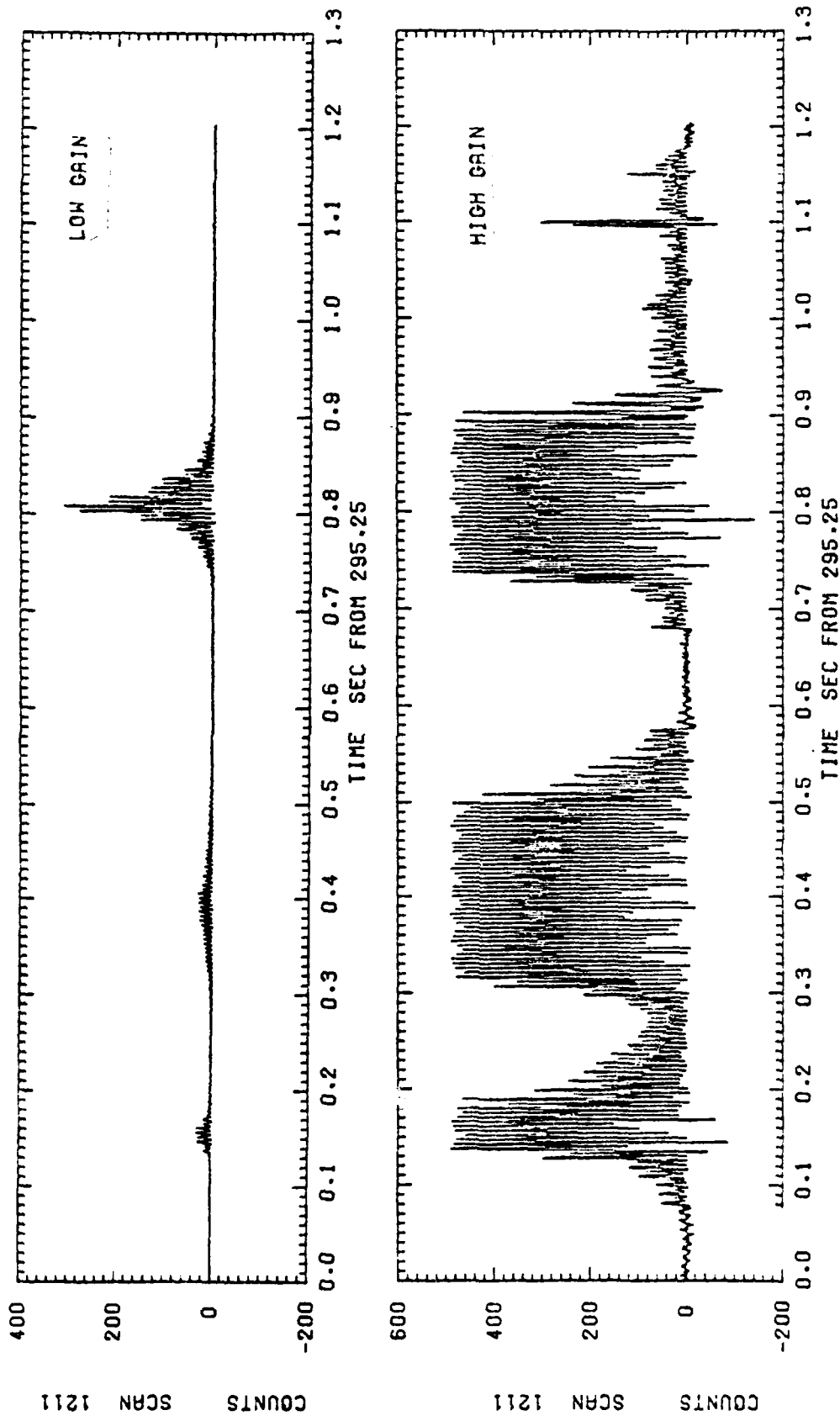


Figure 3, 3-3

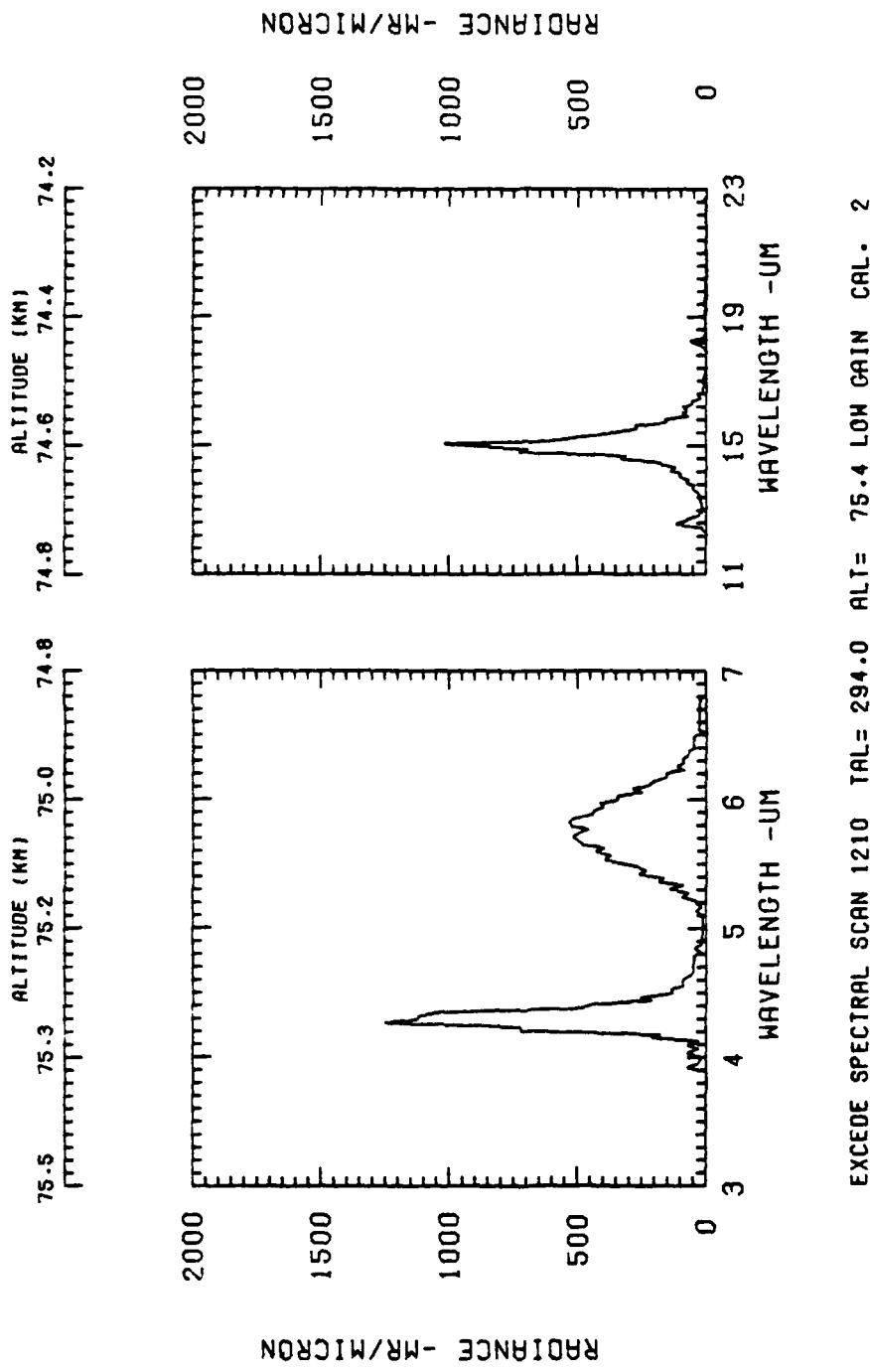


Figure 3.3-4 Example of unfiltered spectrum obtained with the EXCDE chopped CVF.

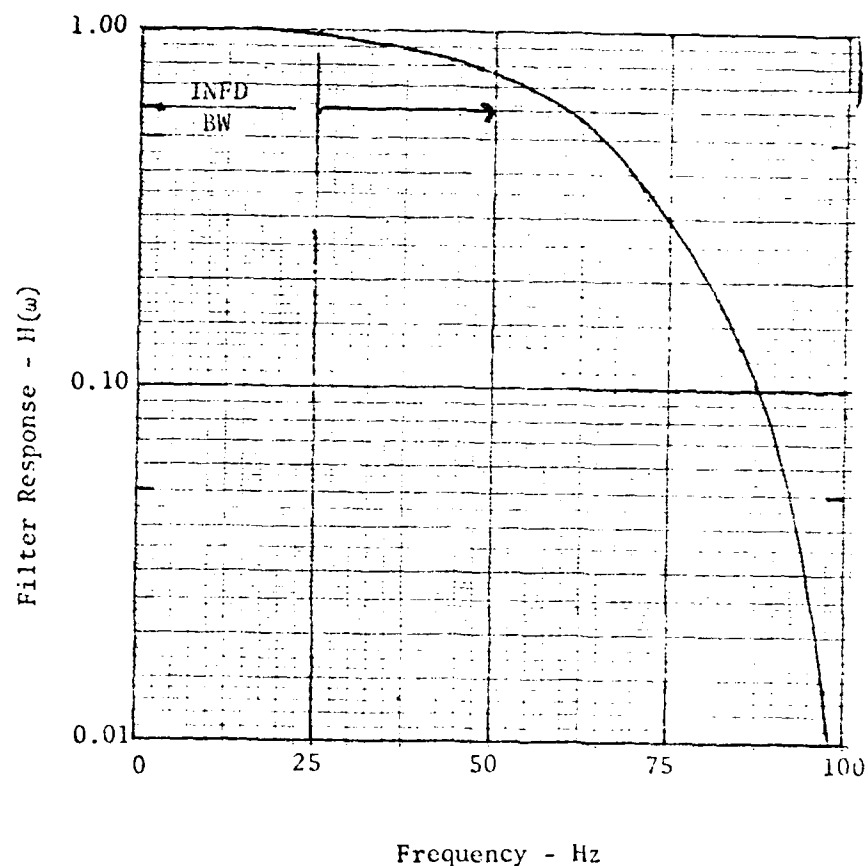


Figure 3.3-5. Frequency response of smoothing filter used after decimating data base to a sampling frequency of 205 Hz EXCEDE information bandwidth is 50 Hz.

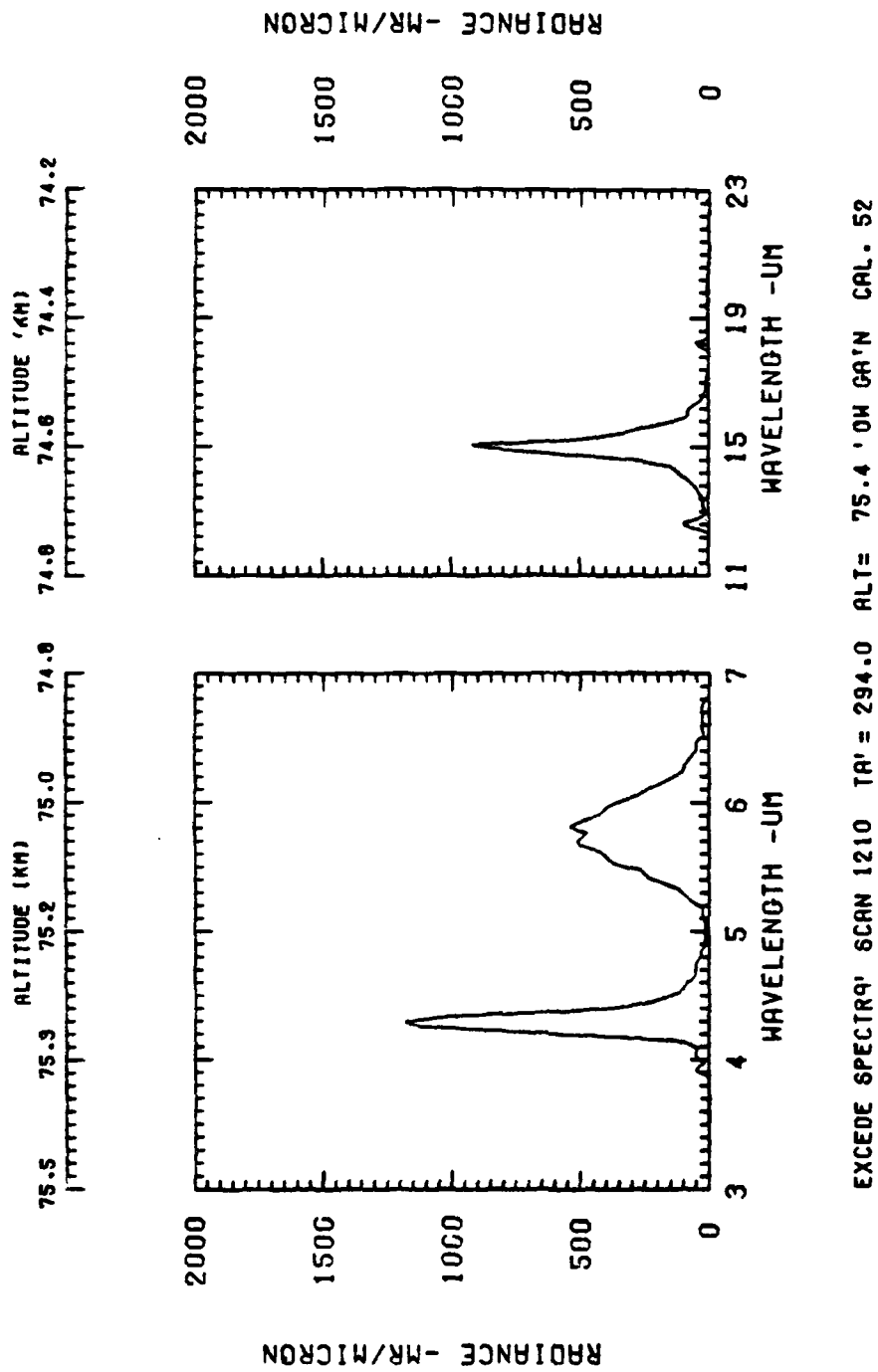


Figure 3.3-6 Example of smoothed spectrum using a 5 point smoothing filter.

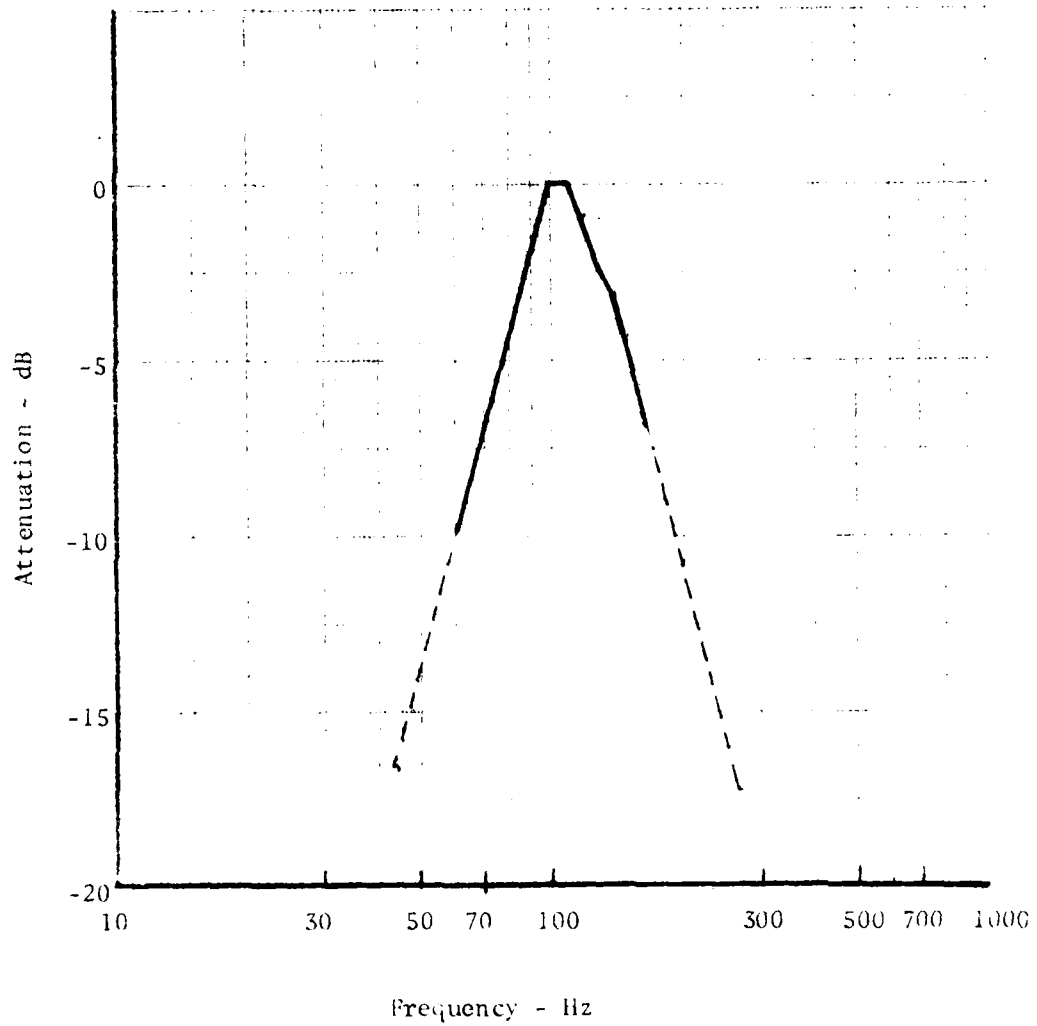


Figure 3.4-1 Characteristics of the electronic filter for CVF HS-3B-1

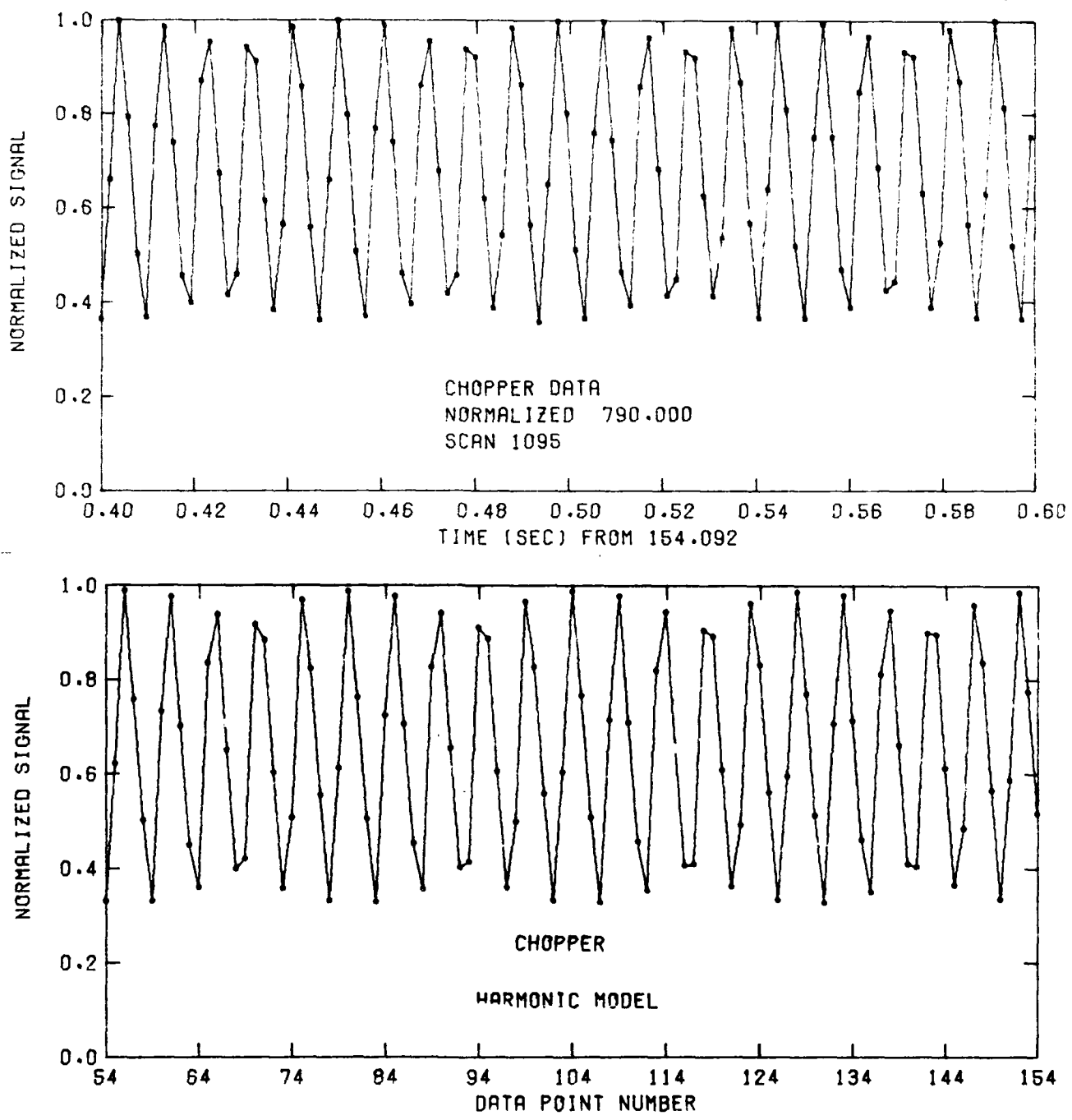


Figure 3.4-2. Comparison of chopper data with model of the form
 $S = K_1 + K_2 [\cos \omega_c t + \sin(2\omega_c t - \delta)]$ where K_1 and K_2 are scale factors, and $\omega_c t = 2\pi f_c(n-1)f_S$, and $\delta = 9^\circ$.

APPENDIX A

Spectral Scan Start Times and
Other Data for NS-6-4 CVF

Data in this appendix is defined as follows:

| <u>Column</u> | <u>Title</u> | <u>Definition</u> |
|---------------|-----------------|--|
| 1 | Scan Number | Number assigned to the spectral scan |
| 2 | Length | Number of data points in spectral scan |
| 3 | Length sec | Duration of the spectral scan in seconds |
| 4 | Time A-L | Time after launch in seconds of scan start |
| 5 | Altitude | Payload altitude corresponding to T.A.L. |
| 6 | Time U.T. | T.A.L. in U.T. seconds |
| 7 | Clock Time U.T. | T.A.L. in clock form |

FIGURE 11 NS-E SURFACE CLOUD STAIRS

| SUPERFICIAL | TYPE | DEPTH | LEADERS | STAIRS |
|-------------|------|-------|---------|--------|
| 1000 | 1 | 0 | 0 | 0 |
| 1000 | 1 | 100 | 0 | 0 |
| 1000 | 1 | 200 | 0 | 0 |
| 1000 | 1 | 300 | 0 | 0 |
| 1000 | 1 | 400 | 0 | 0 |
| 1000 | 1 | 500 | 0 | 0 |
| 1000 | 1 | 600 | 0 | 0 |
| 1000 | 1 | 700 | 0 | 0 |
| 1000 | 1 | 800 | 0 | 0 |
| 1000 | 1 | 900 | 0 | 0 |
| 1000 | 1 | 1000 | 0 | 0 |
| 1000 | 1 | 1100 | 0 | 0 |
| 1000 | 1 | 1200 | 0 | 0 |
| 1000 | 1 | 1300 | 0 | 0 |
| 1000 | 1 | 1400 | 0 | 0 |
| 1000 | 1 | 1500 | 0 | 0 |
| 1000 | 1 | 1600 | 0 | 0 |
| 1000 | 1 | 1700 | 0 | 0 |
| 1000 | 1 | 1800 | 0 | 0 |
| 1000 | 1 | 1900 | 0 | 0 |
| 1000 | 1 | 2000 | 0 | 0 |
| 1000 | 1 | 2100 | 0 | 0 |
| 1000 | 1 | 2200 | 0 | 0 |
| 1000 | 1 | 2300 | 0 | 0 |
| 1000 | 1 | 2400 | 0 | 0 |
| 1000 | 1 | 2500 | 0 | 0 |
| 1000 | 1 | 2600 | 0 | 0 |
| 1000 | 1 | 2700 | 0 | 0 |
| 1000 | 1 | 2800 | 0 | 0 |
| 1000 | 1 | 2900 | 0 | 0 |
| 1000 | 1 | 3000 | 0 | 0 |
| 1000 | 1 | 3100 | 0 | 0 |
| 1000 | 1 | 3200 | 0 | 0 |
| 1000 | 1 | 3300 | 0 | 0 |
| 1000 | 1 | 3400 | 0 | 0 |
| 1000 | 1 | 3500 | 0 | 0 |
| 1000 | 1 | 3600 | 0 | 0 |
| 1000 | 1 | 3700 | 0 | 0 |
| 1000 | 1 | 3800 | 0 | 0 |
| 1000 | 1 | 3900 | 0 | 0 |
| 1000 | 1 | 4000 | 0 | 0 |
| 1000 | 1 | 4100 | 0 | 0 |
| 1000 | 1 | 4200 | 0 | 0 |
| 1000 | 1 | 4300 | 0 | 0 |
| 1000 | 1 | 4400 | 0 | 0 |
| 1000 | 1 | 4500 | 0 | 0 |
| 1000 | 1 | 4600 | 0 | 0 |
| 1000 | 1 | 4700 | 0 | 0 |
| 1000 | 1 | 4800 | 0 | 0 |
| 1000 | 1 | 4900 | 0 | 0 |
| 1000 | 1 | 5000 | 0 | 0 |
| 1000 | 1 | 5100 | 0 | 0 |
| 1000 | 1 | 5200 | 0 | 0 |
| 1000 | 1 | 5300 | 0 | 0 |
| 1000 | 1 | 5400 | 0 | 0 |
| 1000 | 1 | 5500 | 0 | 0 |
| 1000 | 1 | 5600 | 0 | 0 |
| 1000 | 1 | 5700 | 0 | 0 |
| 1000 | 1 | 5800 | 0 | 0 |
| 1000 | 1 | 5900 | 0 | 0 |
| 1000 | 1 | 6000 | 0 | 0 |
| 1000 | 1 | 6100 | 0 | 0 |
| 1000 | 1 | 6200 | 0 | 0 |
| 1000 | 1 | 6300 | 0 | 0 |
| 1000 | 1 | 6400 | 0 | 0 |
| 1000 | 1 | 6500 | 0 | 0 |
| 1000 | 1 | 6600 | 0 | 0 |
| 1000 | 1 | 6700 | 0 | 0 |
| 1000 | 1 | 6800 | 0 | 0 |
| 1000 | 1 | 6900 | 0 | 0 |
| 1000 | 1 | 7000 | 0 | 0 |
| 1000 | 1 | 7100 | 0 | 0 |
| 1000 | 1 | 7200 | 0 | 0 |
| 1000 | 1 | 7300 | 0 | 0 |
| 1000 | 1 | 7400 | 0 | 0 |
| 1000 | 1 | 7500 | 0 | 0 |
| 1000 | 1 | 7600 | 0 | 0 |
| 1000 | 1 | 7700 | 0 | 0 |
| 1000 | 1 | 7800 | 0 | 0 |
| 1000 | 1 | 7900 | 0 | 0 |
| 1000 | 1 | 8000 | 0 | 0 |
| 1000 | 1 | 8100 | 0 | 0 |
| 1000 | 1 | 8200 | 0 | 0 |
| 1000 | 1 | 8300 | 0 | 0 |
| 1000 | 1 | 8400 | 0 | 0 |
| 1000 | 1 | 8500 | 0 | 0 |
| 1000 | 1 | 8600 | 0 | 0 |
| 1000 | 1 | 8700 | 0 | 0 |
| 1000 | 1 | 8800 | 0 | 0 |
| 1000 | 1 | 8900 | 0 | 0 |
| 1000 | 1 | 9000 | 0 | 0 |
| 1000 | 1 | 9100 | 0 | 0 |
| 1000 | 1 | 9200 | 0 | 0 |
| 1000 | 1 | 9300 | 0 | 0 |
| 1000 | 1 | 9400 | 0 | 0 |
| 1000 | 1 | 9500 | 0 | 0 |
| 1000 | 1 | 9600 | 0 | 0 |
| 1000 | 1 | 9700 | 0 | 0 |
| 1000 | 1 | 9800 | 0 | 0 |
| 1000 | 1 | 9900 | 0 | 0 |
| 1000 | 1 | 10000 | 0 | 0 |

6/27/61 13.77.61.

PAGE

1

EXCELSIOR 11

四庫全書

PAGE ?

EXCERPT II USES OF SUPPORTIVE SUPER STAFFS

〔五〕 二二〇 一三〇 三七〇 六一〇

Page 3

EXCISE T1 15-4 SPECIFIC SURFP CHARTS

00/02/90 13-37-41.

PAGE 5

13-37-41.

SECTIONAL SURFP CHARTS

LATITUDE

LONGITUD

0000

0000

0000

0000

0000

0000

0000

0000

0000

0000

0000

0000

0000

0000

0000

0000

0000

0000

0000

0000

0000

0000

0000

0000

0000

0000

0000

0000

0000

0000

0000

0000

0000

0000

0000

0000

0000

0000

0000

0000

0000

0000

0000

0000

0000

0000

0000

0000

0000

0000

0000

0000

0000

0000

0000

0000

0000

0000

0000

0000

0000

0000

0000

0000

0000

0000

0000

0000

0000

0000

0000

0000

0000

0000

0000

0000

0000

0000

0000

0000

0000

0000

0000

0000

0000

0000

0000

0000

0000

0000

0000

0000

0000

0000

0000

0000

0000

0000

0000

0000

0000

0000

0000

0000

0000

0000

0000

0000

0000

0000

0000

0000

0000

0000

0000

0000

0000

0000

0000

0000

0000

0000

0000

0000

0000

0000

0000

0000

0000

0000

0000

0000

0000

0000

0000

0000

0000

0000

0000

0000

0000

0000

0000

0000

0000

0000

0000

0000

0000

0000

0000

0000

0000

0000

0000

0000

0000

0000

0000

0000

0000

0000

0000

0000

0000

0000

0000

0000

0000

0000

0000

0000

0000

0000

0000

0000

0000

0000

0000

0000

0000

0000

0000

0000

0000

0000

0000

0000

0000

0000

0000

0000

0000

0000

0000

0000

0000

0000

0000

0000

0000

0000

0000

0000

0000

0000

0000

0000

0000

0000

0000

0000

0000

0000

0000

0000

0000

0000

0000

0000

0000

0000

0000

0000

0000

0000

0000

0000

0000

0000

0000

0000

0000

0000

0000

0000

0000

0000

0000

0000

0000

0000

0000

0000

0000

0000

0000

0000

0000

0000

0000

0000

0000

0000

0000

0000

0000

0000

0000

0000

0000

0000

0000

0000

0000

0000

0000

0000

0000

0000

0000

0000

0000

0000

0000

0000

0000

0000

0000

0000

0000

0000

0000

EXCELSIOR: THE JOURNAL OF THE UNIVERSITY OF TORONTO

INTERFACIAL SURFACE ACTANTS

۱۷

1

1

۲۷۶

318013 J3-R3 1431393 9-551 11 3U3KA

THE JOURNAL OF CLIMATE

卷之三

卷之六

一

2

2

1

1

2

1. **What is the primary purpose of the study?**
The primary purpose of the study is to evaluate the effectiveness of a new treatment for hypertension compared to a standard treatment. The study will also assess the safety and side effects of the new treatment.

Impact of the new policy on the number of patients with a primary diagnosis of stroke

INFECTED -

EXCELSIOR 11 NOVEMBER 1911

CE/C/AC 92.27.41.

6

56

EXCERPT II NS-6 SPECIAL OPERATIONS

| SPECIAL OPS | LENGTH | ROUTE SER | TIME A/L | ALTITUDE | TIME U/T | UT CLOCK TIME |
|-------------|--------|-----------|----------|----------|-----------|---------------|
| 565 | 696 | 565.9610 | 565.9610 | 10.2415 | 2114.8010 | 51521 15.4010 |
| 566 | 696 | 566.2693 | 566.2693 | 10.2205 | 2114.2693 | 51521 26.2840 |
| 567 | 696 | 567.7627 | 567.7627 | 10.2217 | 2114.7627 | 51521 26.7470 |
| 568 | 696 | 568.7627 | 568.7627 | 10.2217 | 2114.7627 | 51521 26.7470 |
| 569 | 696 | 569.7627 | 569.7627 | 10.2217 | 2114.7627 | 51521 26.7470 |
| 570 | 696 | 570.7627 | 570.7627 | 10.2217 | 2114.7627 | 51521 26.7470 |

PAGE 9

PAGE

9

APPENDIX B

Spectral Scan Start Times and Other Data for HS-3B-1 CVF

Data in this appendix is defined as follows:

| <u>Column</u> | <u>Title</u> | <u>Definition</u> |
|---------------|-----------------|--|
| 1 | Scan Number | Number assigned to the spectral scan |
| 2 | Length | Number of data points in spectral scan |
| 3 | Length sec | Duration of the spectral scan in seconds |
| 4 | Time A-L | Time after launch in seconds of scan start |
| 5 | Altitude | Payload altitude corresponding to T.A.L. |
| 6 | Time U.T. | T.A.L. in U.T. seconds |
| 7 | Clock Time U.T. | T.A.L. in clock form |

2

۲۰۷

17.0 37.0 17.0

Digitized by srujanika@gmail.com

162

三

二二

APPENDIX C

Chopper Reference Phase Angle and Other Data for HS-3B-1 CVF

Constants A, b, and c are defined by Equation 3-12 of the text. The frequency (FREQ) is the best fit chopper frequency and THETA is the chopper phase angle θ_c relative to the scan start. MEAN HI and LO are the spectral mean counts for the high and low gain. NPTS is the number of points of the scan. CHISQ and INTER are the goodness of fit parameter and the number of iterations required to fit the data.

118,07,42.

7.000-10.000-15.000-20.000-25.000-30.000-35.000-40.000-45.000-50.000-55.000-60.000-65.000-70.000-75.000-80.000-85.000-90.000-95.000-100.000-105.000-110.000-115.000-120.000-125.000-130.000-135.000-140.000-145.000-150.000-155.000-160.000-165.000-170.000-175.000-180.000-185.000-190.000-195.000-200.000-205.000-210.000-215.000-220.000-225.000-230.000-235.000-240.000-245.000-250.000-255.000-260.000-265.000-270.000-275.000-280.000-285.000-290.000-295.000-300.000-305.000-310.000-315.000-320.000-325.000-330.000-335.000-340.000-345.000-350.000-355.000-360.000-365.000-370.000-375.000-380.000-385.000-390.000-395.000-400.000-405.000-410.000-415.000-420.000-425.000-430.000-435.000-440.000-445.000-450.000-455.000-460.000-465.000-470.000-475.000-480.000-485.000-490.000-495.000-500.000-505.000-510.000-515.000-520.000-525.000-530.000-535.000-540.000-545.000-550.000-555.000-560.000-565.000-570.000-575.000-580.000-585.000-590.000-595.000-600.000-605.000-610.000-615.000-620.000-625.000-630.000-635.000-640.000-645.000-650.000-655.000-660.000-665.000-670.000-675.000-680.000-685.000-690.000-695.000-700.000-705.000-710.000-715.000-720.000-725.000-730.000-735.000-740.000-745.000-750.000-755.000-760.000-765.000-770.000-775.000-780.000-785.000-790.000-795.000-800.000-805.000-810.000-815.000-820.000-825.000-830.000-835.000-840.000-845.000-850.000-855.000-860.000-865.000-870.000-875.000-880.000-885.000-890.000-895.000-900.000-905.000-910.000-915.000-920.000-925.000-930.000-935.000-940.000-945.000-950.000-955.000-960.000-965.000-970.000-975.000-980.000-985.000-990.000-995.000-1000.000

የመተዳደሪያዎች በመሆኑ የሚከተሉት ስልክ ነው፡፡ የመተዳደሪያዎች በመሆኑ የሚከተሉት ስልክ ነው፡፡

କାହାର ପାଇଁ କାହାର ପାଇଁ କାହାର ପାଇଁ କାହାର ପାଇଁ କାହାର ପାଇଁ କାହାର ପାଇଁ କାହାର ପାଇଁ

APPENDIX D

Sample Data Base for CVF NS-6-4

This appendix contains selected spectral data developed from CVF NS-6-4 measurements. Scans and scan start times (time after launch in seconds) follow

| <u>Scan</u> | <u>T. A. L.</u> | <u>Scan</u> | <u>T. A. L.</u> |
|-------------|-----------------|-------------|-----------------|
| 116 | 96.1080 | 271 | 171.4120 |
| 119 | 97.5590 | 276 | 173.8840 |
| 121 | 98.5300 | 395 | 232.7120 |
| 126 | 100.9500 | 424 | 247.0380 |
| 136 | 105.7810 | 447 | 257.6770 |
| 139 | 107.2340 | 467 | 267.3540 |
| 153 | 114.0030 | 487 | 277.0310 |
| 156 | 115.4520 | -497 | 281.8680 |
| 159 | 116.9030 | 502 | 284.2890 |
| 171 | 122.7050 | 505 | 285.7450 |
| 174 | 124.1570 | 507 | 286.7110 |
| 181 | 127.5440 | 510 | 288.1610 |
| 223 | 147.8600 | -512 | 289.1290 |
| 228 | 150.2780 | 520 | 292.9960 |
| 231 | 151.7300 | -522 | 293.963 |

- indicates difficulty in detecting scan start time.

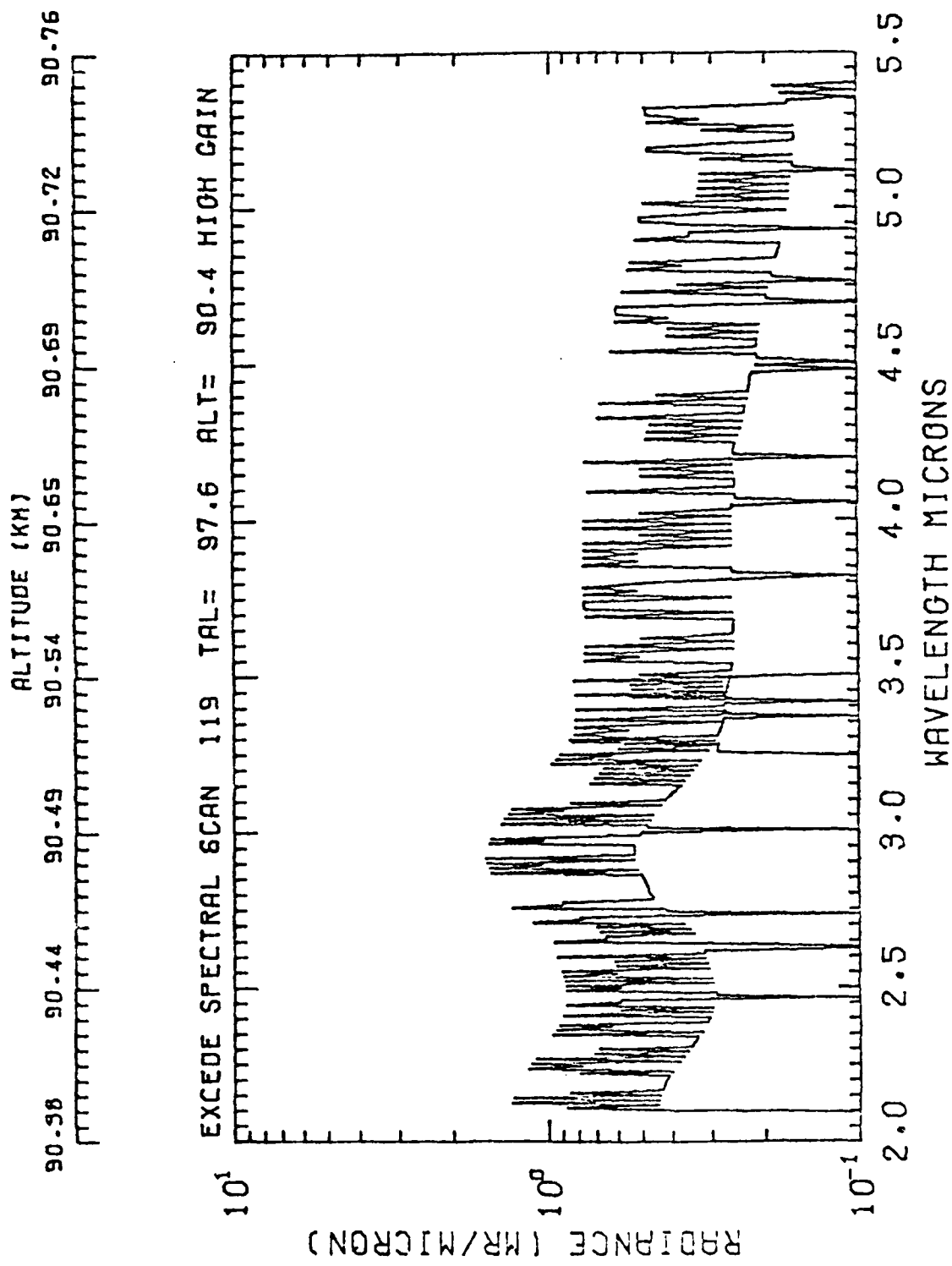
ALTITUDE (KM)
88.14 88.20 88.25 89.30 89.42 88.45 88.49 88.52

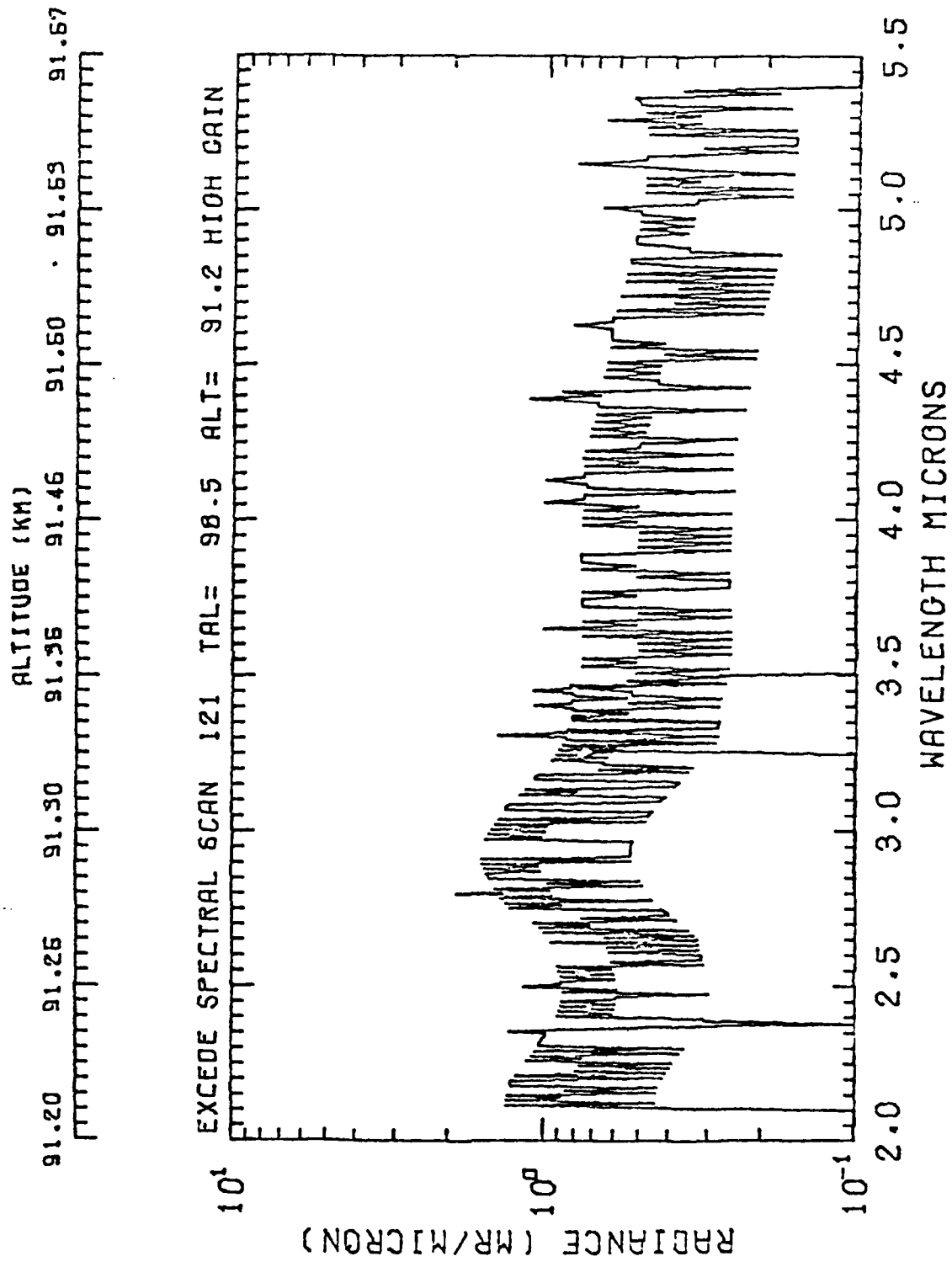
EXCITE SPECTRAL SCAN 116 TAL= 96.1 ALT= 89.1 HIGH GAIN
10¹

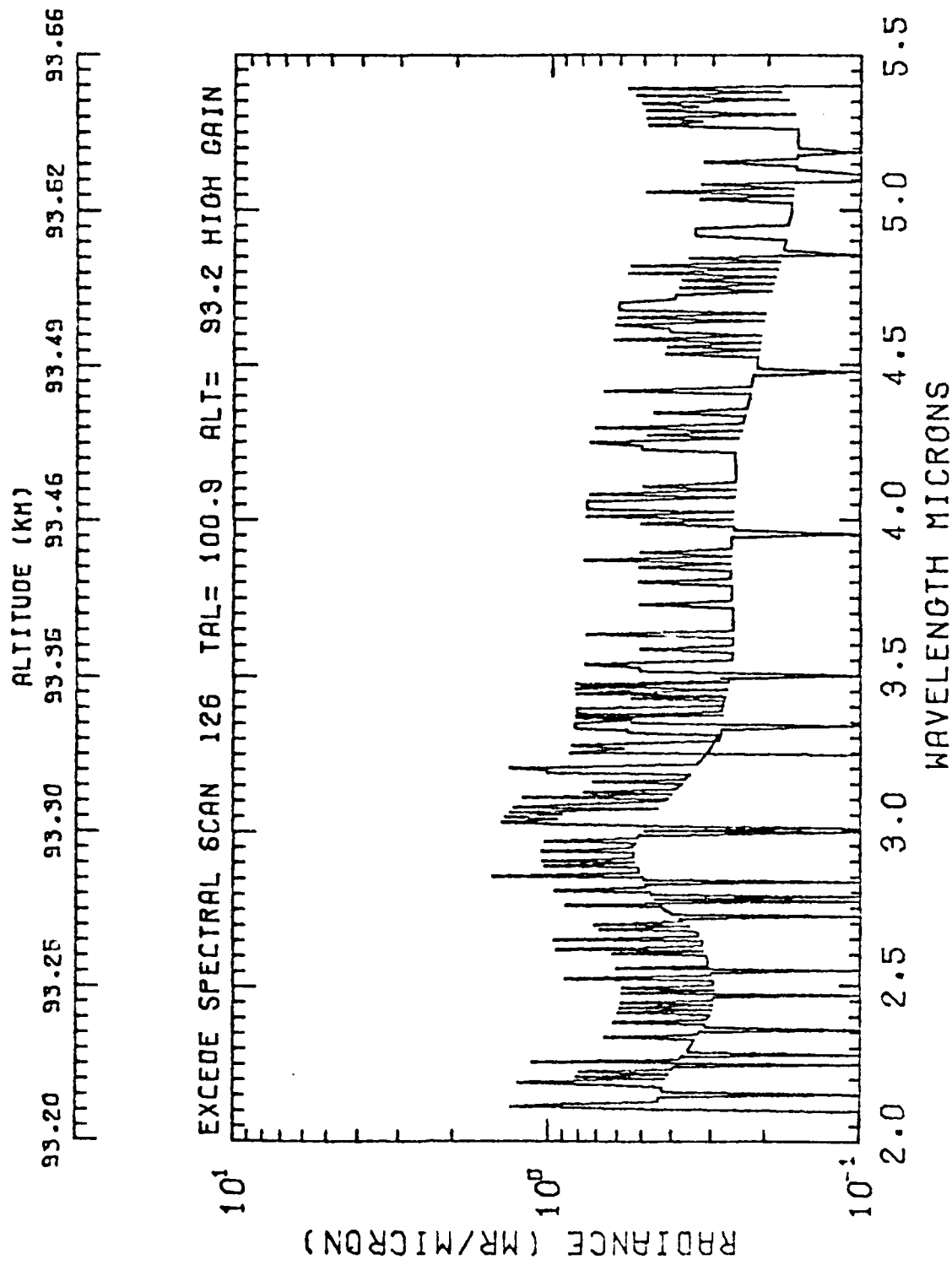
RADIANCE (MR/MICRON)

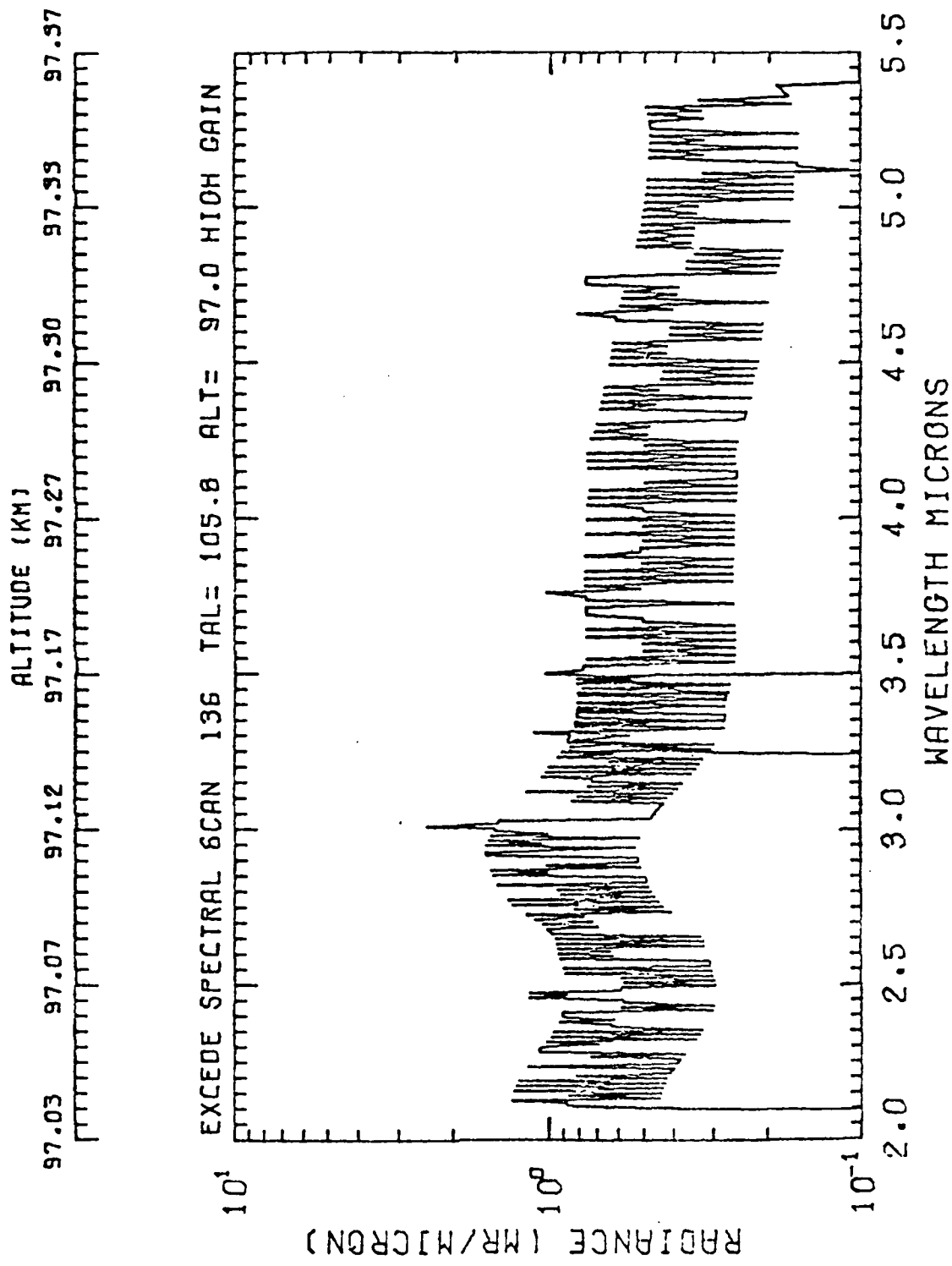
10⁰

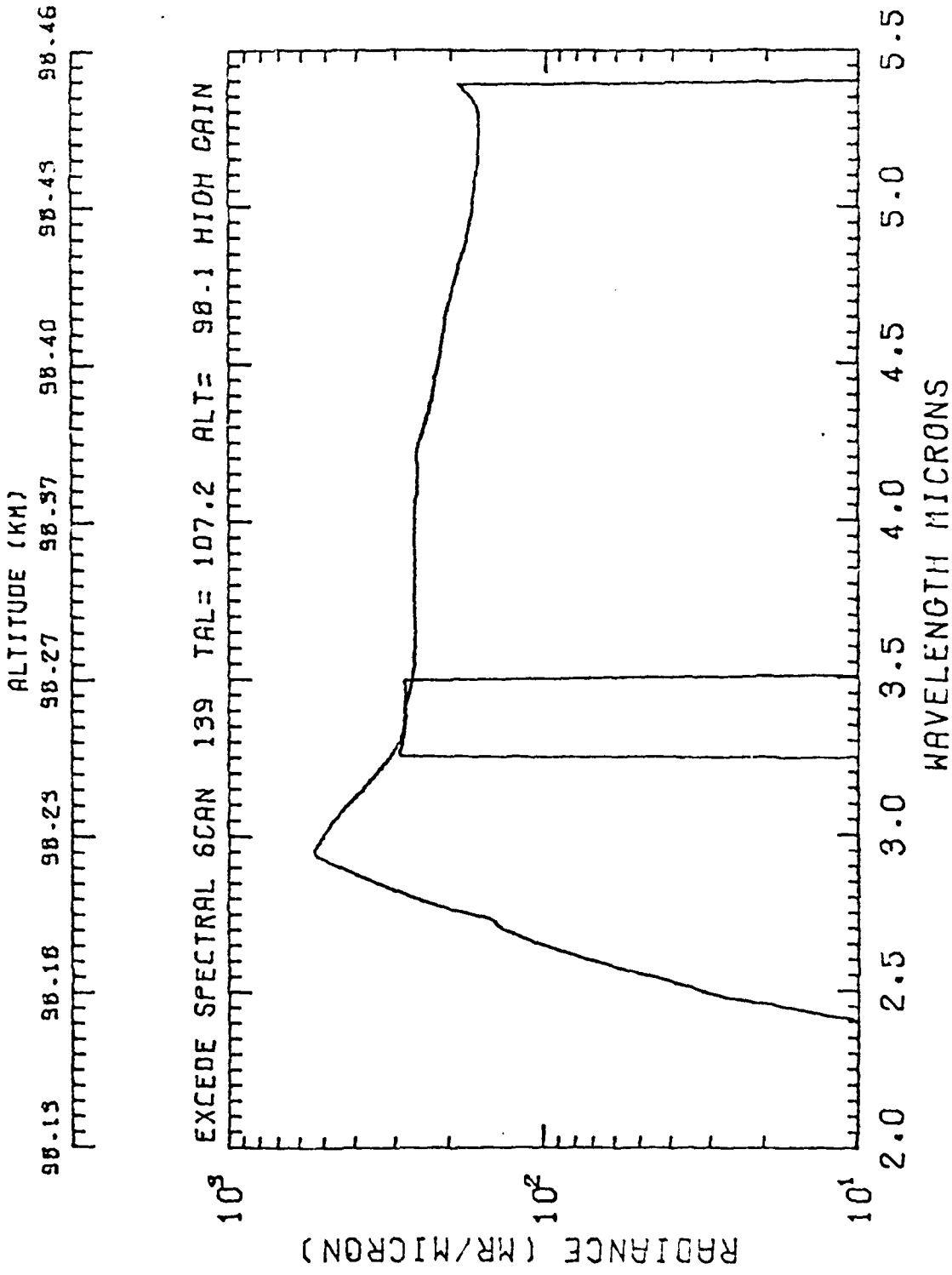
10⁻¹
2.0 2.5 3.0 3.5 4.0 4.5 5.0 5.5
WAVELENGTH MICRONS

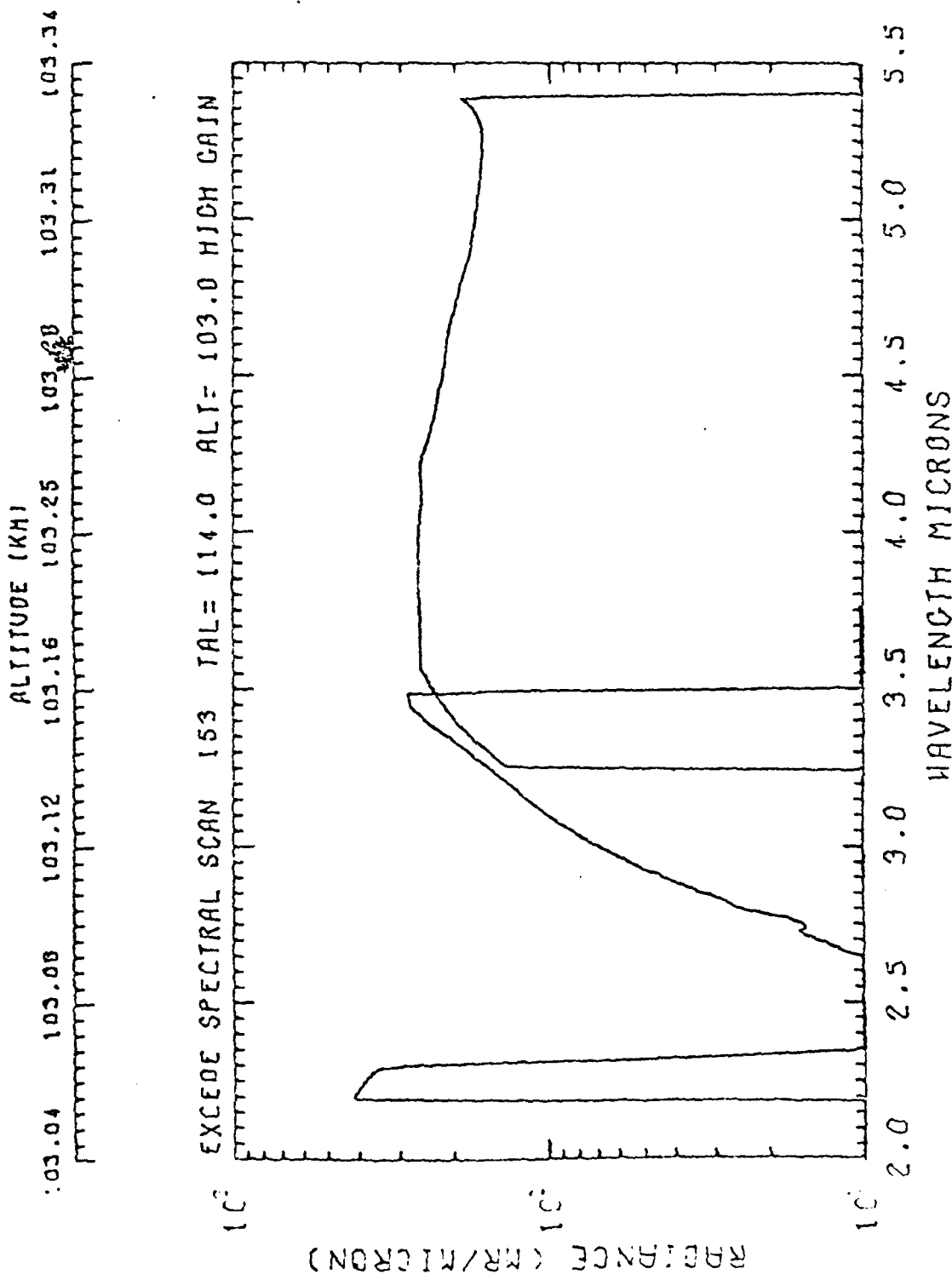


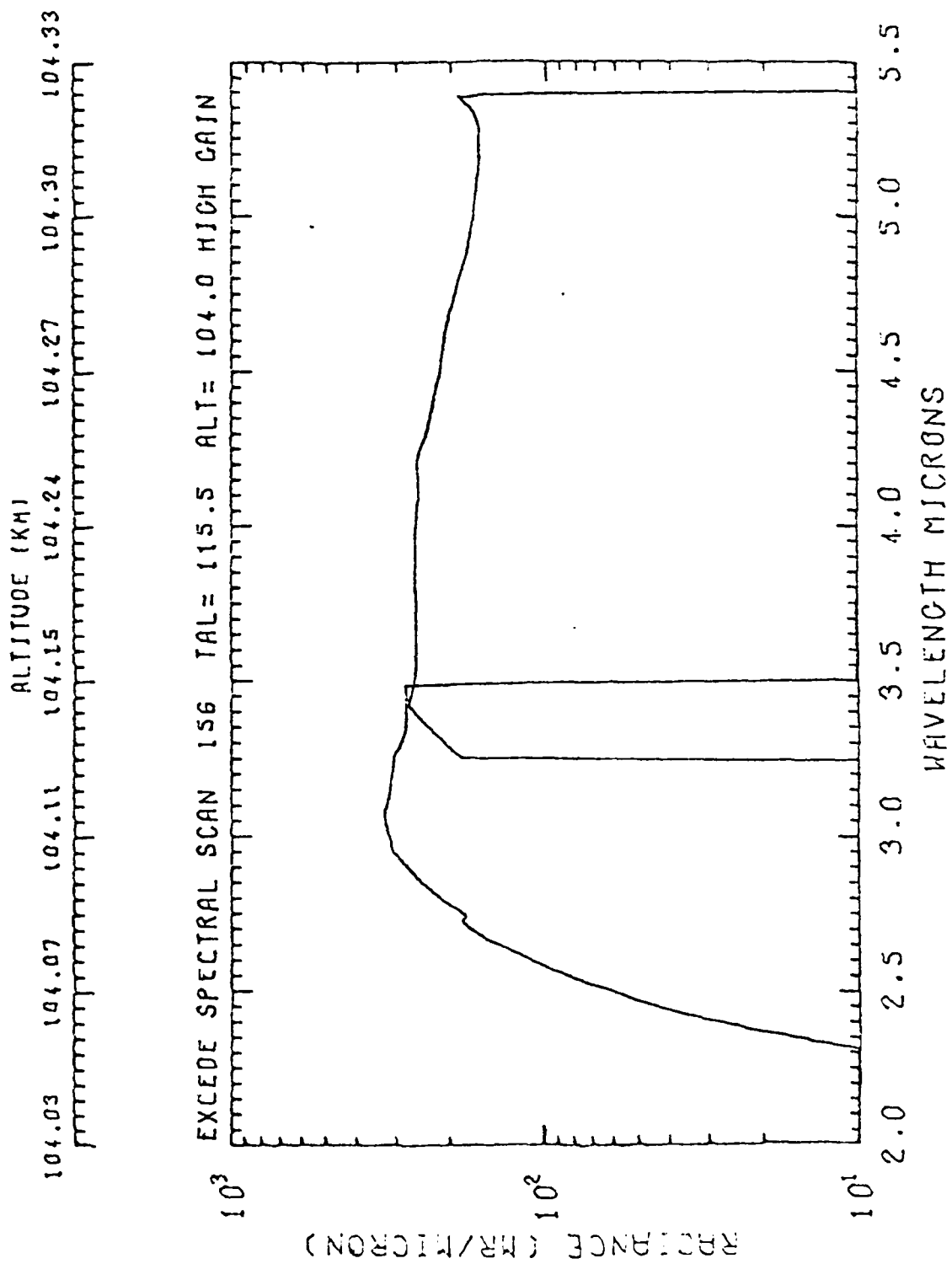




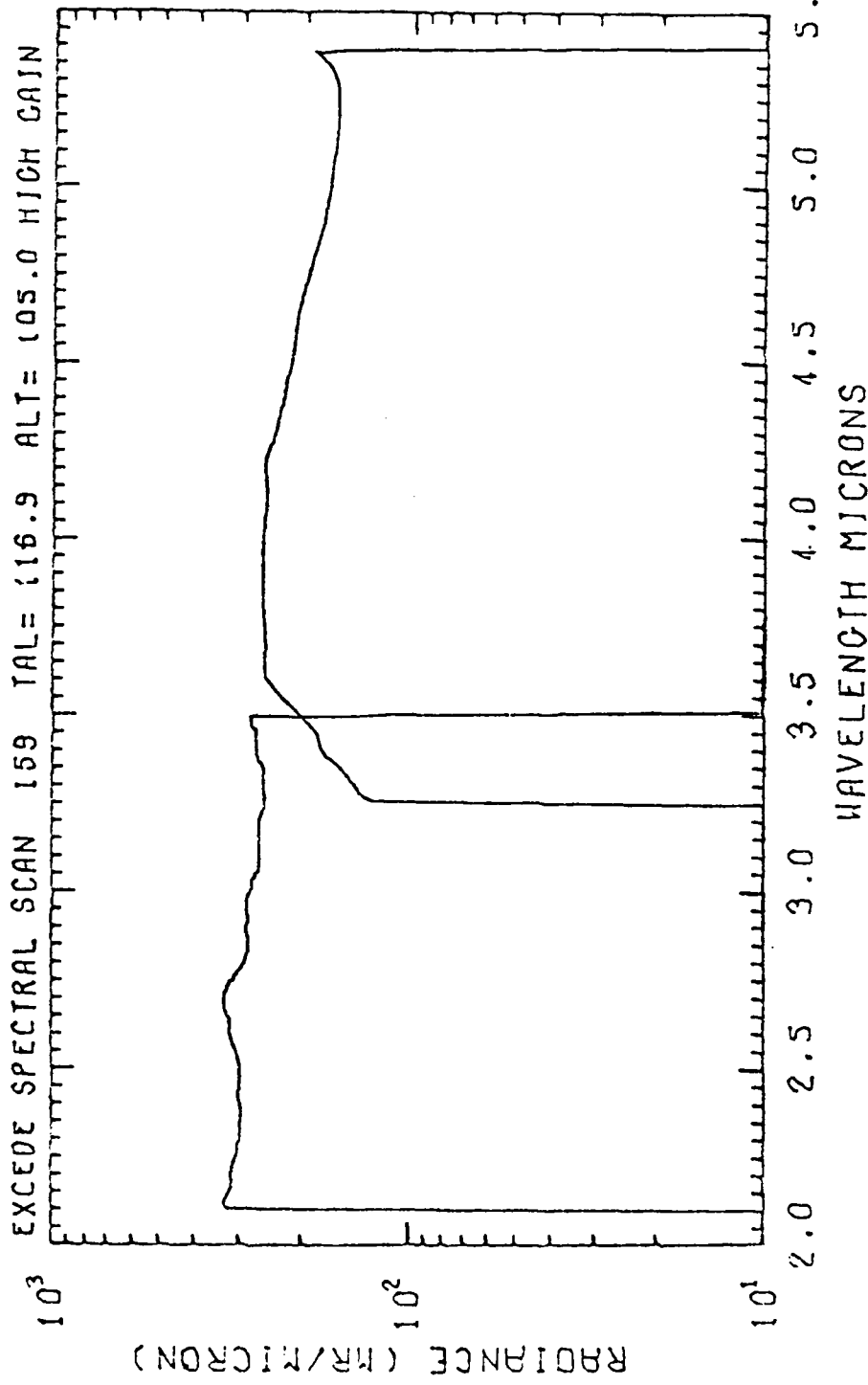


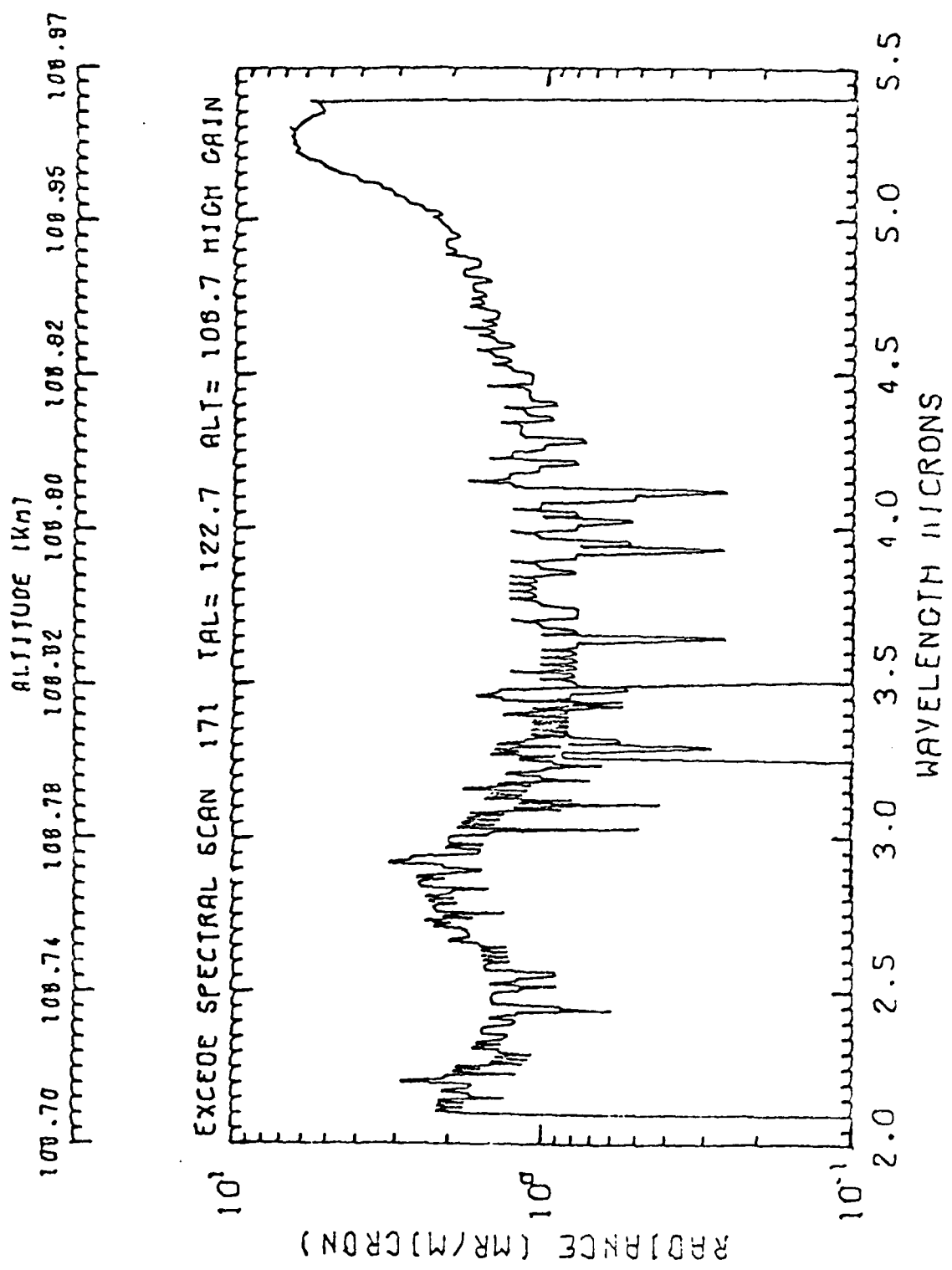


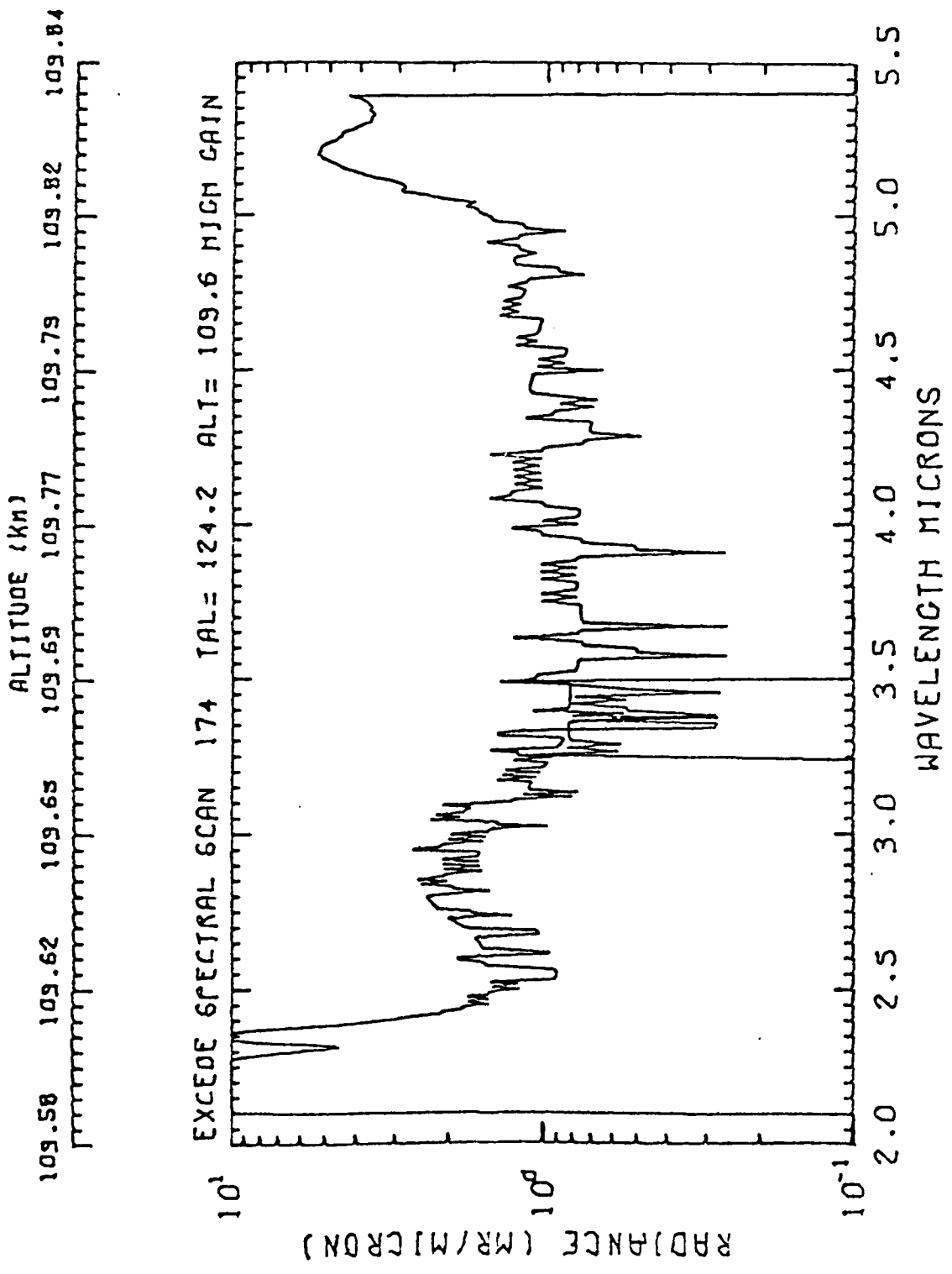


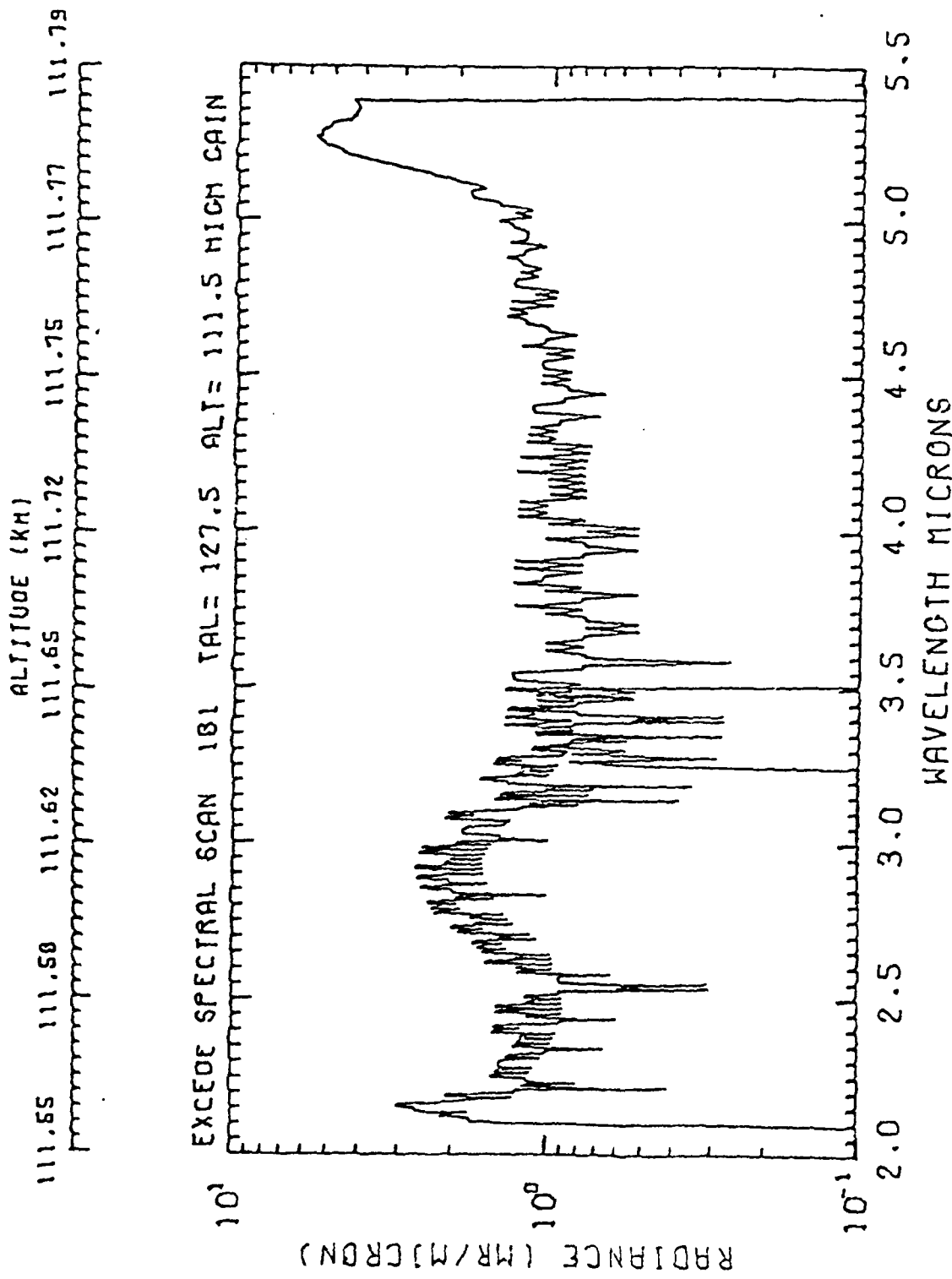


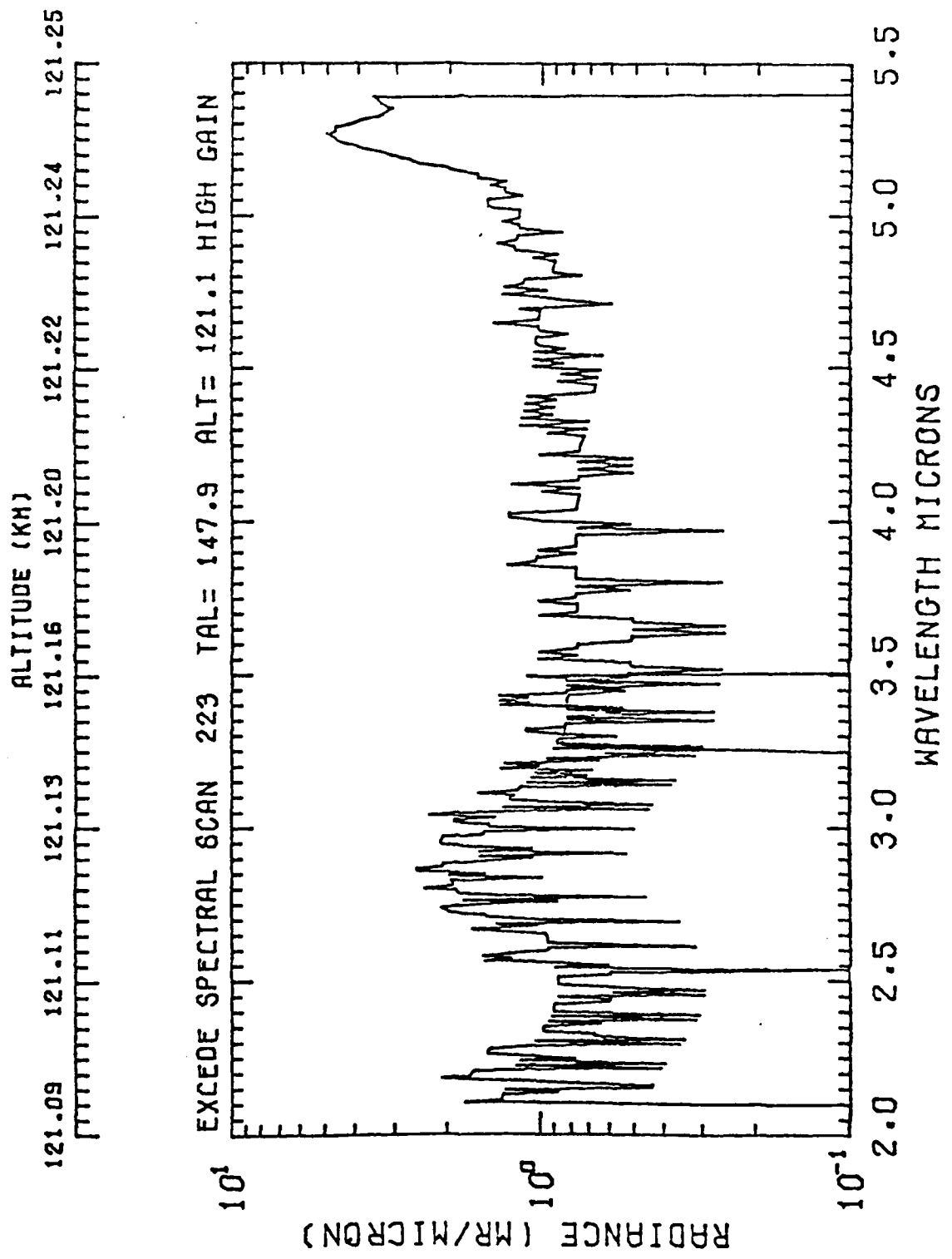
ALTITUDE (KM)
105.00 105.04 105.08 105.13 105.21 105.24 105.27 105.29

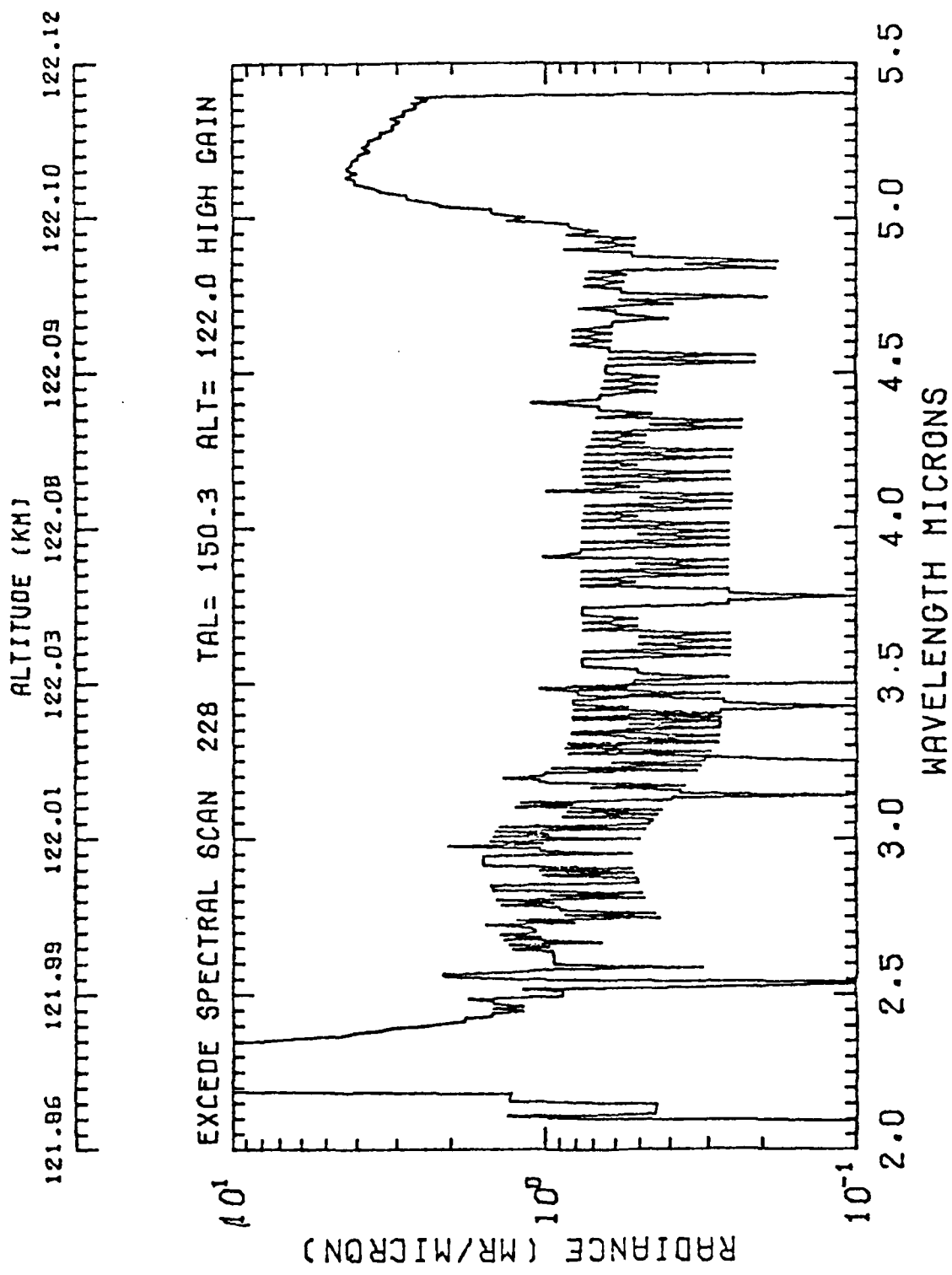




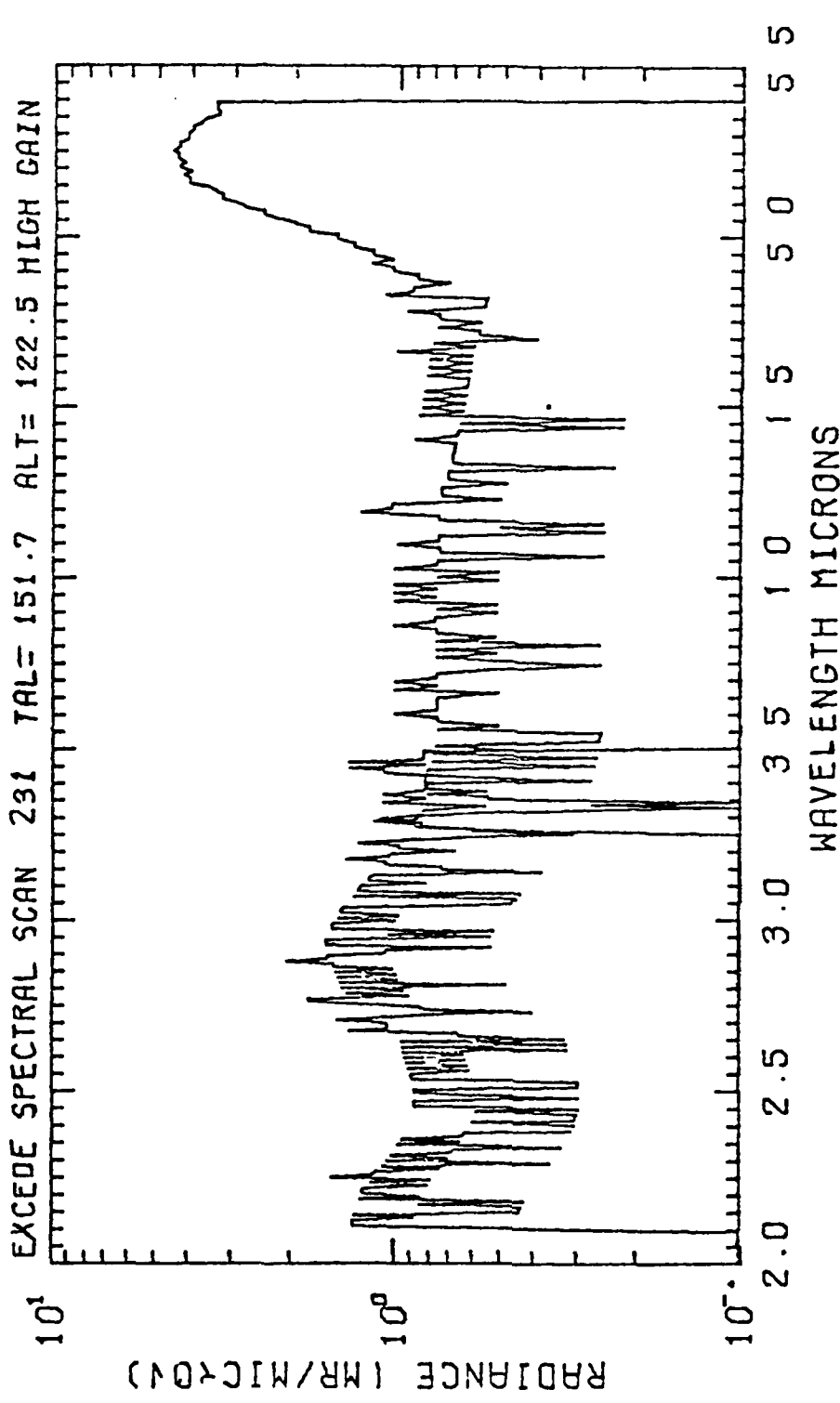


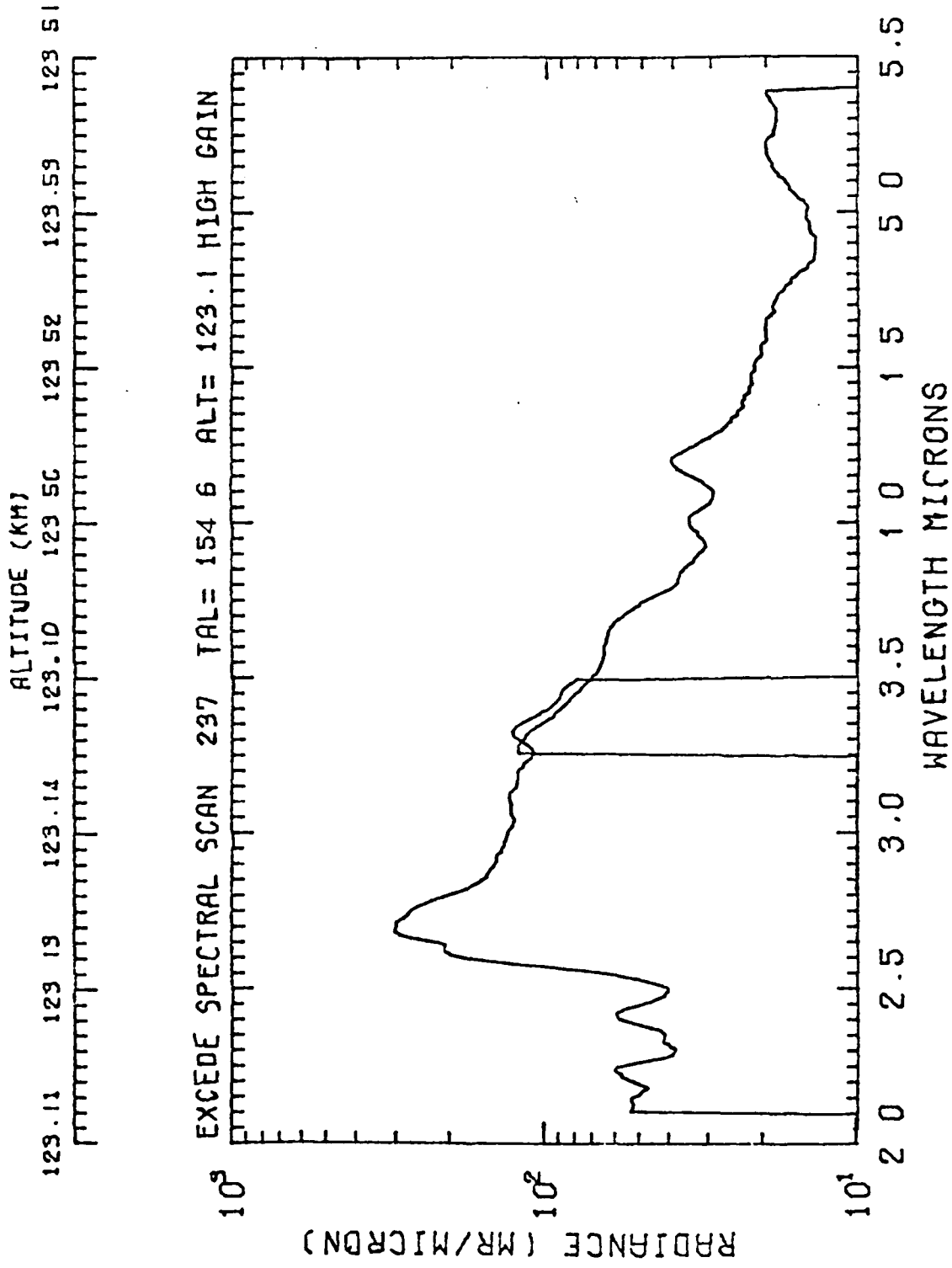


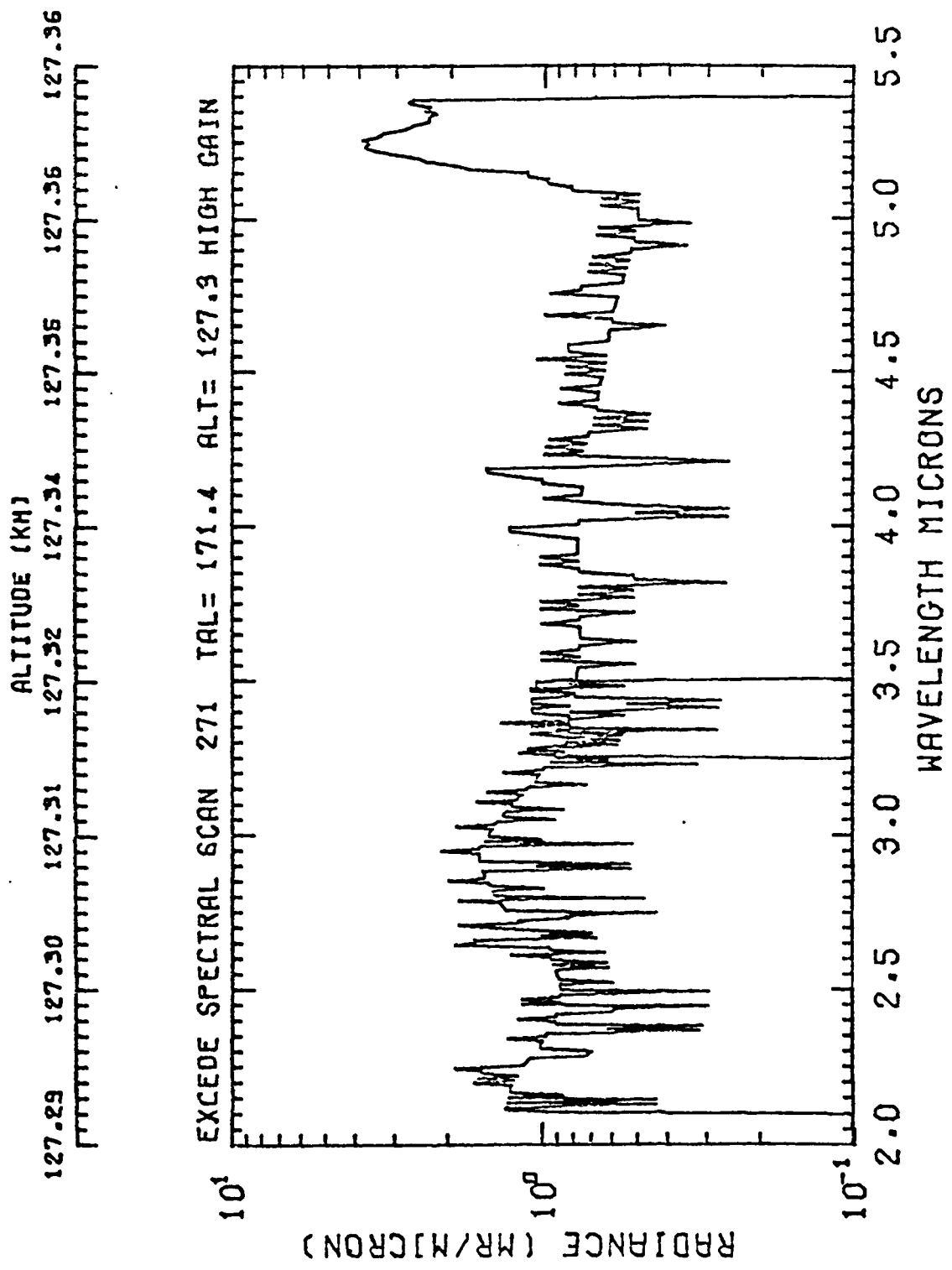


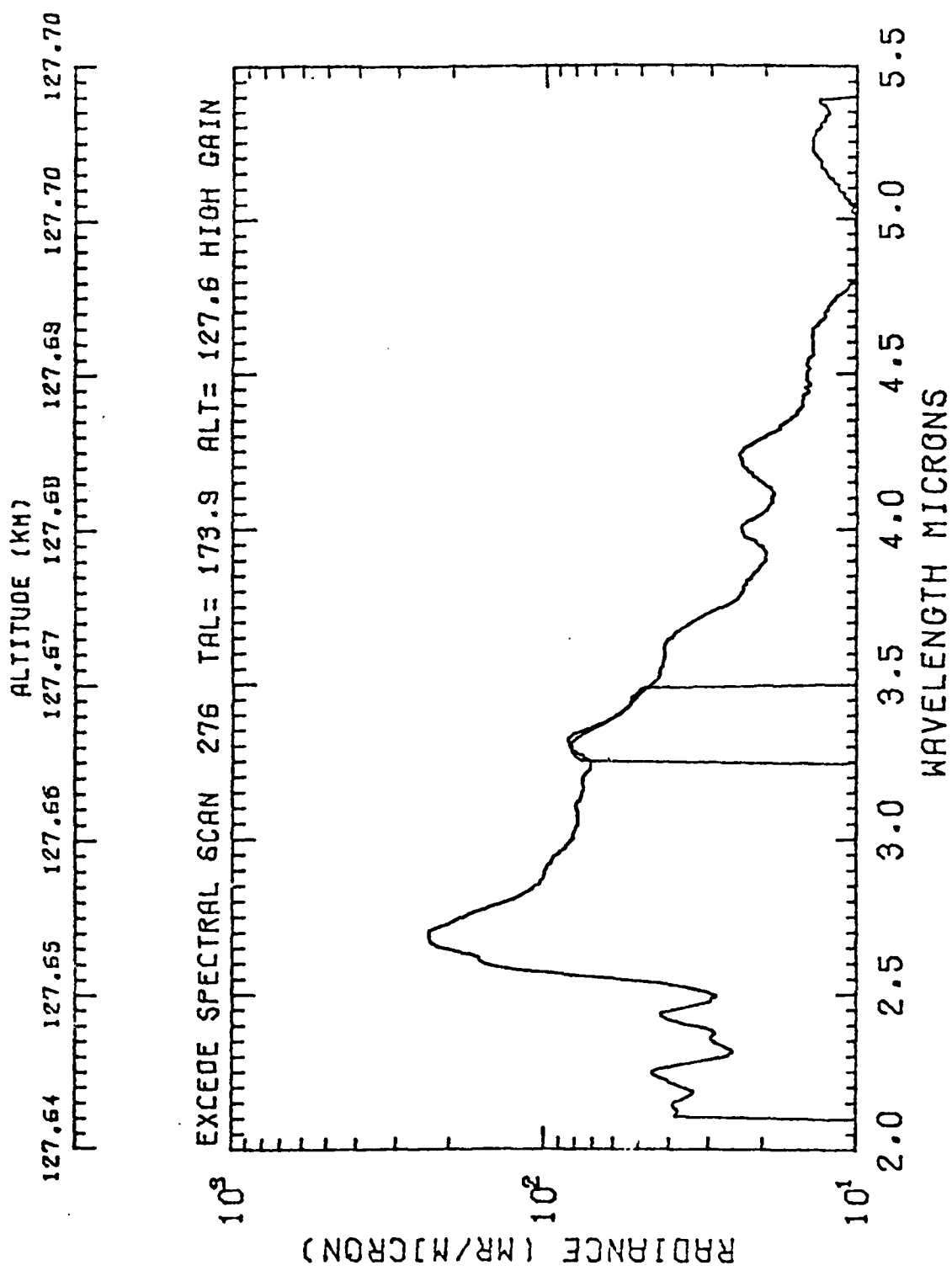


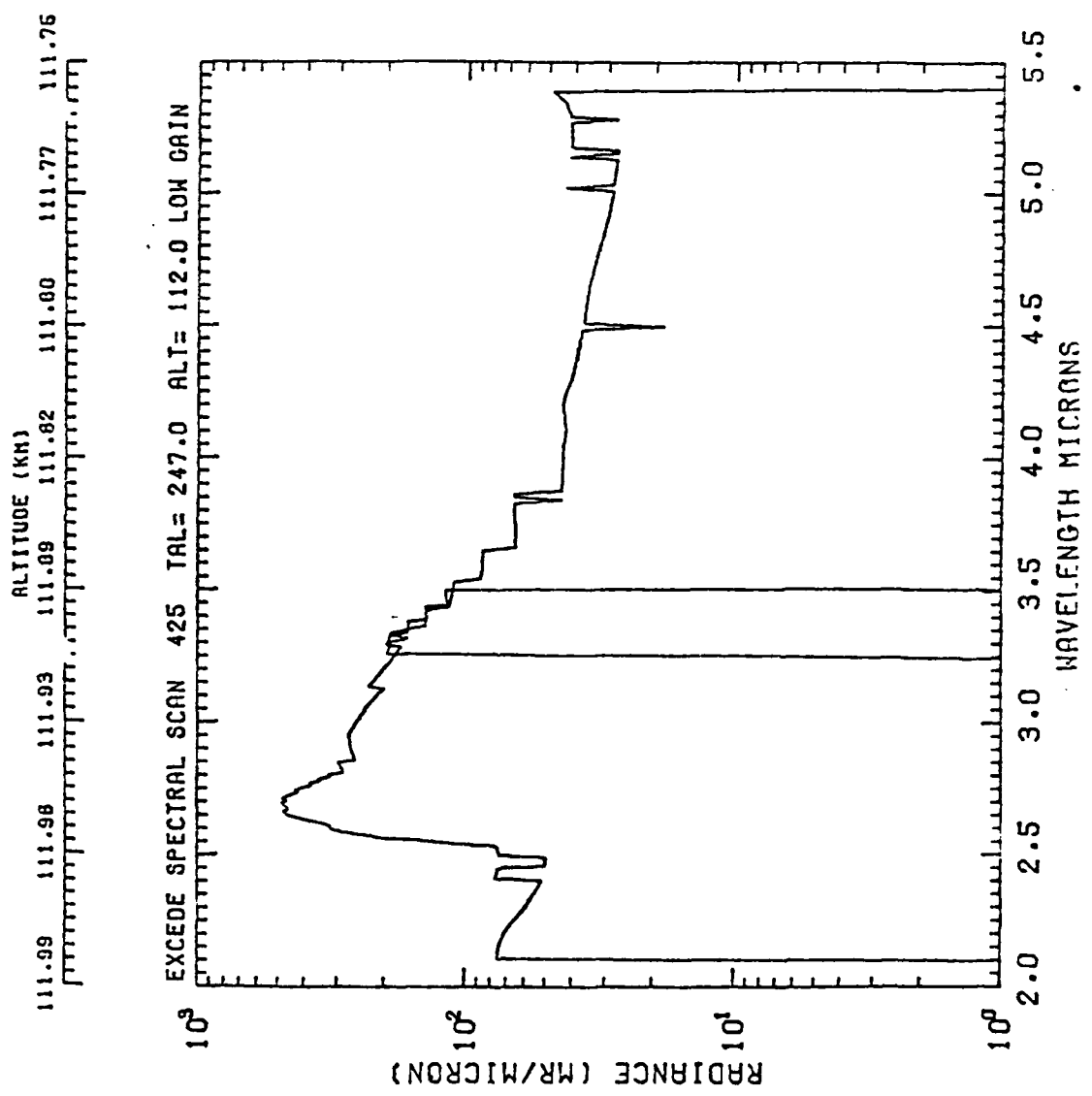
122.10 122.16 122.54 122.53 122.57 122.59 122.60 122.64

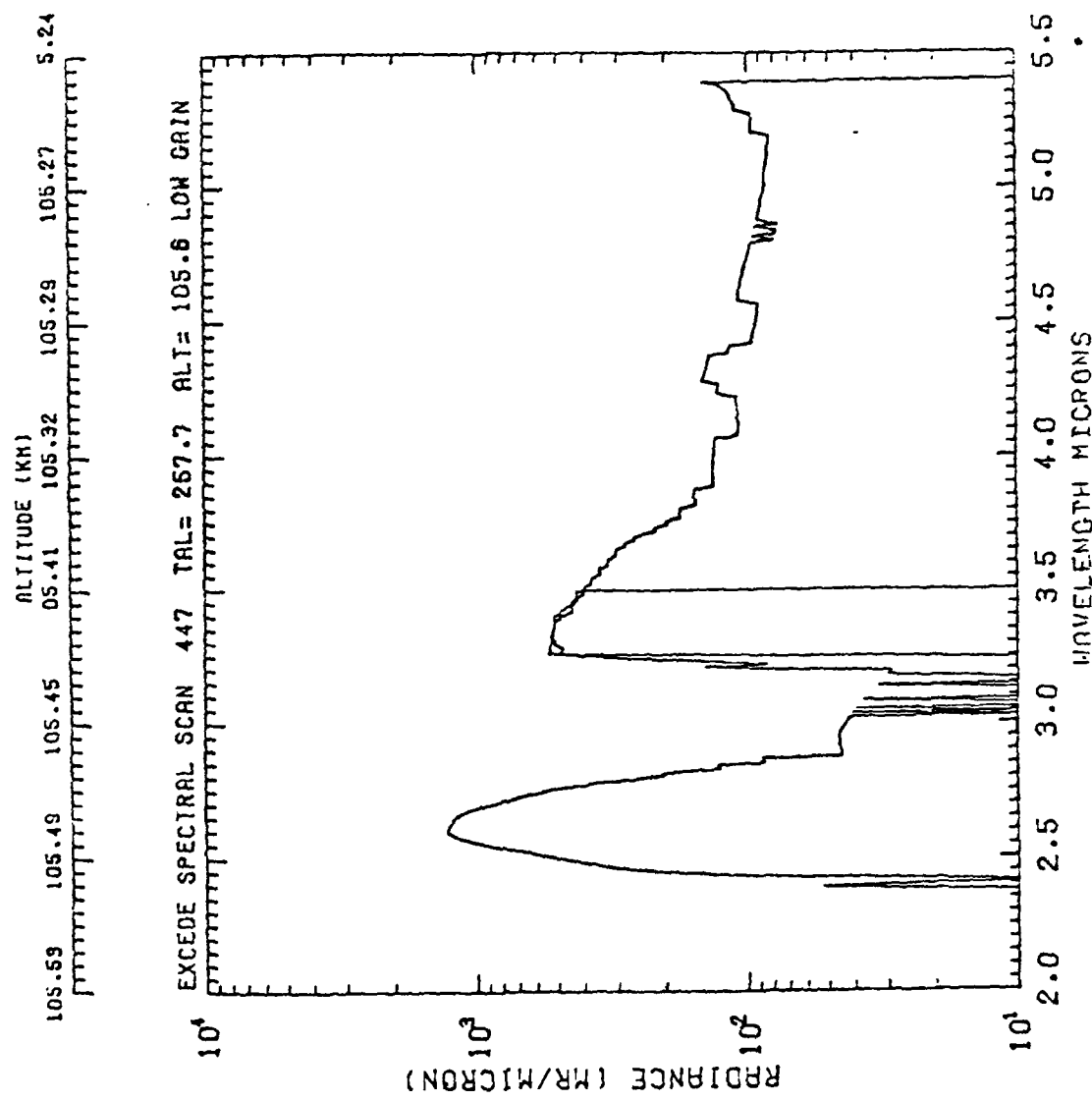


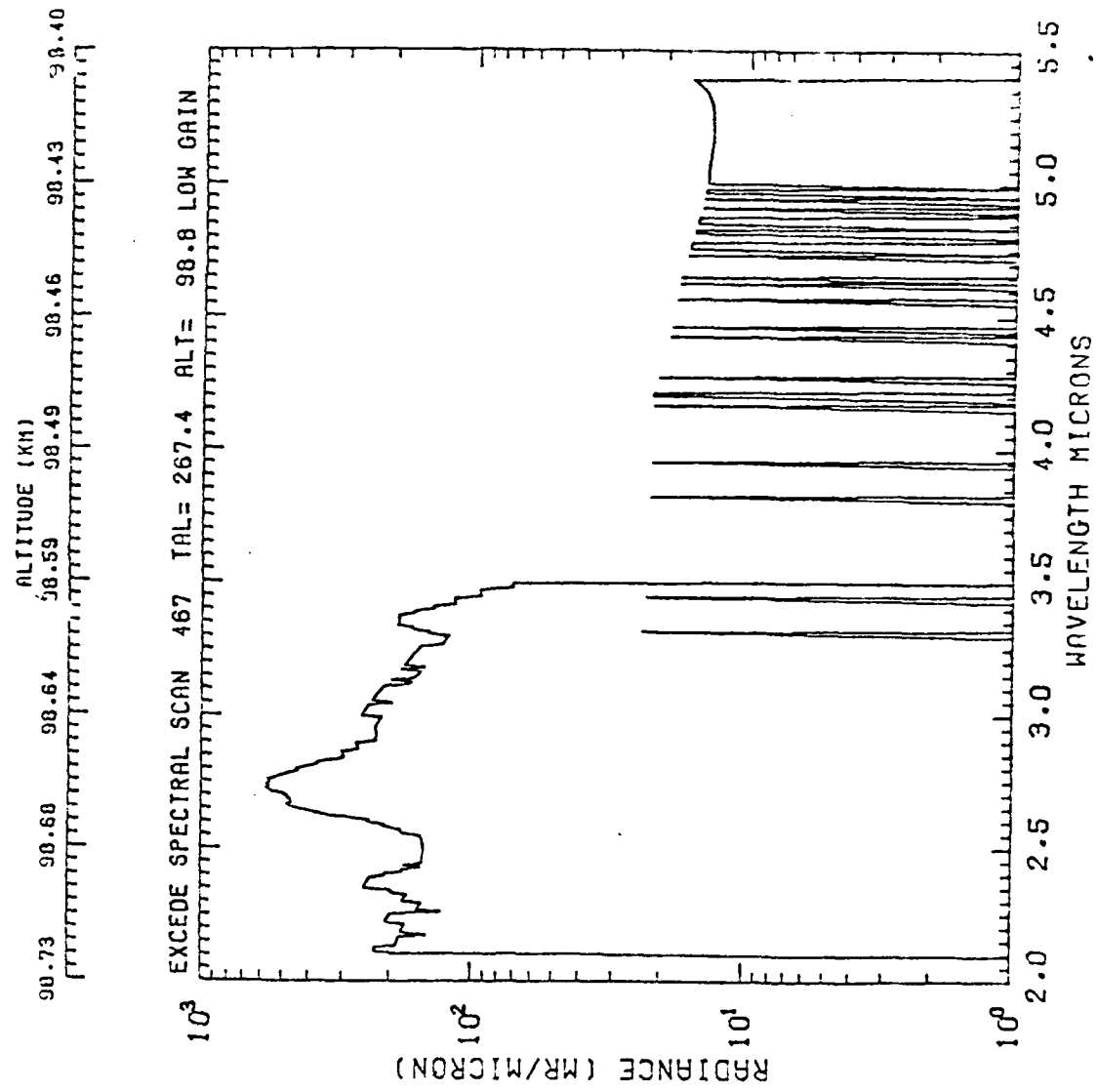






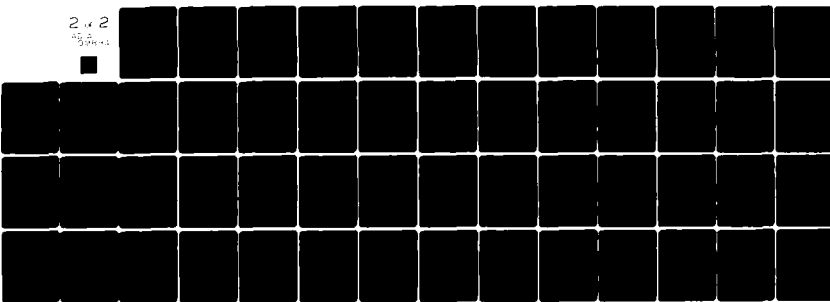




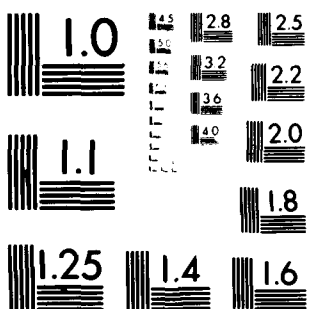


AD-A109 894 BOSTON COLL CHESTNUT HILL MA SPACE DATA ANALYSIS LAB F/G 20/6
ANALYSIS OF PROJECT EXCDE II CIRCULAR VARIABLE FILTER SPECTROM--ETC(U)
JAN 81 W F GRIEDER, C I FOLEY F1962R-79-C-0139
UNCLASSIFIED BC-SDAL-80-3 AFGL-TR-81-0224 NL

2 x 2
30 Jan 81

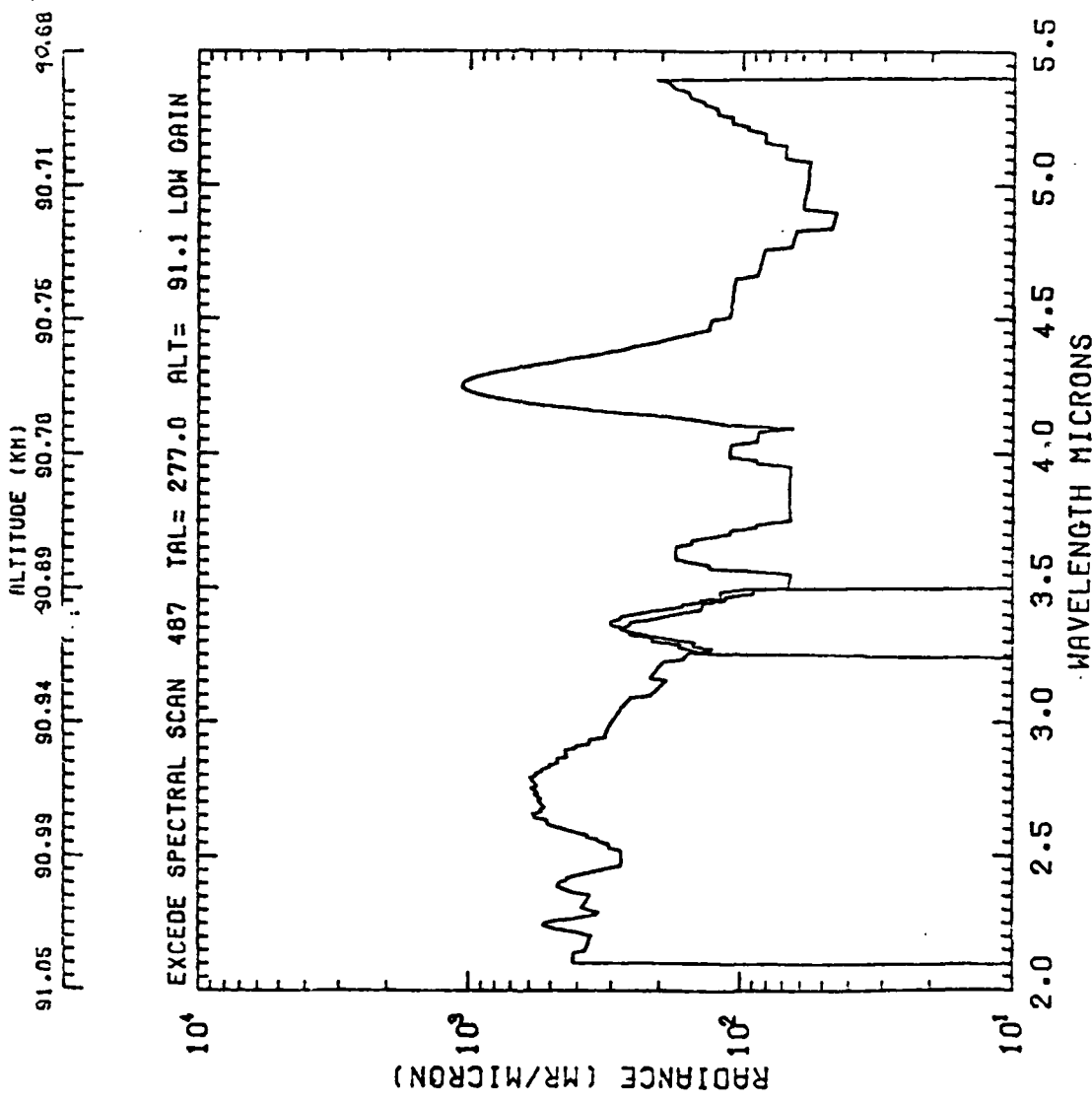


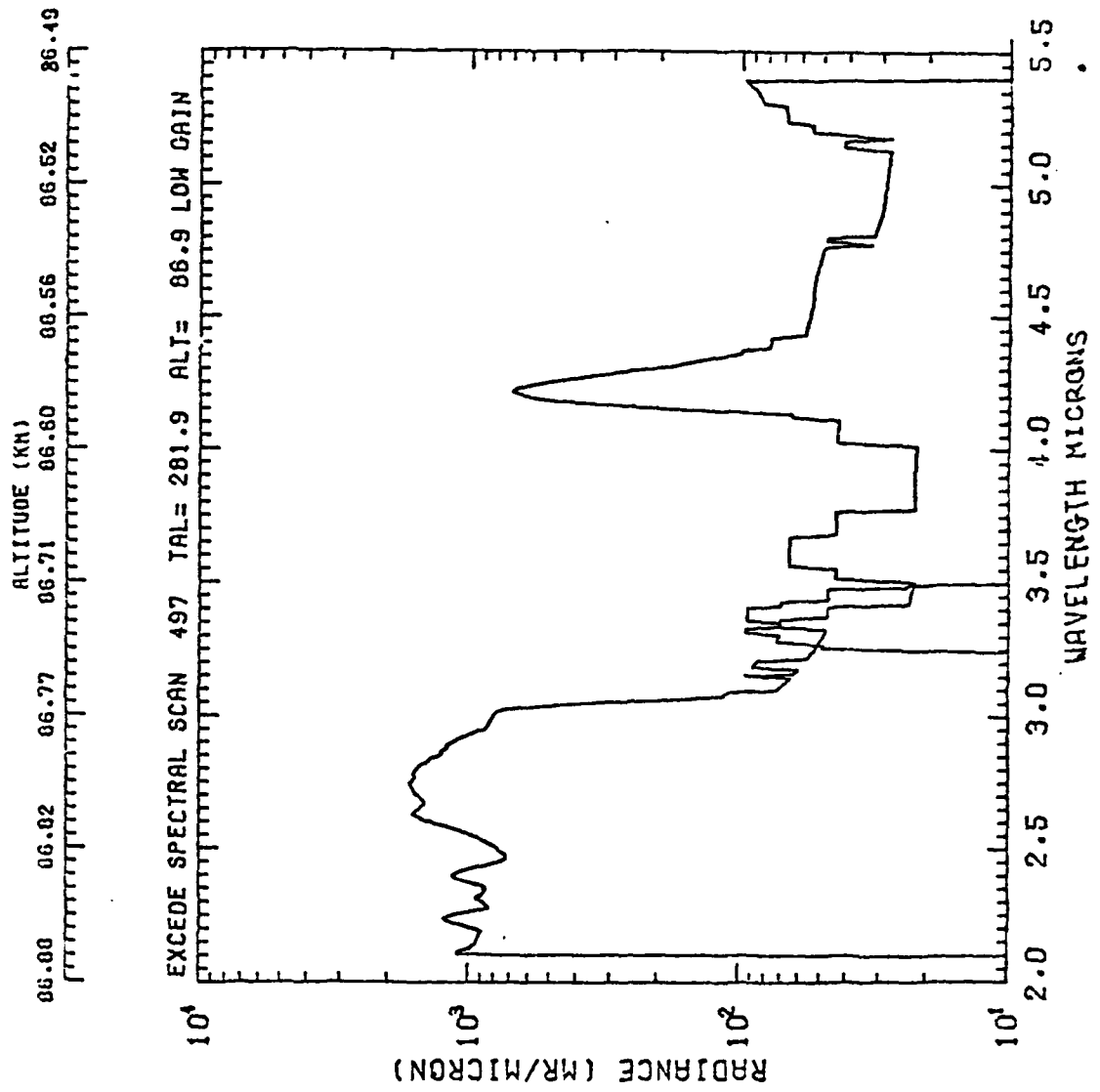
END
DATA
FILED
3-82
DTIC

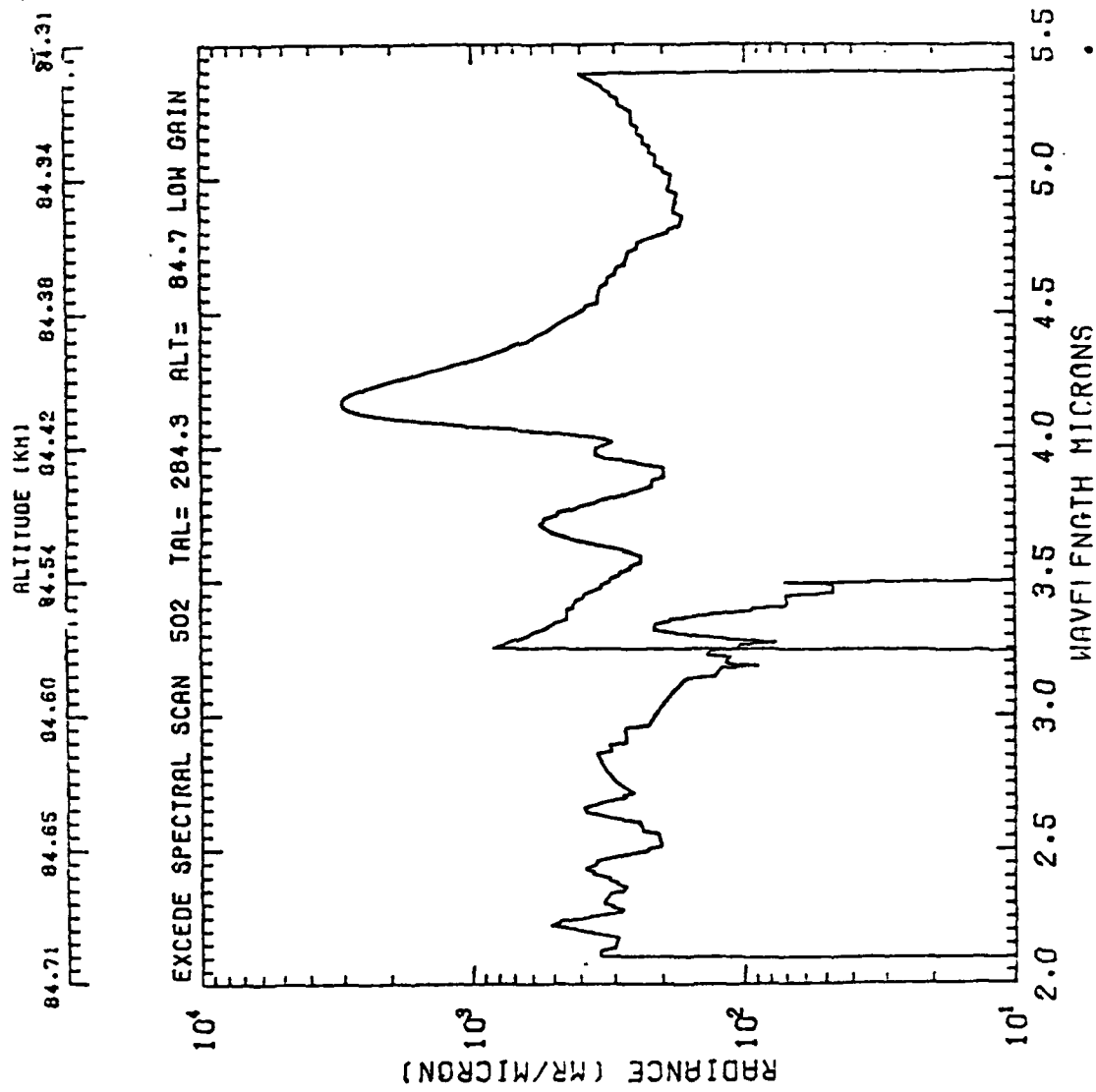


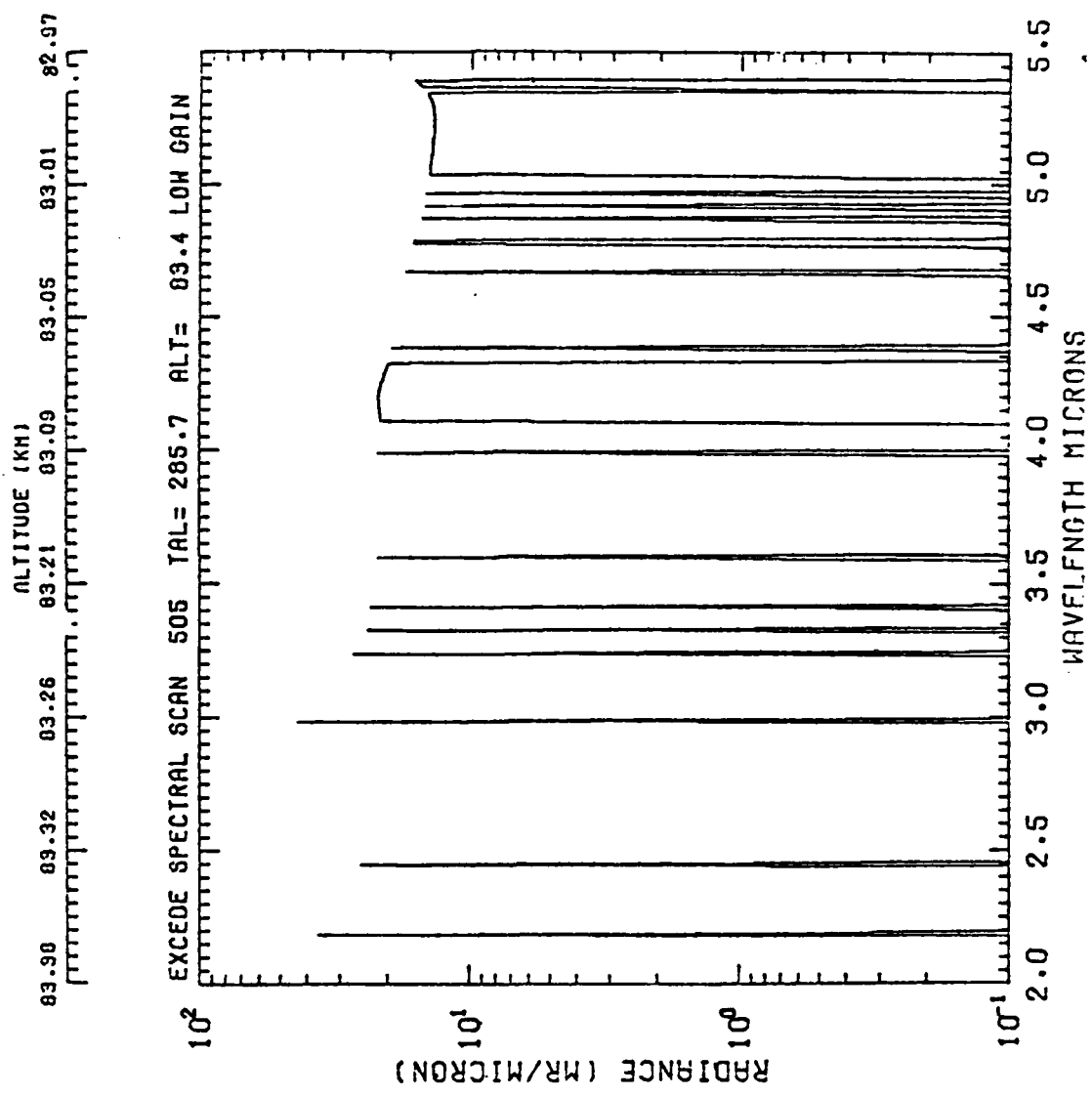
MICROCOPY RESOLUTION TEST CHART

NATIONAL INSTRUMENTS

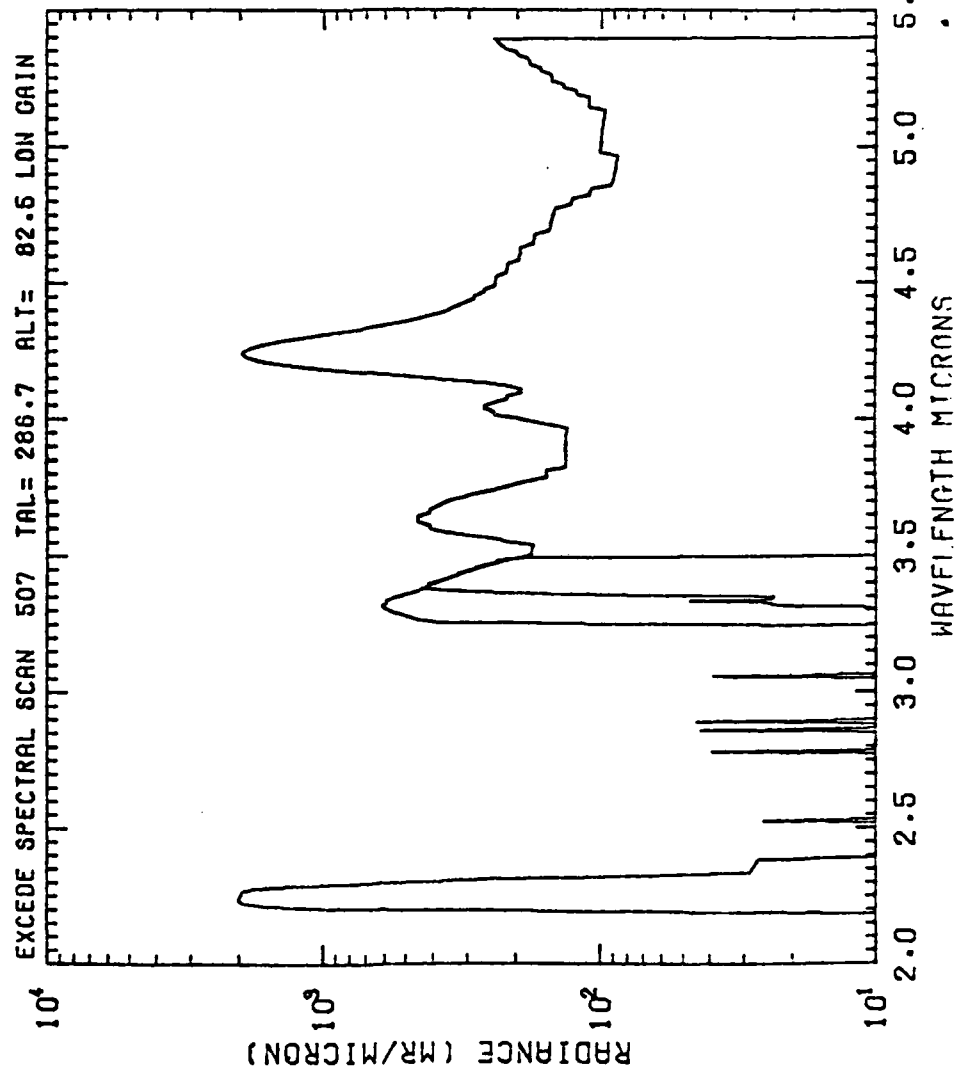


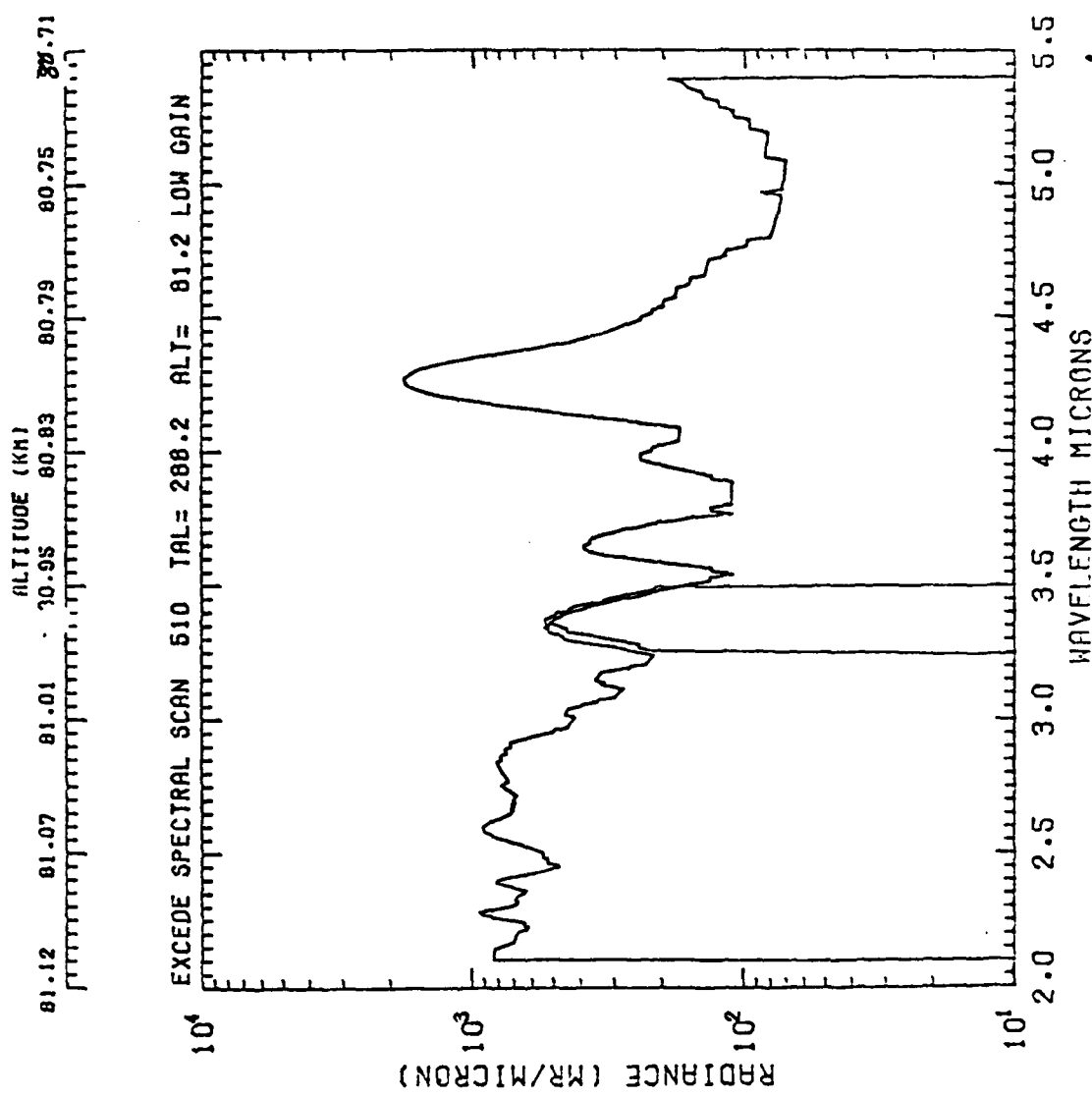


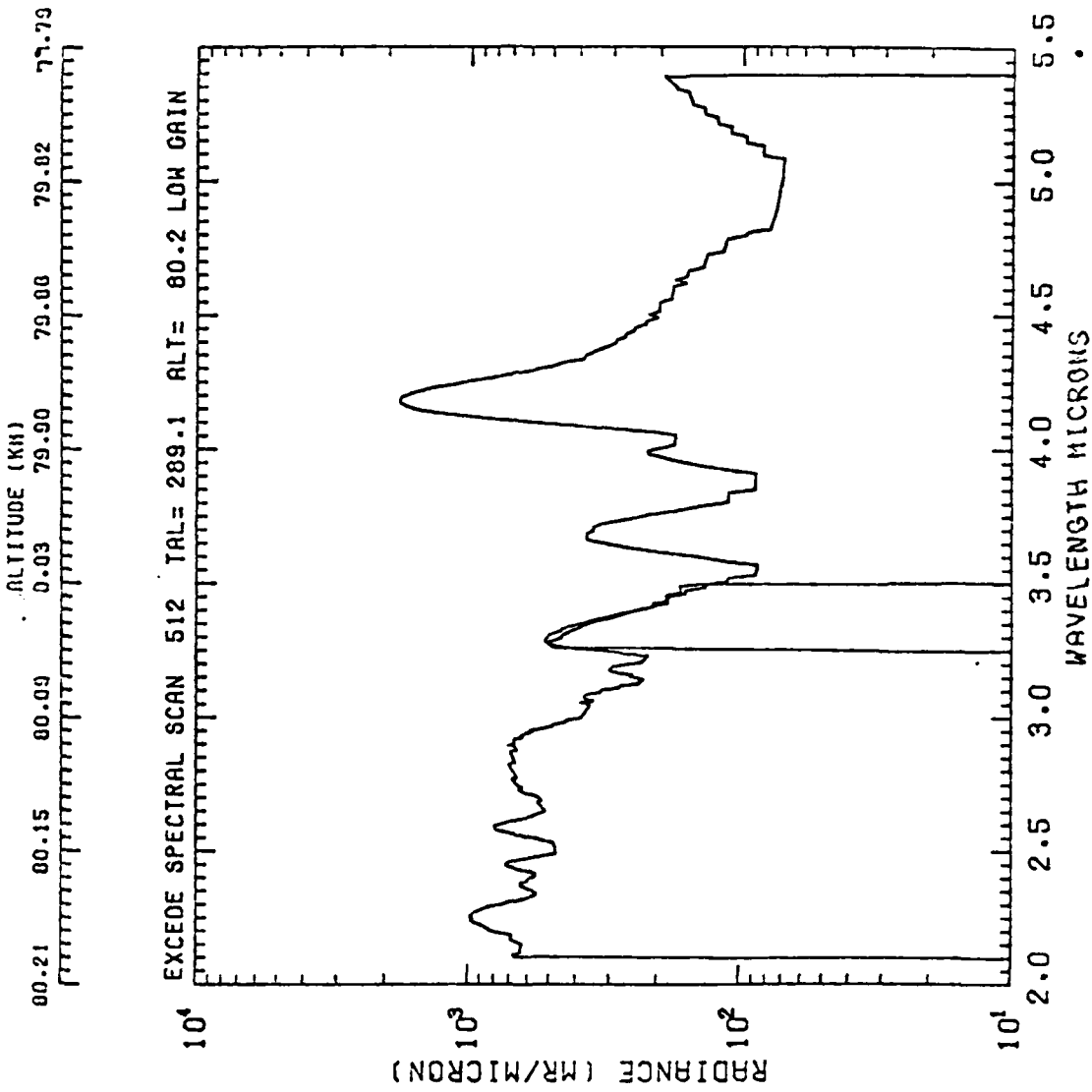


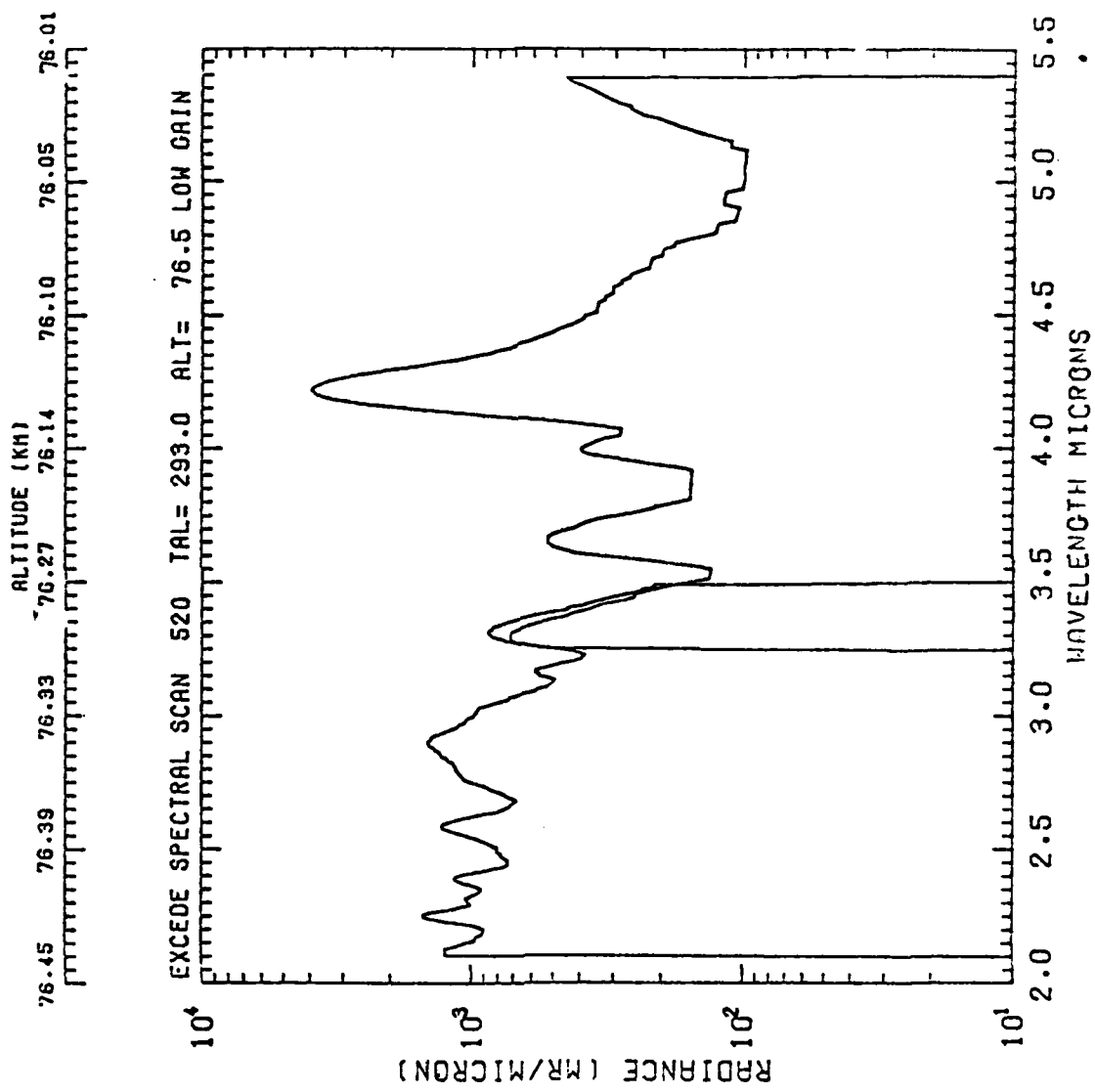


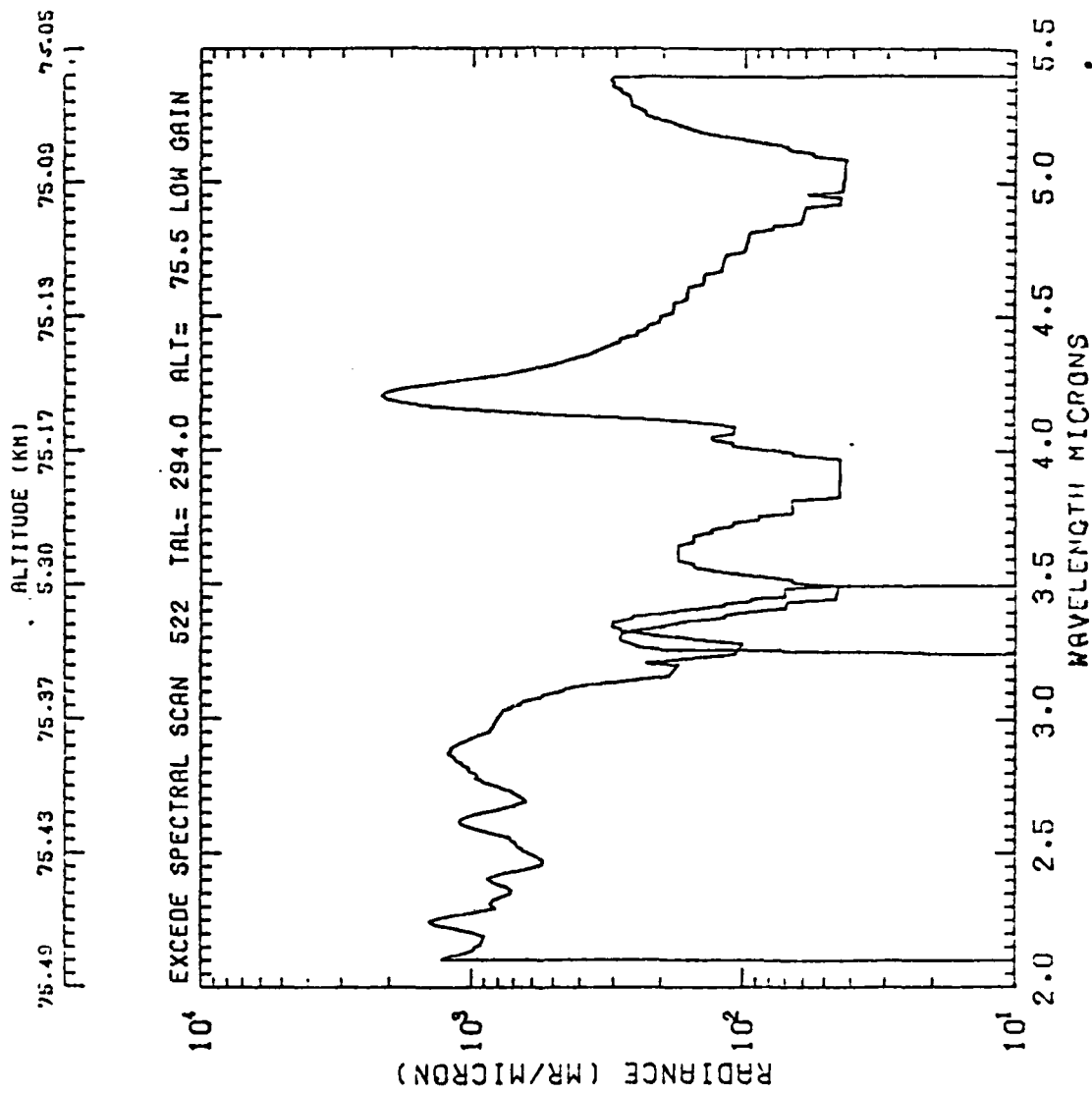
82.48 82.42 82.37 82.31 82.19 82.15 82.11 82.07











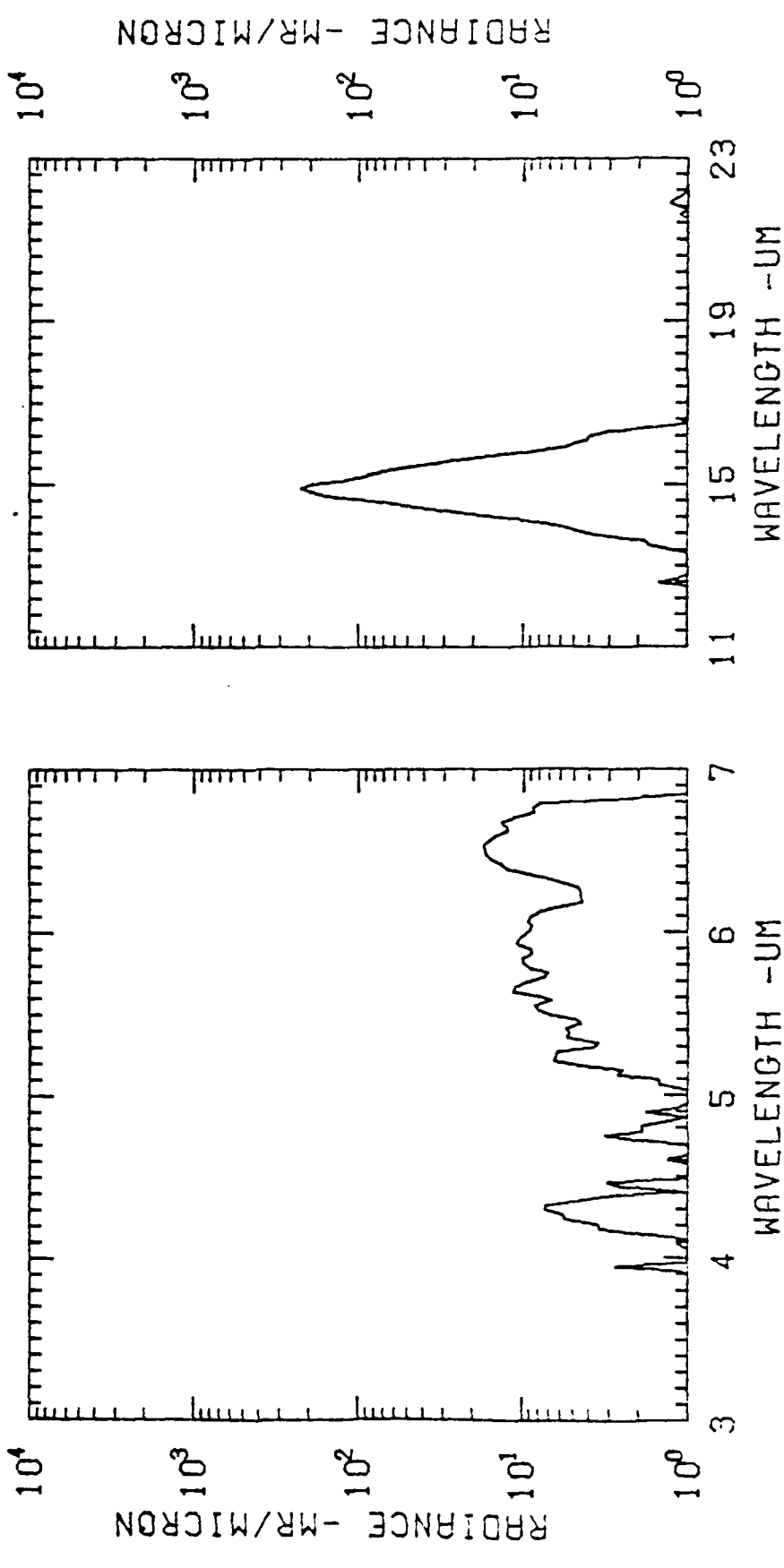
APPENDIX E

Sample Data Base for CVF HS-3B-1

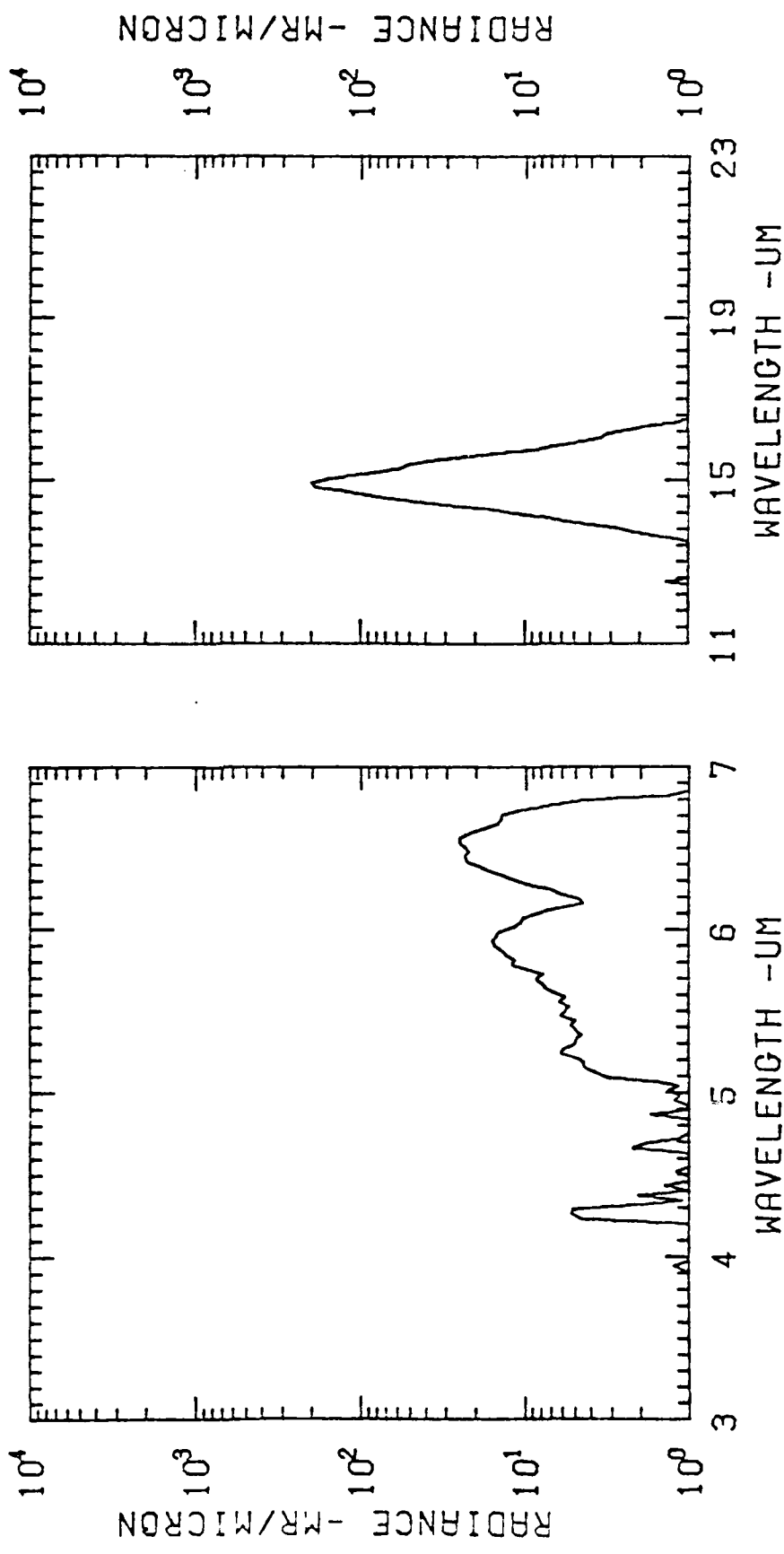
This appendix contains selected spectral data developed from CVF HS-3B-1 measurements. Scans and scan start times (time after launch in seconds) follow

| <u>Scan</u> | <u>T.A.L.</u> | <u>Scan</u> | <u>T.A.L.</u> |
|-------------|---------------|-------------|---------------|
| 1047 | 96.1650 | 1111 | 173.7760 |
| 1048 | 97.3730 | 1159 | 232.9600 |
| 1049 | 98.5790 | 1171 | 246.9950 |
| 1051 | 100.9930 | 1180 | 257.8540 |
| 1055 | 105.8200 | 1188 | 267.5050 |
| 1056 | 107.0260 | 1196 | 277.1560 |
| 1062 | 114.2680 | 1200 | 281.9820 |
| 1063 | 115.4730 | 1202 | 284.3940 |
| 1064 | 116.6810 | 1203 | 285.6000 |
| 1069 | 122.7150 | 1204 | 286.8070 |
| 1070 | 123.9220 | 1205 | 288.0130 |
| 1073 | 127.5420 | 1206 | 289.2200 |
| 1090 | 148.0560 | 1209 | 292.8380 |
| 1092 | 150.4700 | 1210 | 294.0450 |
| 1093 | 151.6770 | 1211 | 295.251 |
| 1095 | 154.0910 | | |
| 1109 | 171.3120 | | |

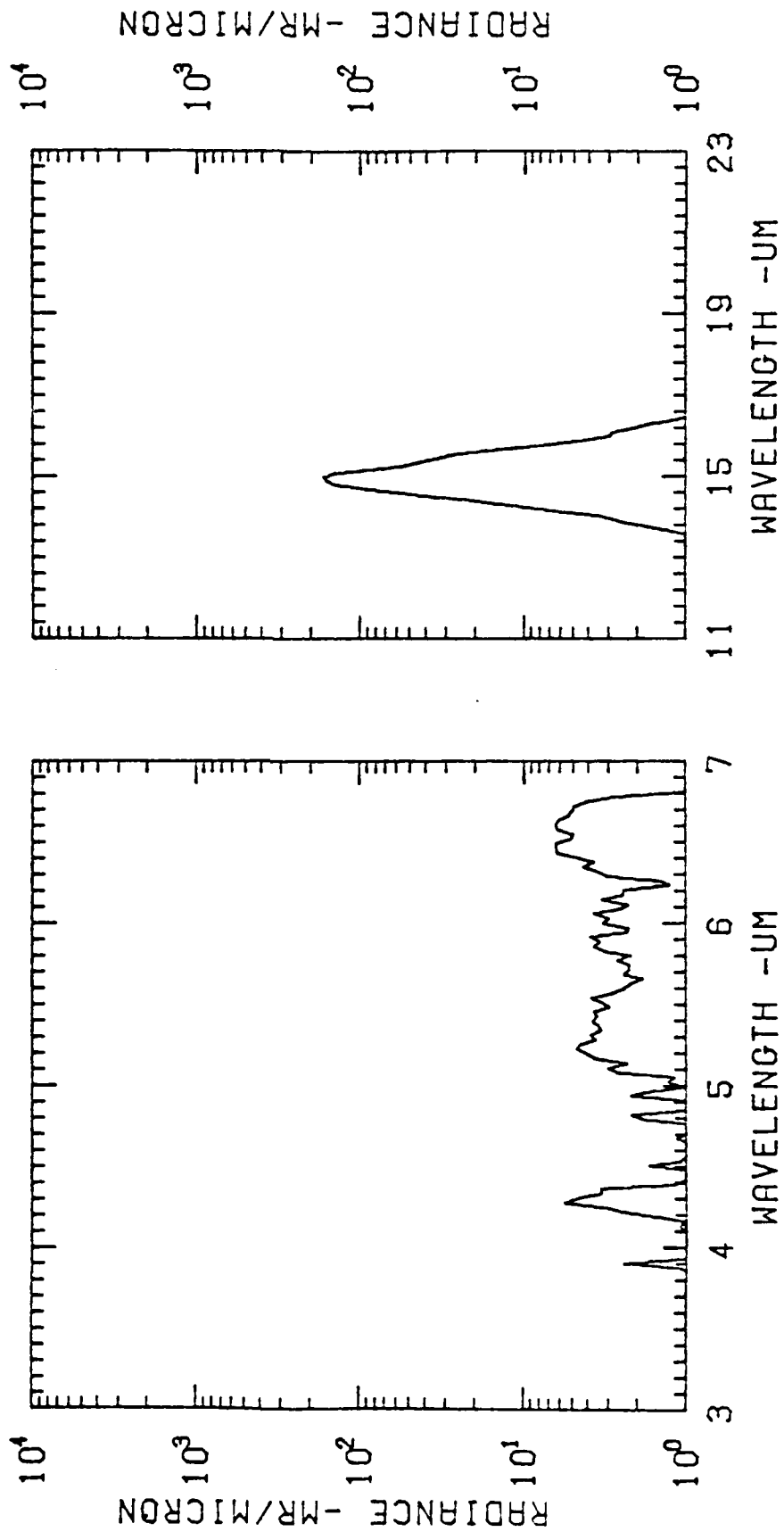
ALTITUDE (KM)
89.1 89.3 89.4 89.5 89.7 89.7 89.9 90.0 90.2



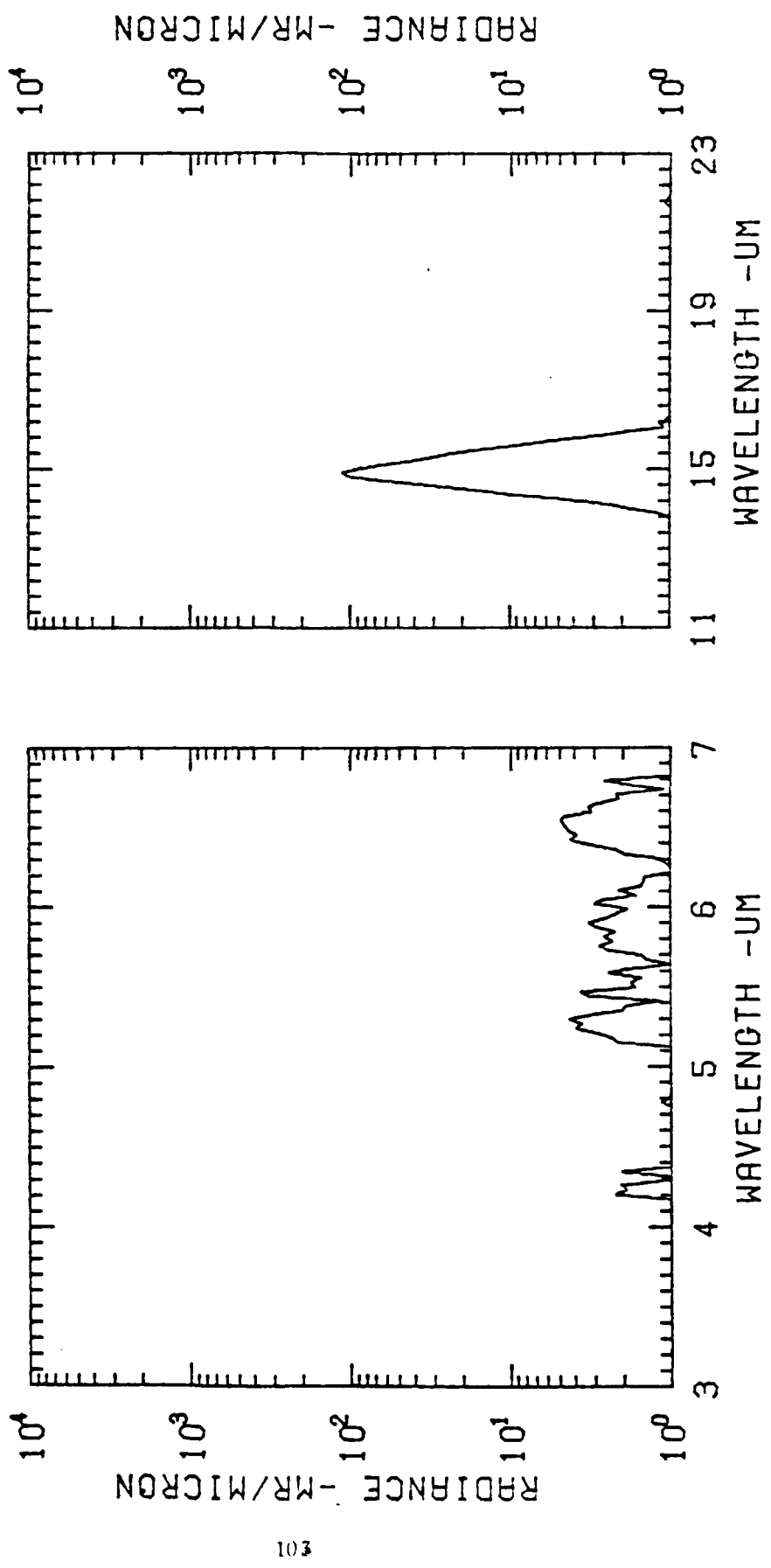
EXC EDE SPECTRAL SCAN 1048 TAL = 37.4 ALT = 90.2 ALL GAIN CAL . 53



ALTITUDE (KM) 91.2 91.3 91.4 91.6 91.7 91.7 91.9 92.1 92.2

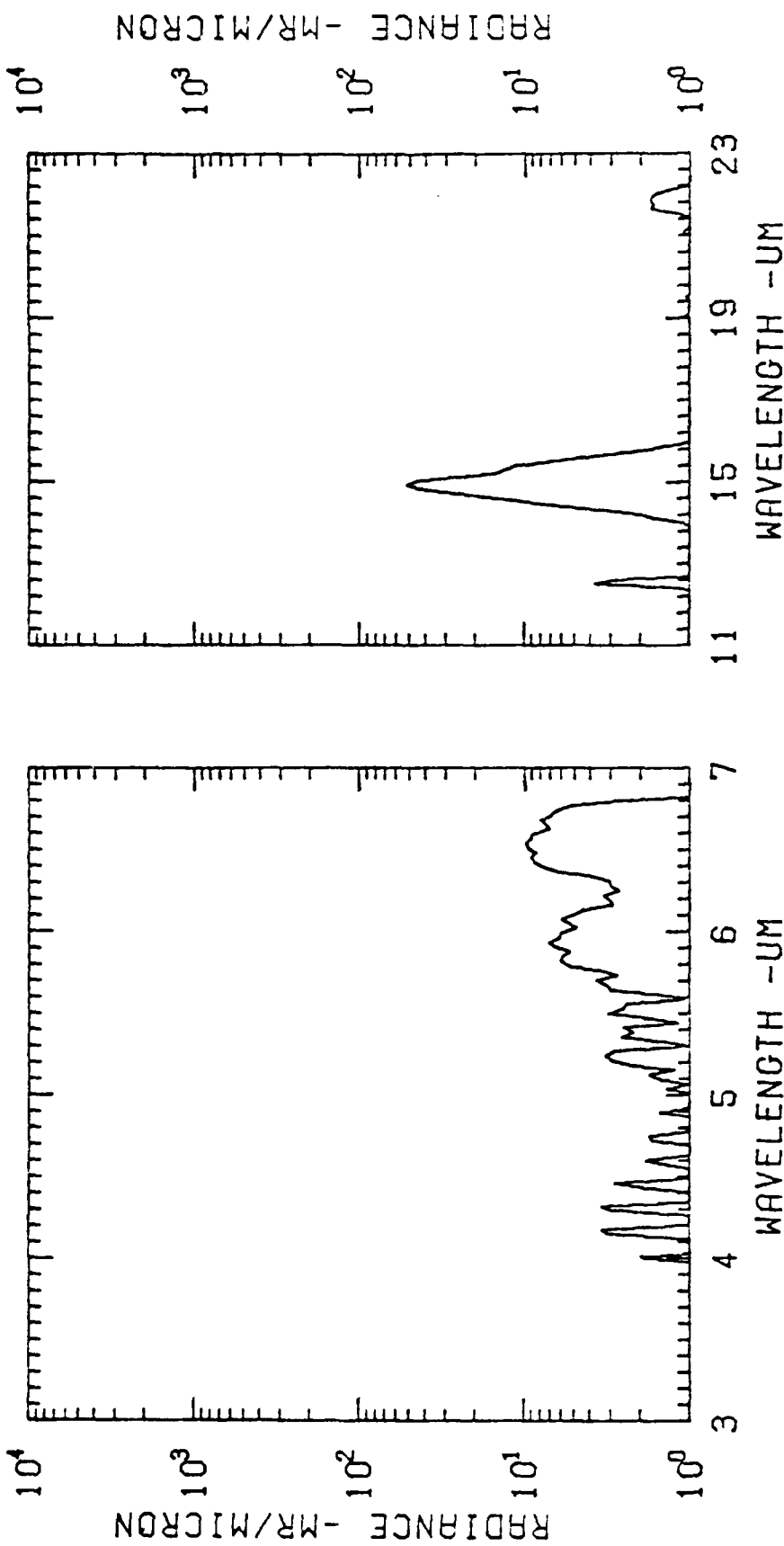


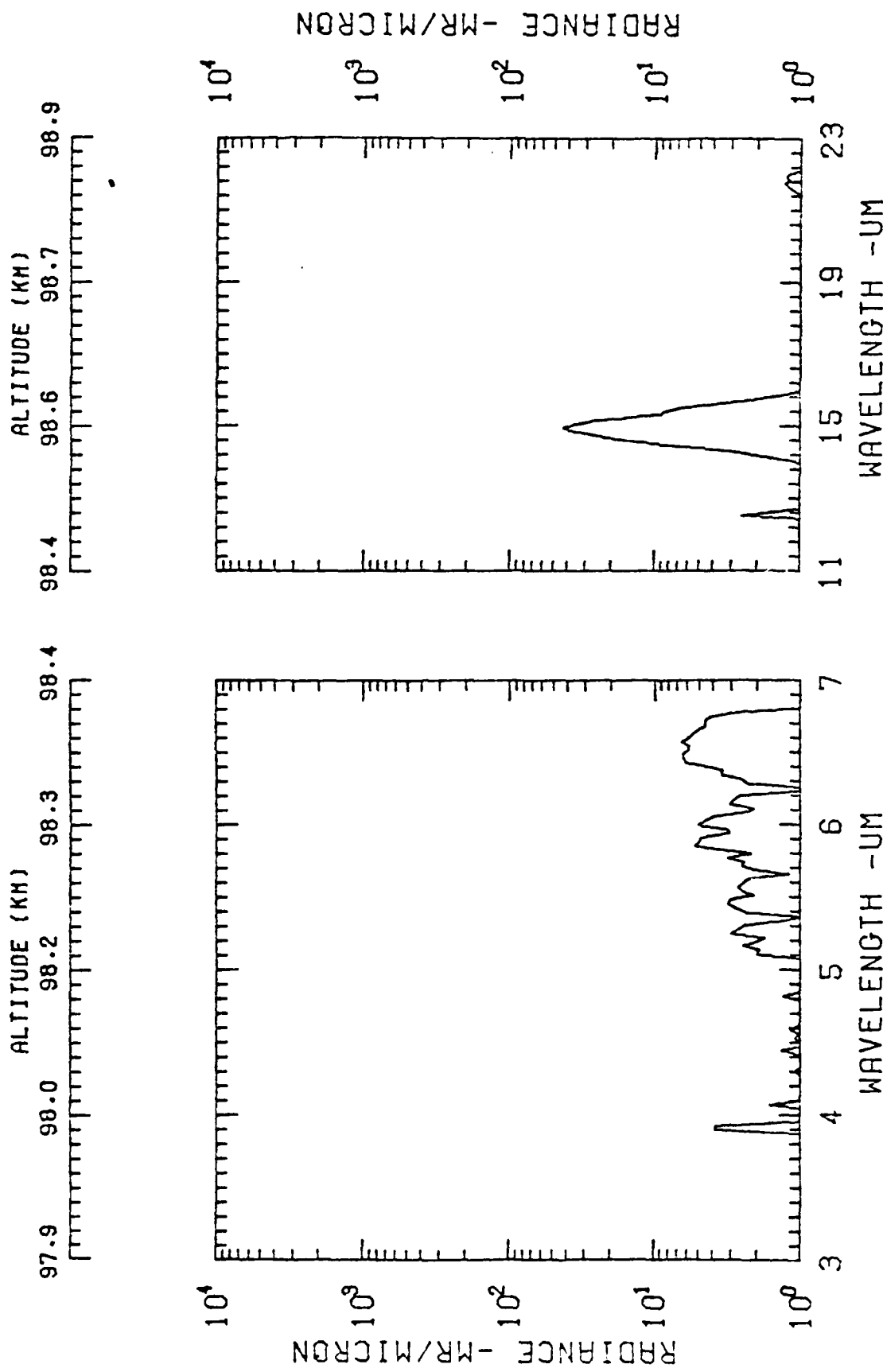
EXCDEE SPECTRAL SCAN 1049 TAL= 90.6 ALT= 91.2 ALL GAIN CAL. 53



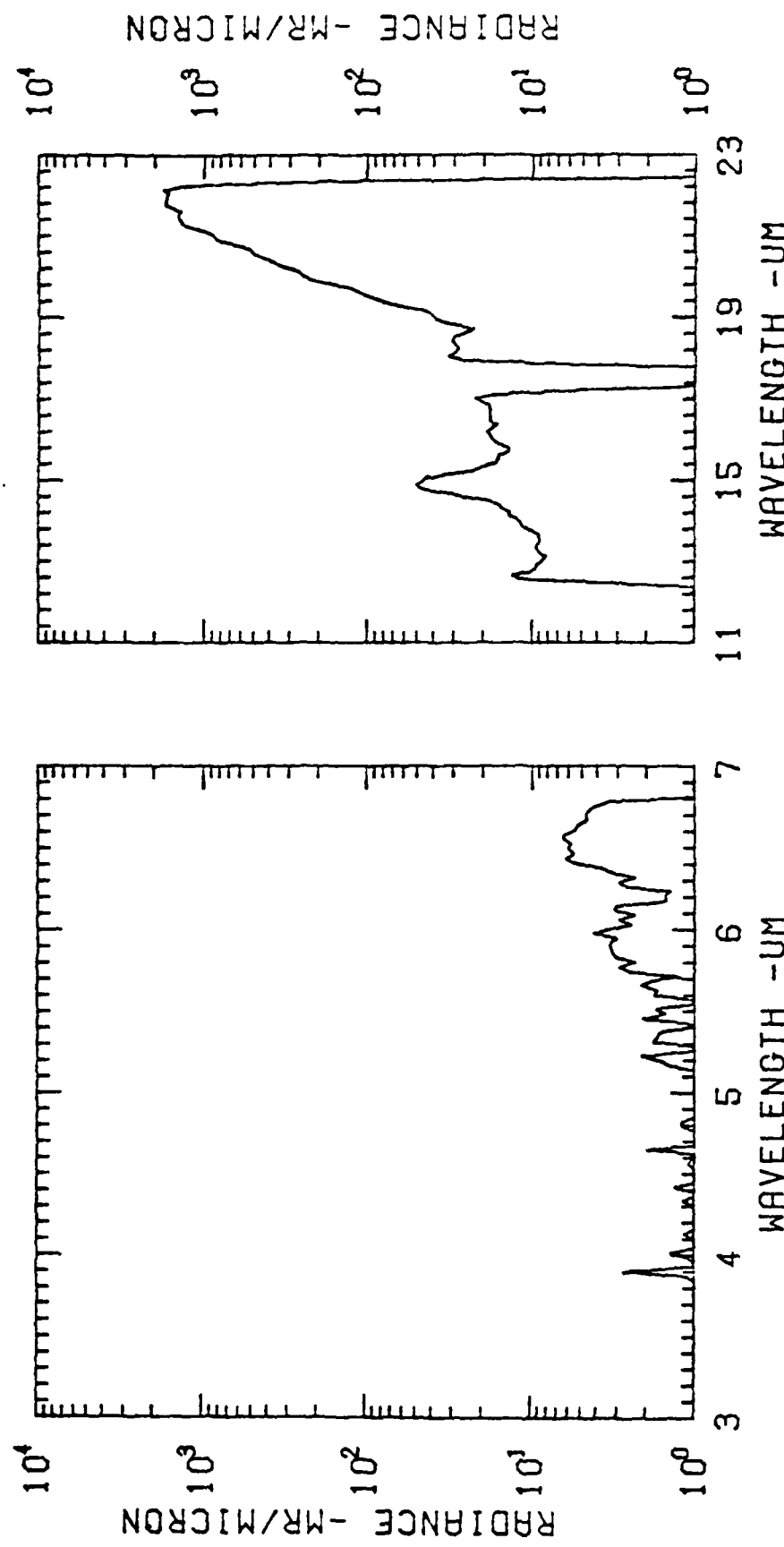
EXC EDE SPECTRAL SCAN 1051 TAL= 101.0 ALT= 93.2 ALL GAIN CAL. 53

EXC 002E SPECTRAL SCAN 1055 TAL= 105.0 ALT= 97.0 AUL GAIN CAL. 53





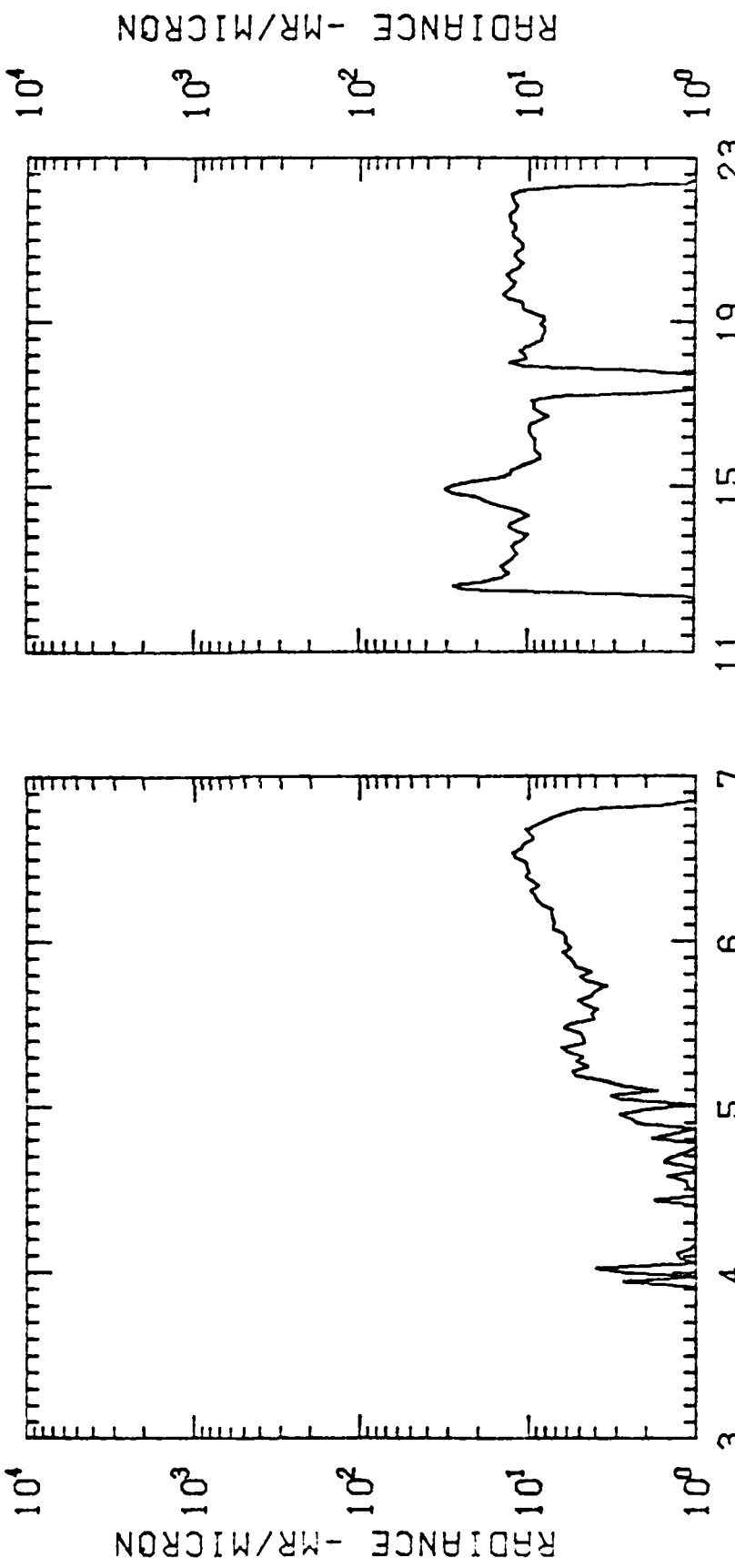
98.8 98.9 ALTITUDE (KM) 99.1 99.2 99.3 99.3 99.5 99.6 99.8
 98.8 98.9 ALTITUDE (KM) 99.1 99.2 99.3 99.3 99.5 99.6 99.8



EXCITE SPECTRAL SCAN 1067 TAL= 108.2 ALT= 98.9 ALL GRIN CAL. 53

EXCDE SPECTRAL SCAN 1062 ALT= 114.3 ALT= 103.2 ALL GAIN CAL. 53

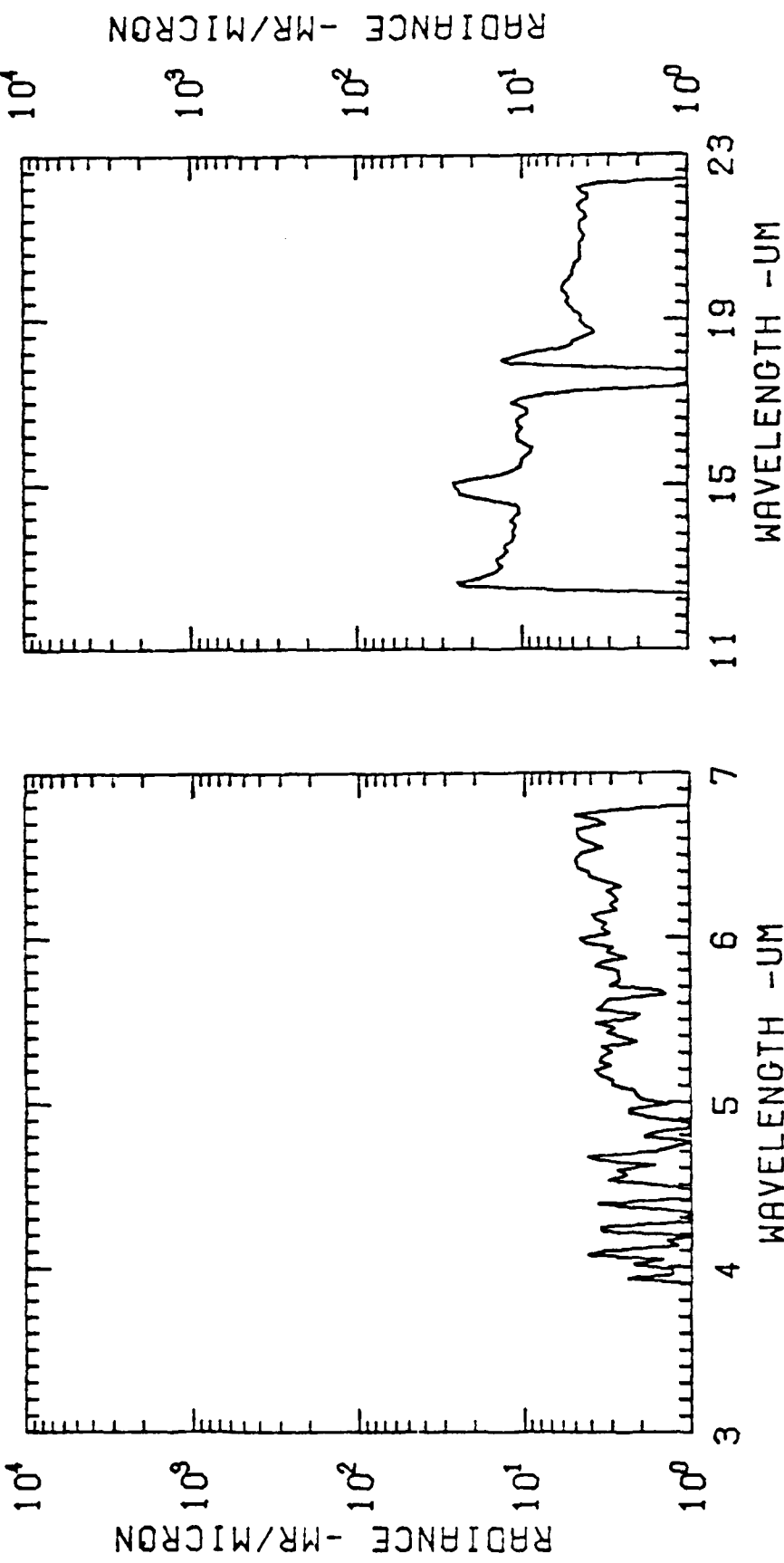
)
WAVELENGTH -UM
11 15 19 23



103.2 103.3 103.4 103.5 103.6 103.6 103.7 103.9 104.0
ALTITUDE (KM)

RADIANCE - MR/MICRON

EXCDE SPECTRAL SCAN 1063 TAL = 115.5 ALT = 104.0 ALL GAIN CAL. 53

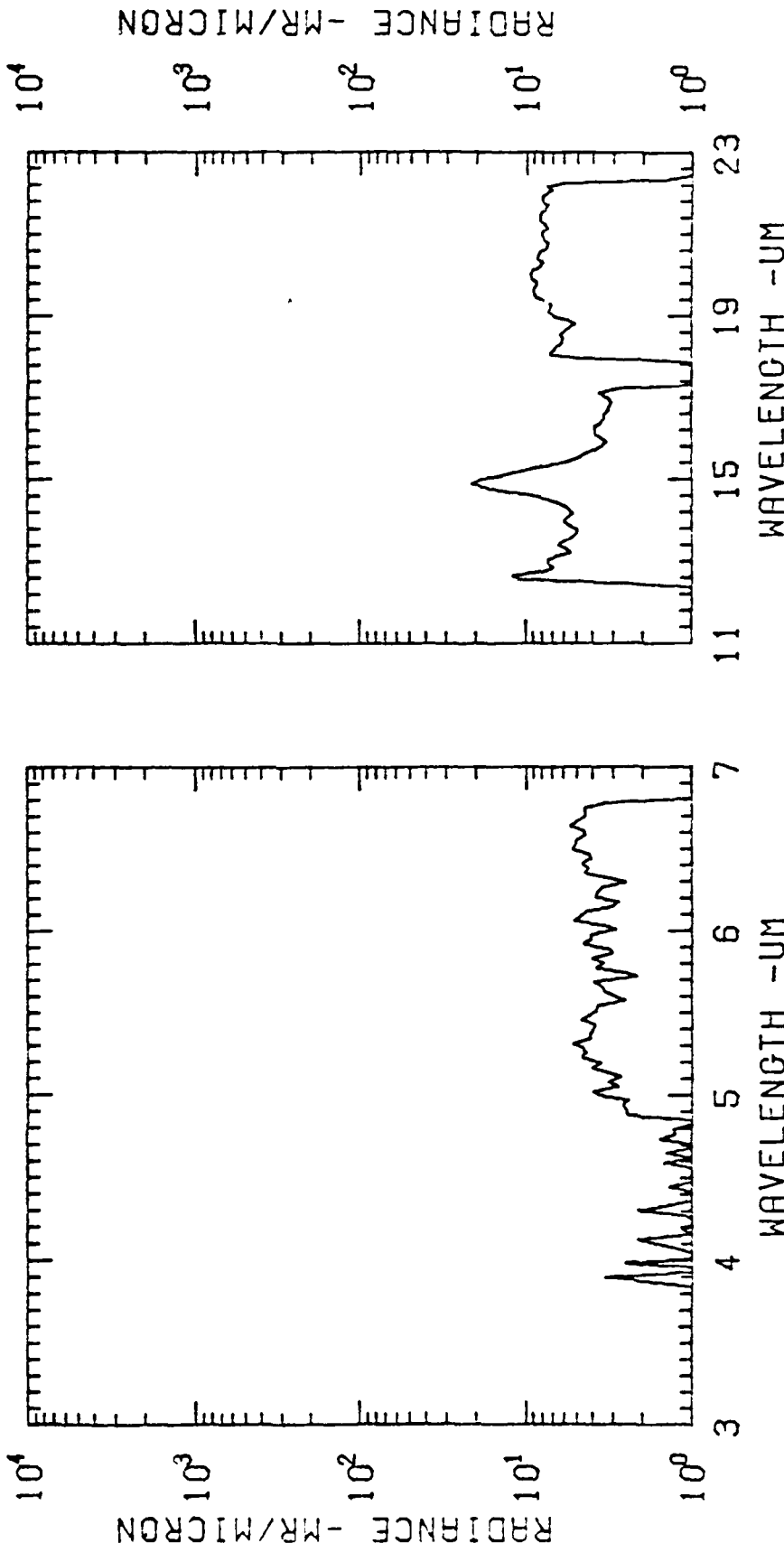


104.0 104.1 104.2 104.3 104.4 104.4 104.6 104.7 104.8
ALTITUDE (KM)

RADIANCE - MR/MICRON

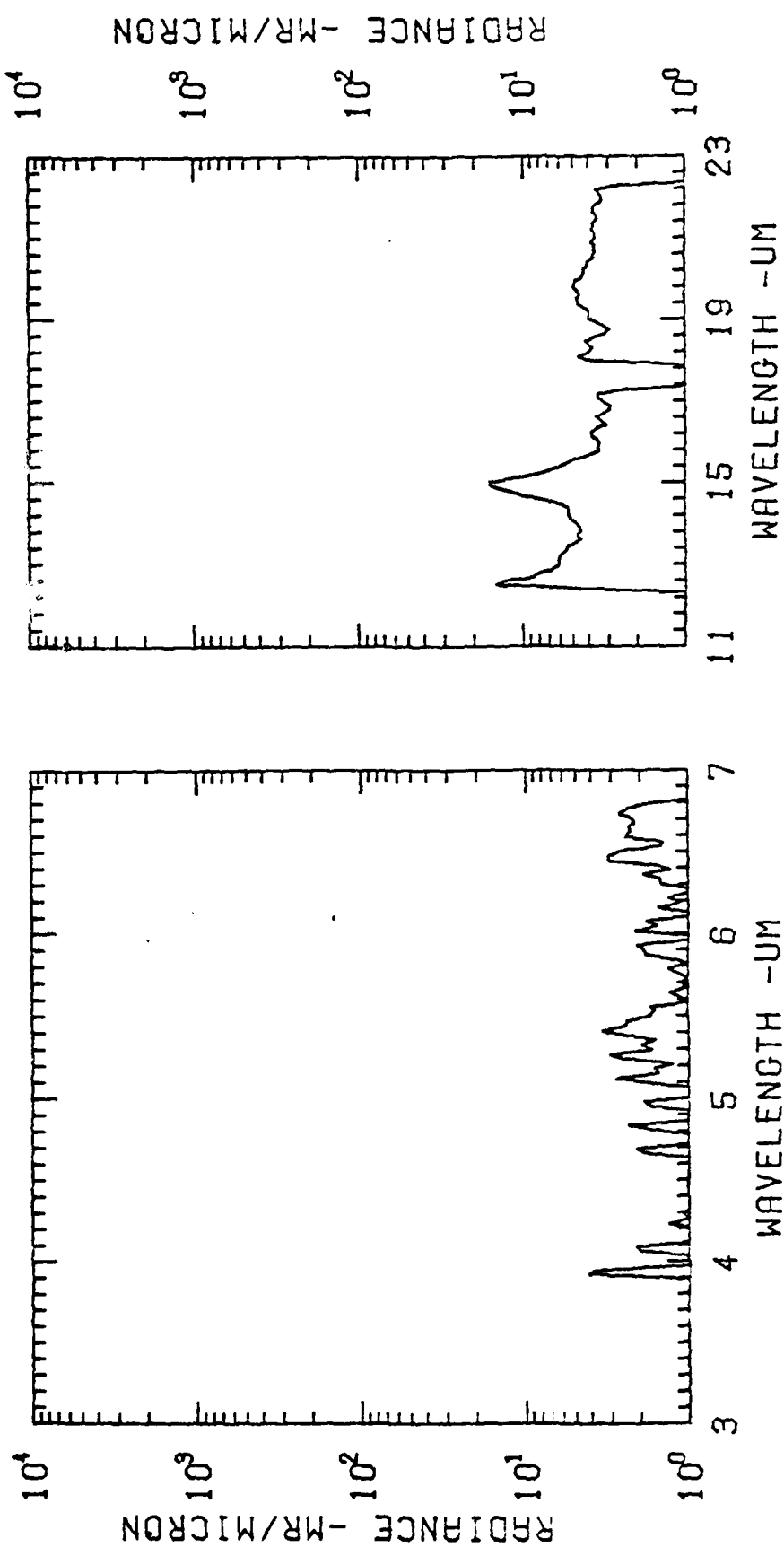
104.8 104.9 105.0 105.1 105.2 105.3 105.4 105.5 105.6

ALTITUDE (KM)



EXC EDE SPECTRAL SCAN 1064 TAL= 116.7 ALT= 104.8 ALL GAIN CAL. 53

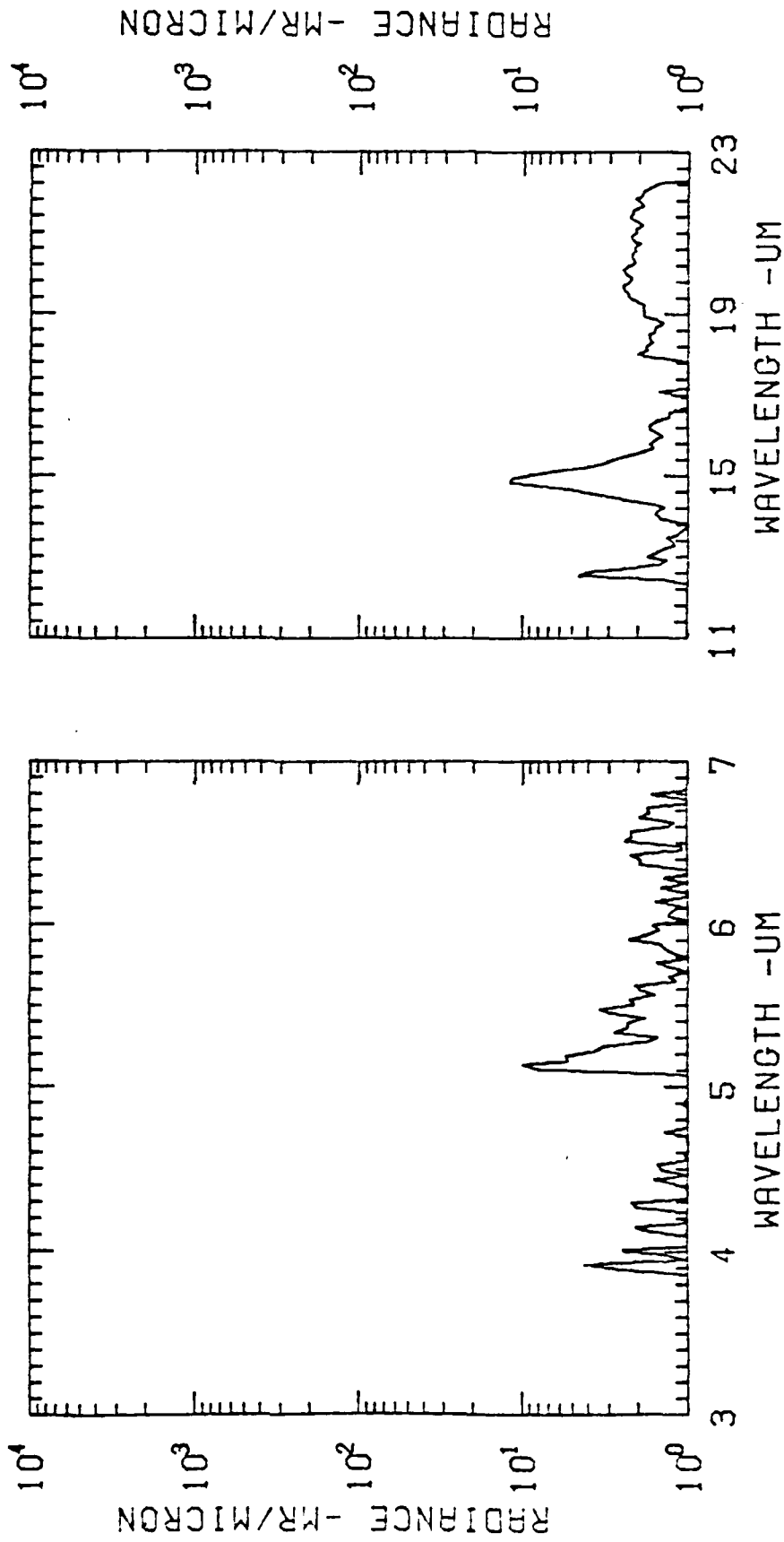
ALTITUDE (KM) 108.7 108.8 108.9 109.0 109.1 109.2 109.3 109.4



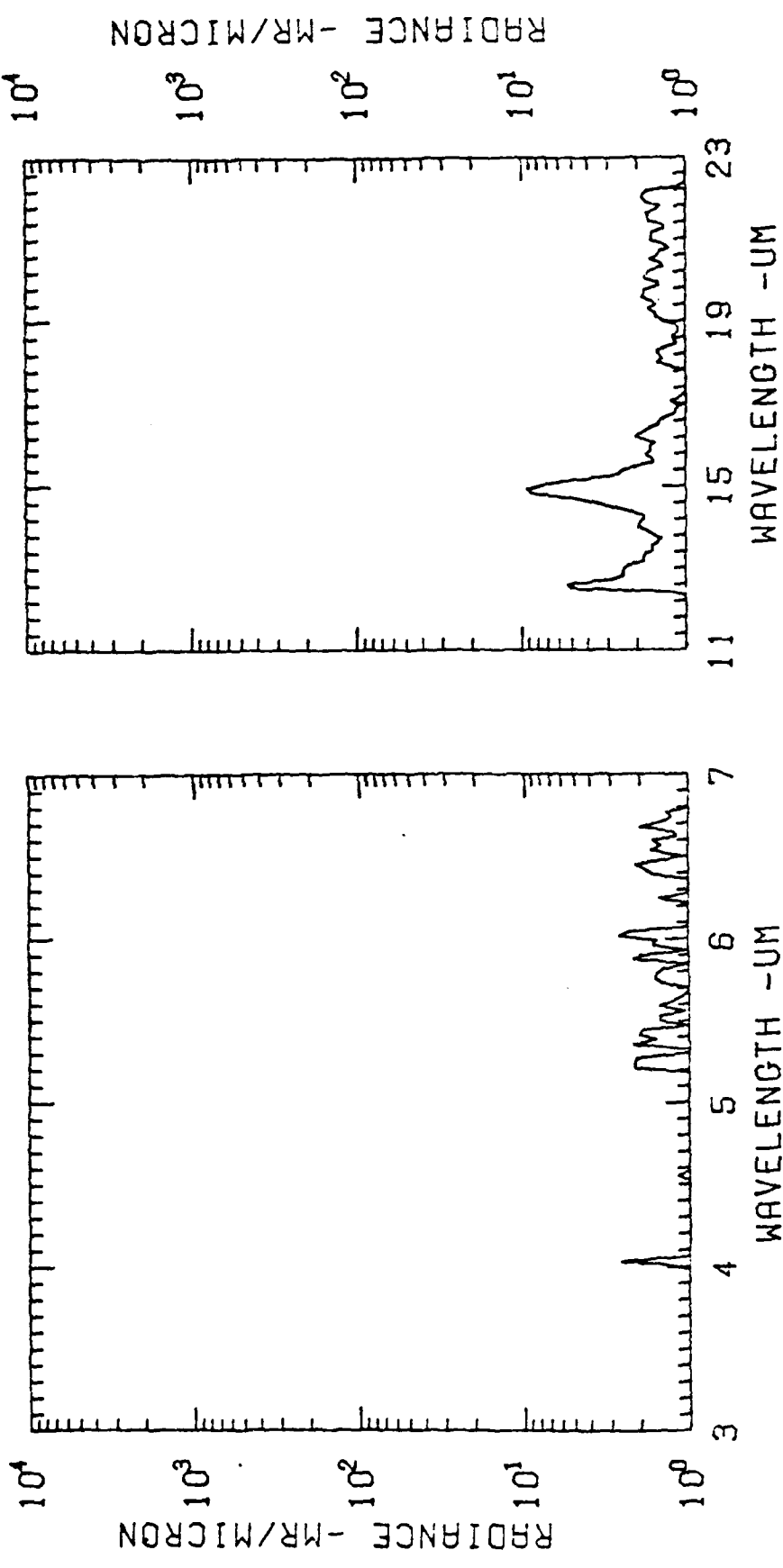
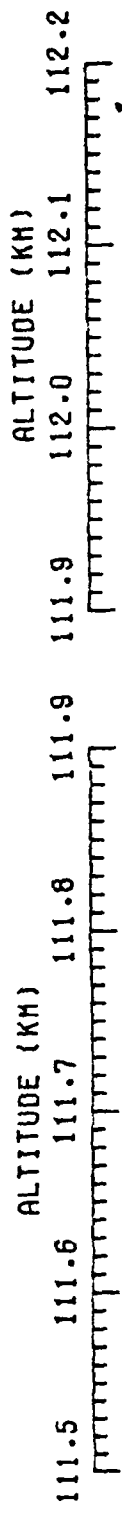
EXCDE SPECTRAL SCAN 1069 TAL= 122.7 ALT= 108.7 ALL GAIN CAL. 53

109.4 109.5 109.6 109.7 109.8 109.9 110.0 110.1

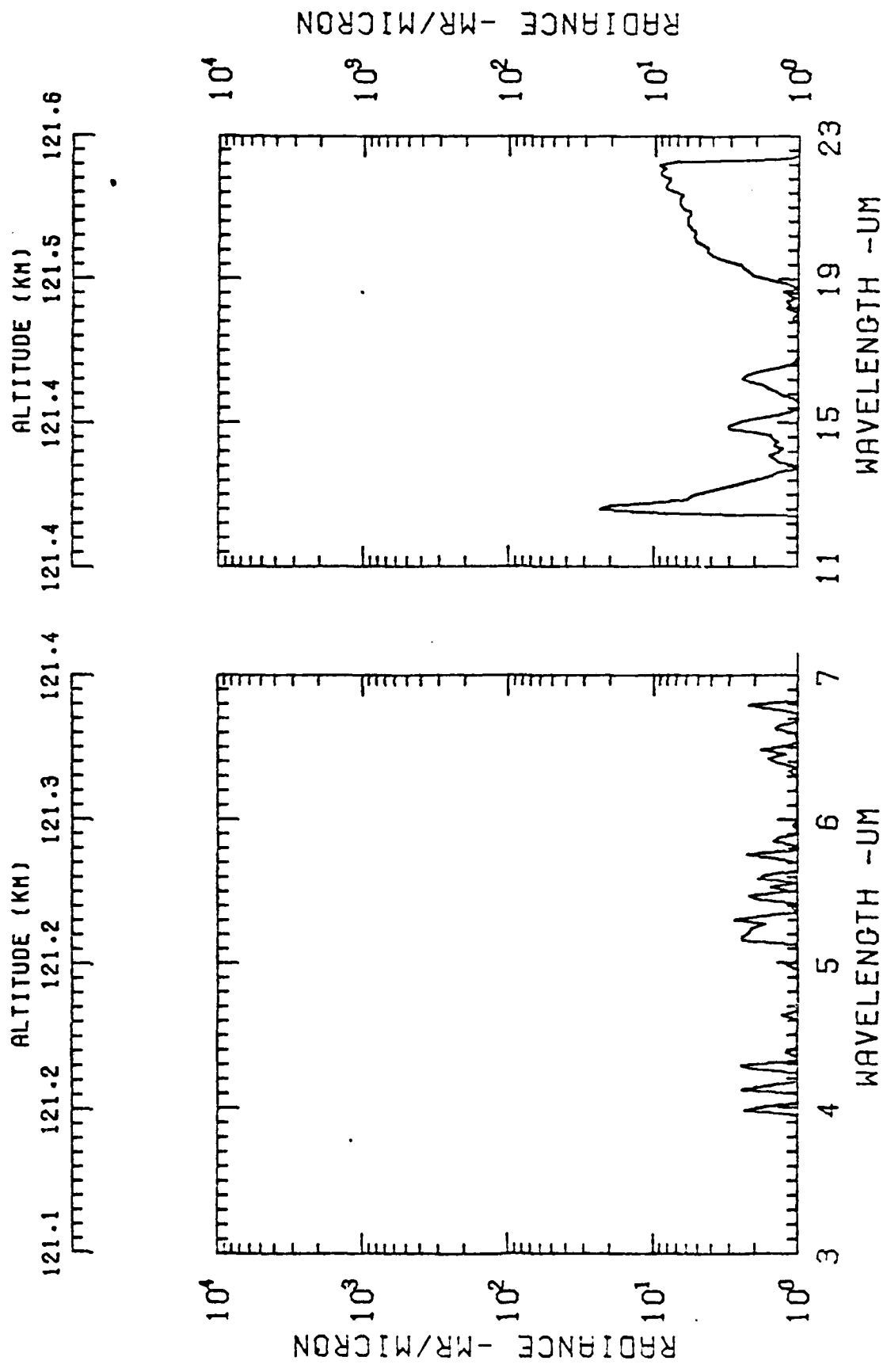
ALTITUDE (KM)



EXC EDE SPECTRAL SCAN 1070 ALT= 123.9 ALT= 109.4 ALL GAIN CAL. 53

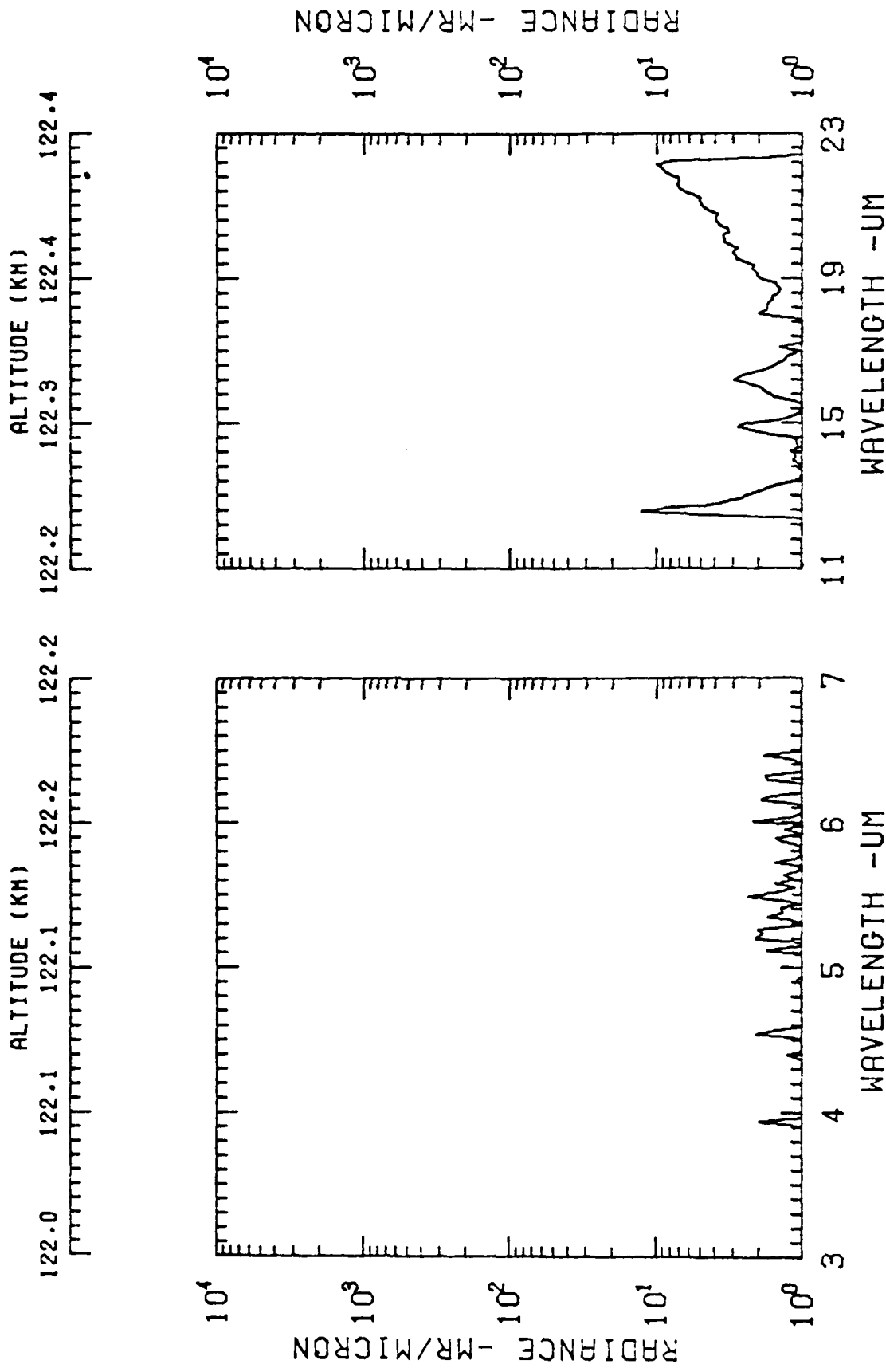


EXC00E SPECTRAL SCAN 1073 TAL= 127.5 ALT= 111.5 ALL GAIN CAL. 53

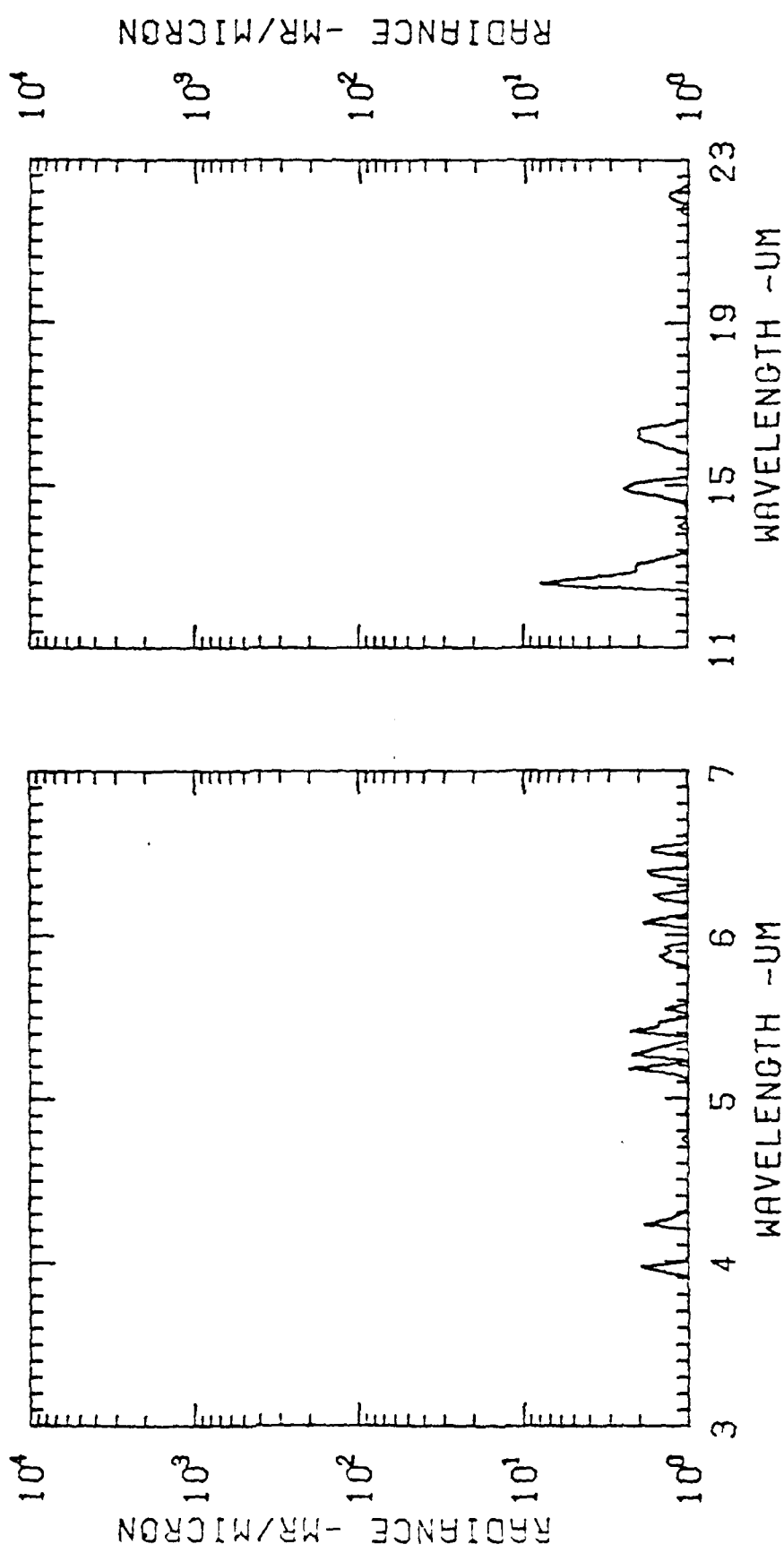


EXC EDE SPECTRAL SCAN 1090 TAL= 148.1 ALT= 121.1 ALL GAIN CAL. 53

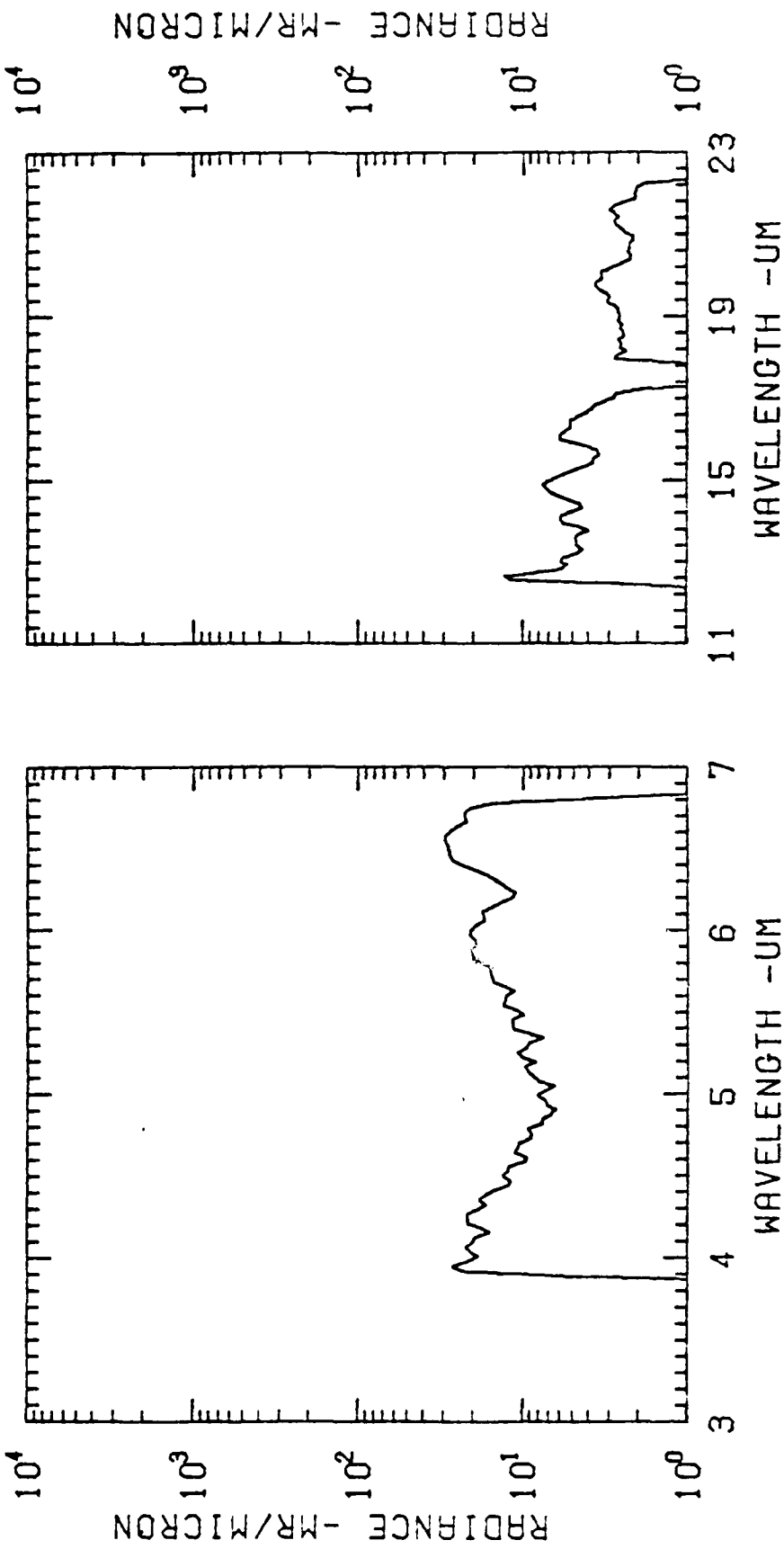
EXCDE SPECTRAL SCAN 1092 TAL= 150.5 ALT= 122.0 ALL GAIN CAL. 53

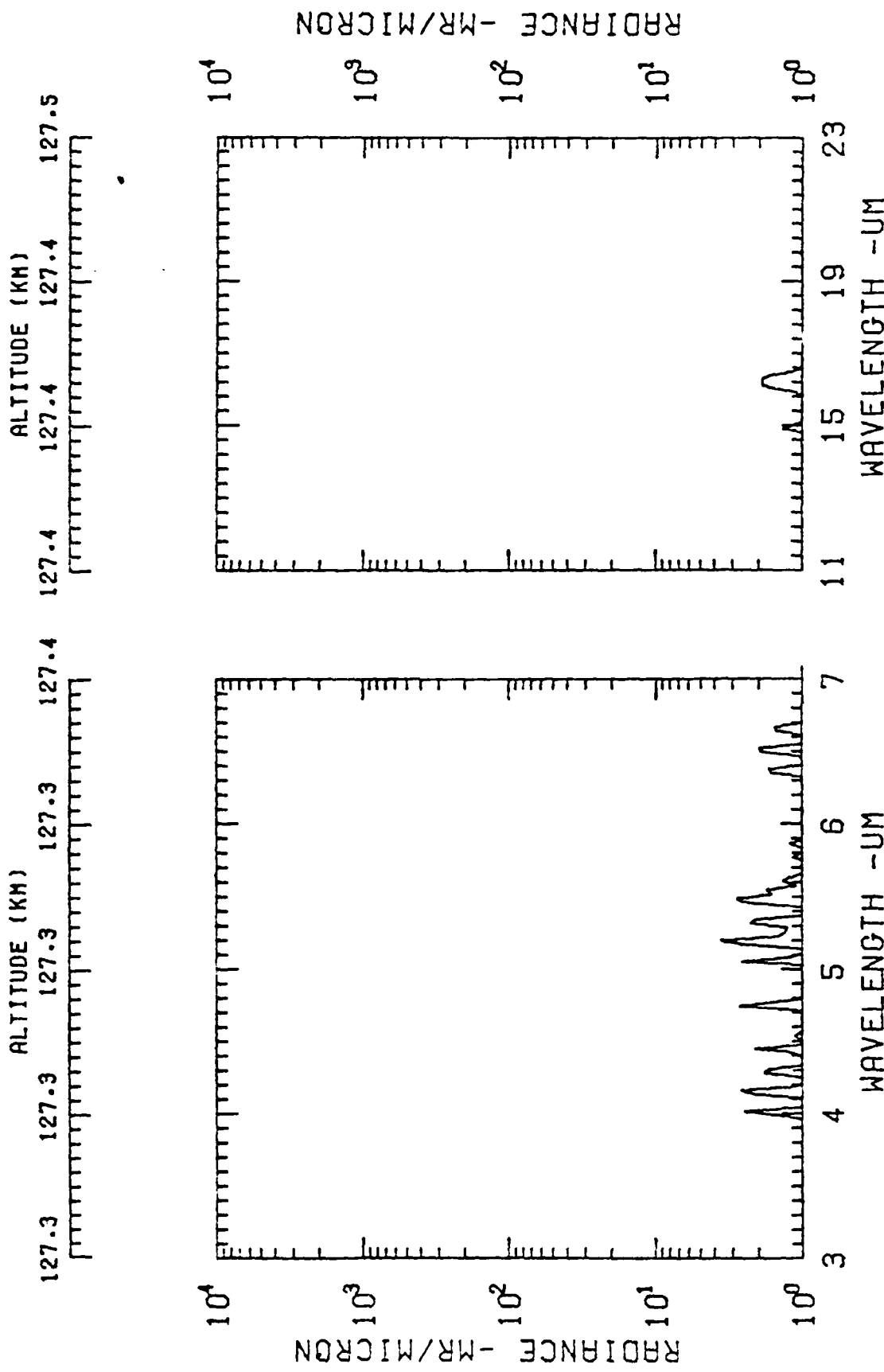


EXC 2000 SPECTRAL SCAN 1093 TBL = 151.7 ALT = 122.4 ALL GAIN CAL. 53



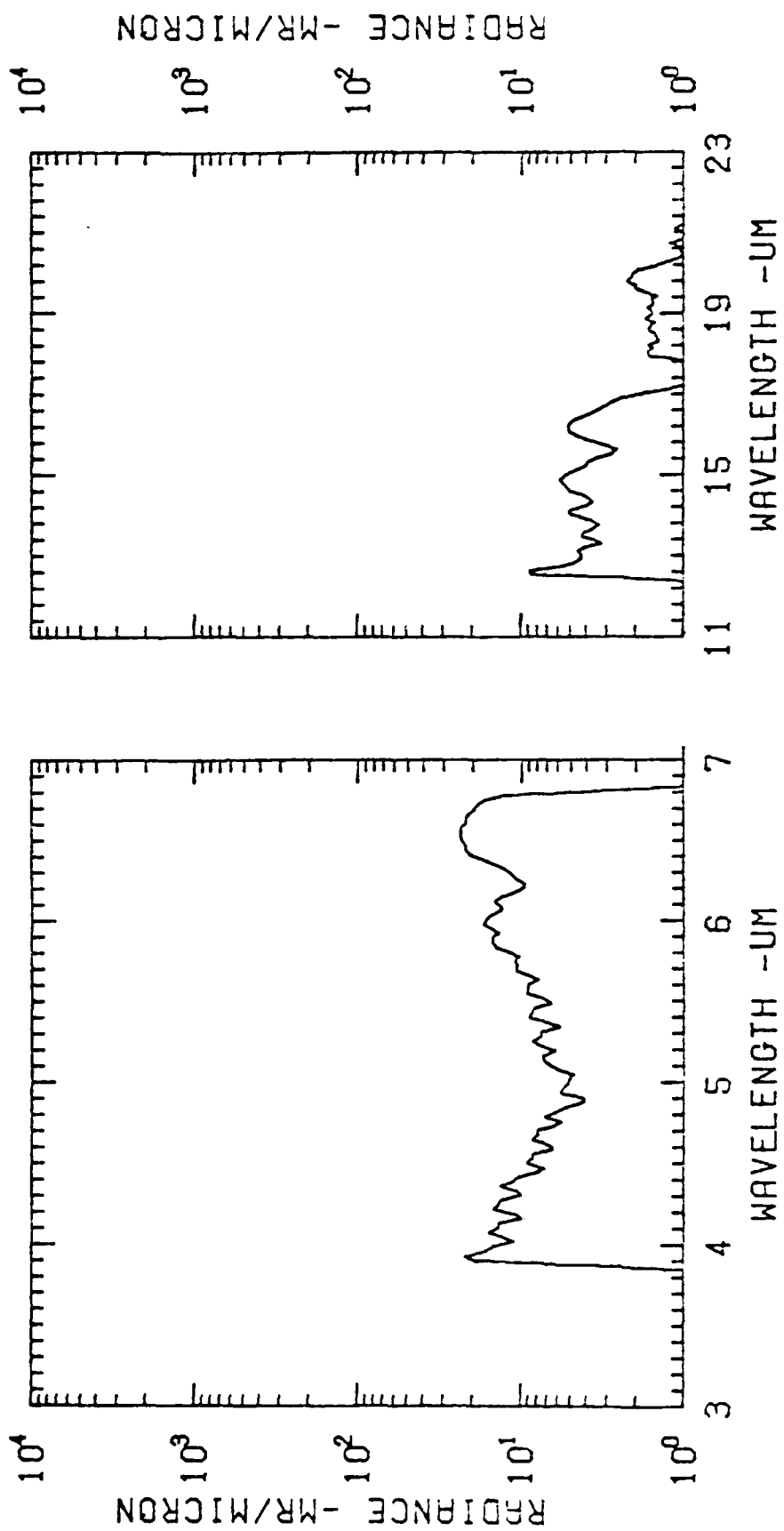
EXCDE SPECTRAL SCAN 1095 TAL= 154.1 ALT= 123.2 ALL GAIN CAL. 53

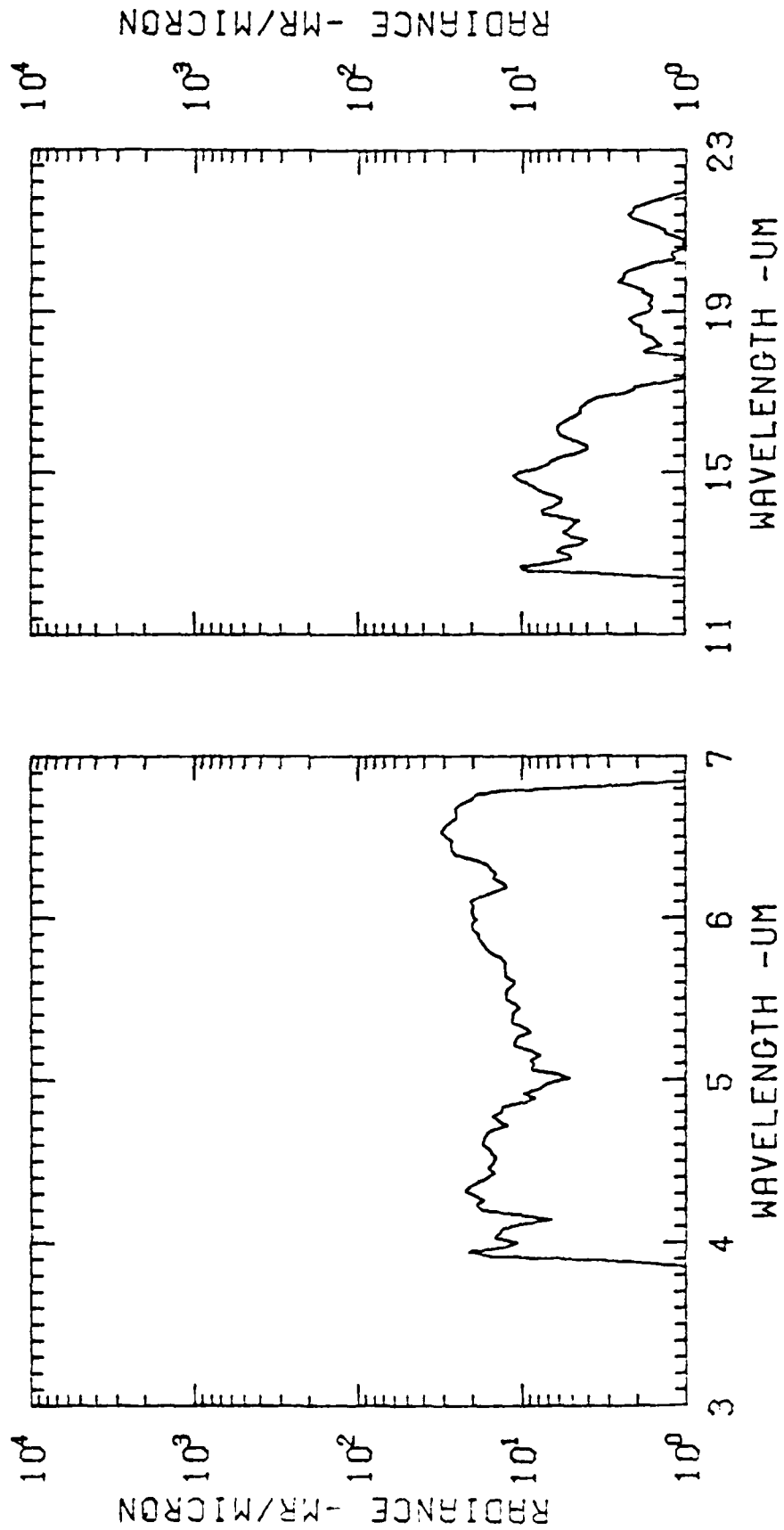




EXC EDE SPECTRAL SCAN 1109 TAL= 171.3 ALT= 127.3 ALL GAIN CAL. 53

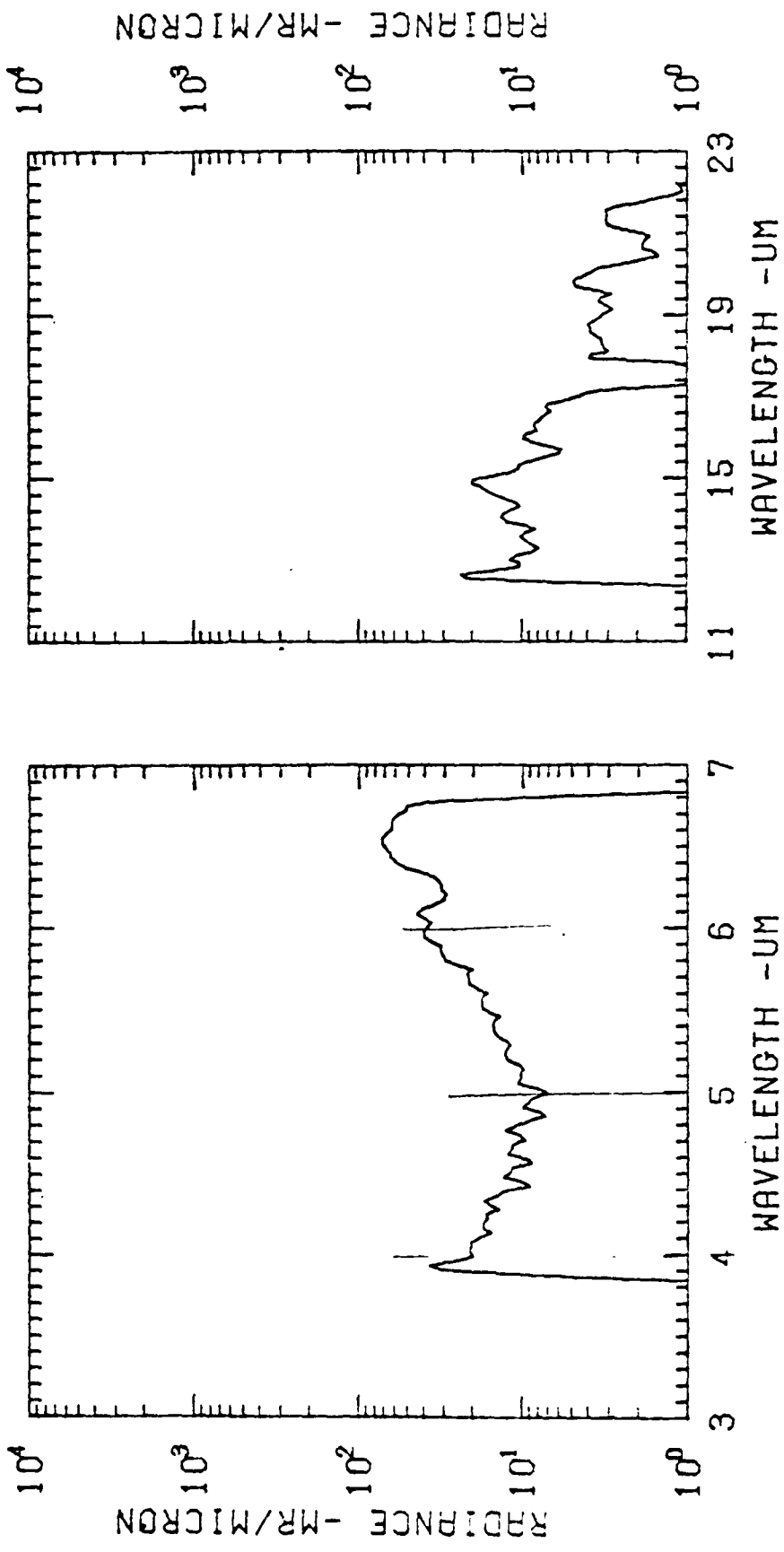
EXC EDE SPECTRAL SCAN 1111 ALT= 173.8 ALT= 127.6 ALL GAIN CAL. 53



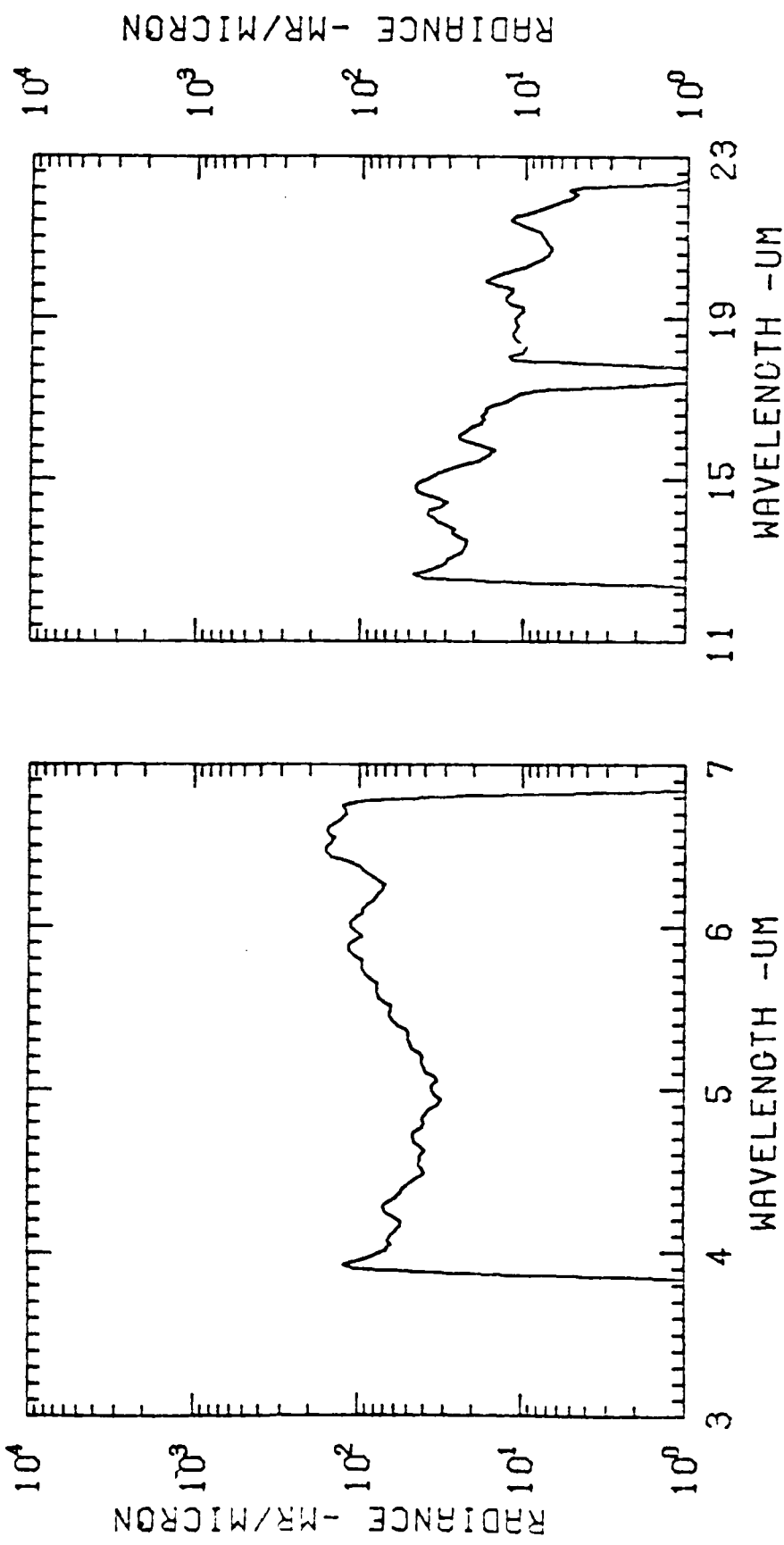


EXCDEE SPECTRAL SCIN 115g TAIL= 233.0 ALT= 118.9 ALL GAIN CAL: 53

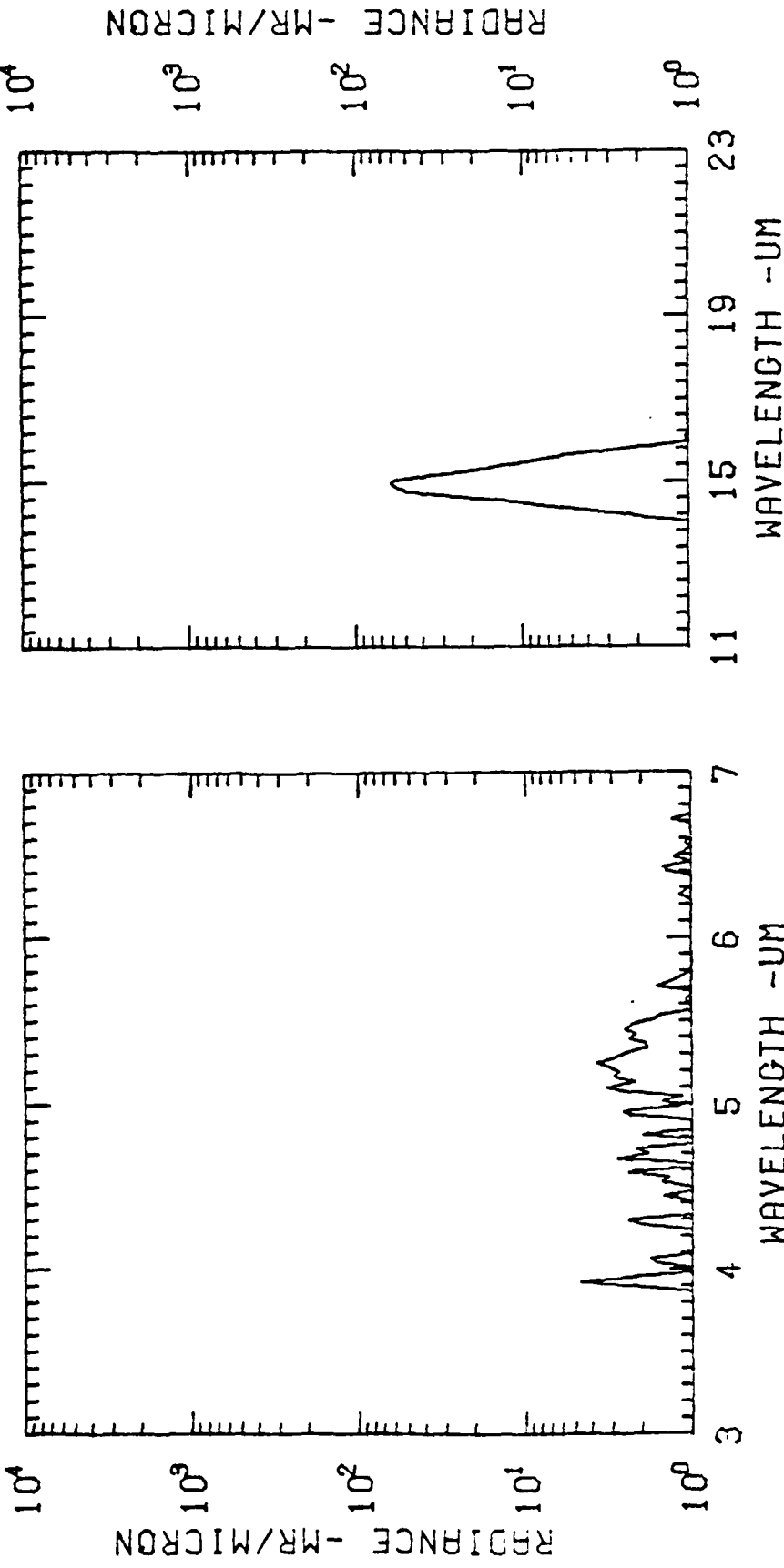
EXC EDE SPECTRAL SCAN 1171 TAL = 247.0 ALT = 112.0 ALL GAIN CAL. 53

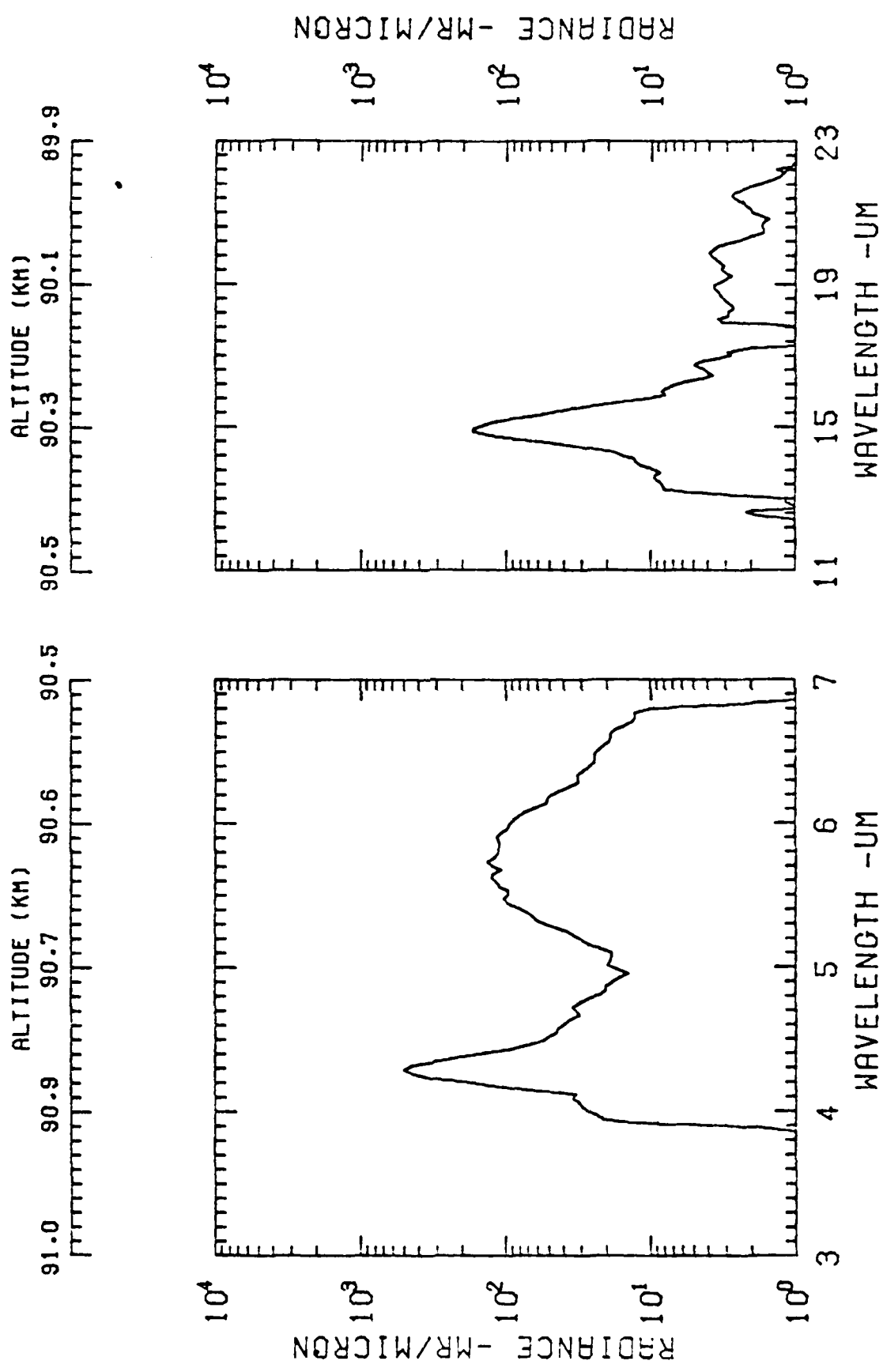


ALTITUDE (KM) 105.5 105.4 105.3 105.2 105.0 105.0 104.9 104.8 104.6



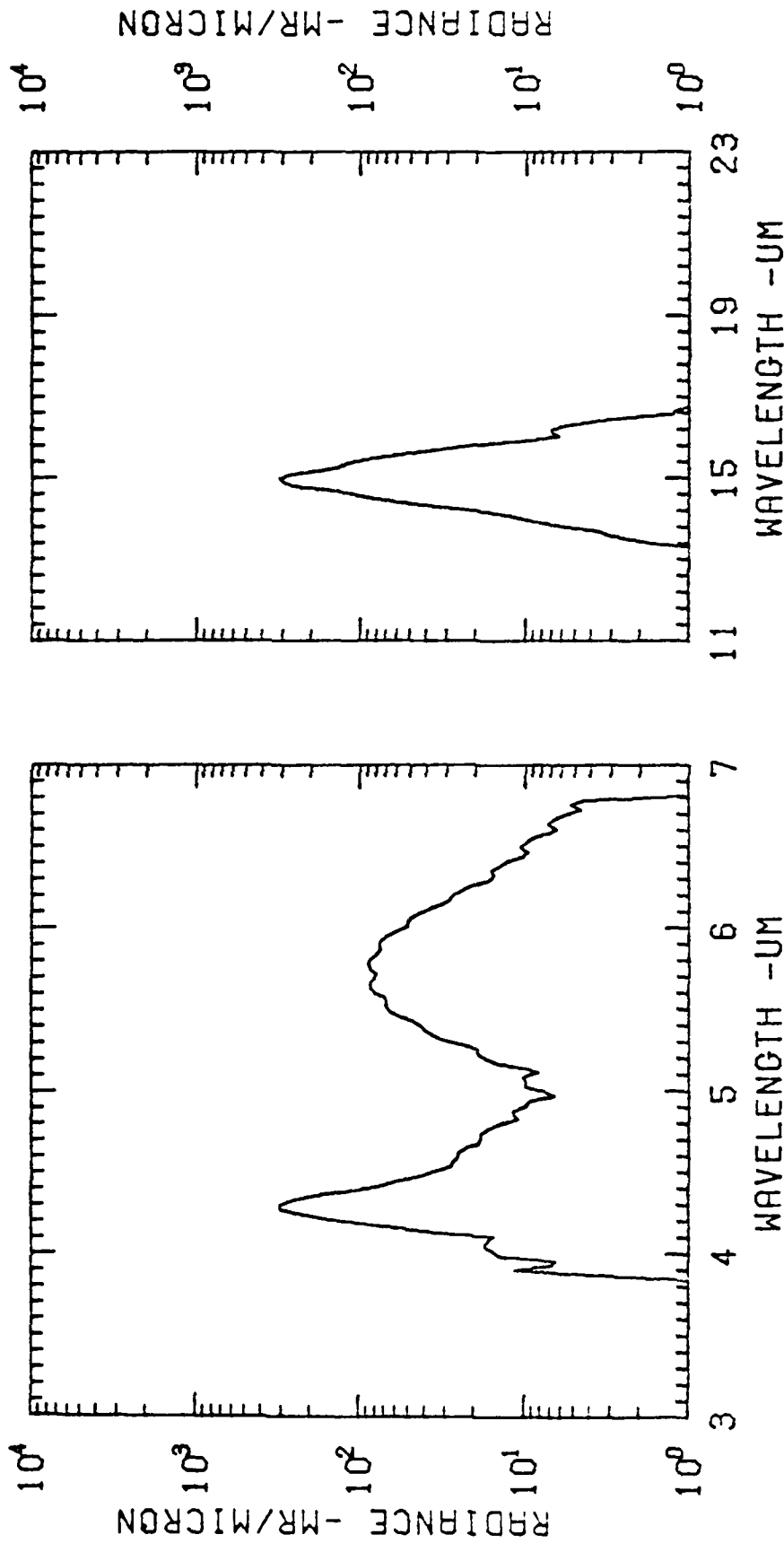
98.7 98.6 98.4 (KM) 98.3 98.2 98.0 97.9 97.7
 ALTITUDE (KM)





EXCDE SPECTRAL SCAN 1196 TAL= 277.2 ALT= 91.0 ALL GAIN CAL. 53

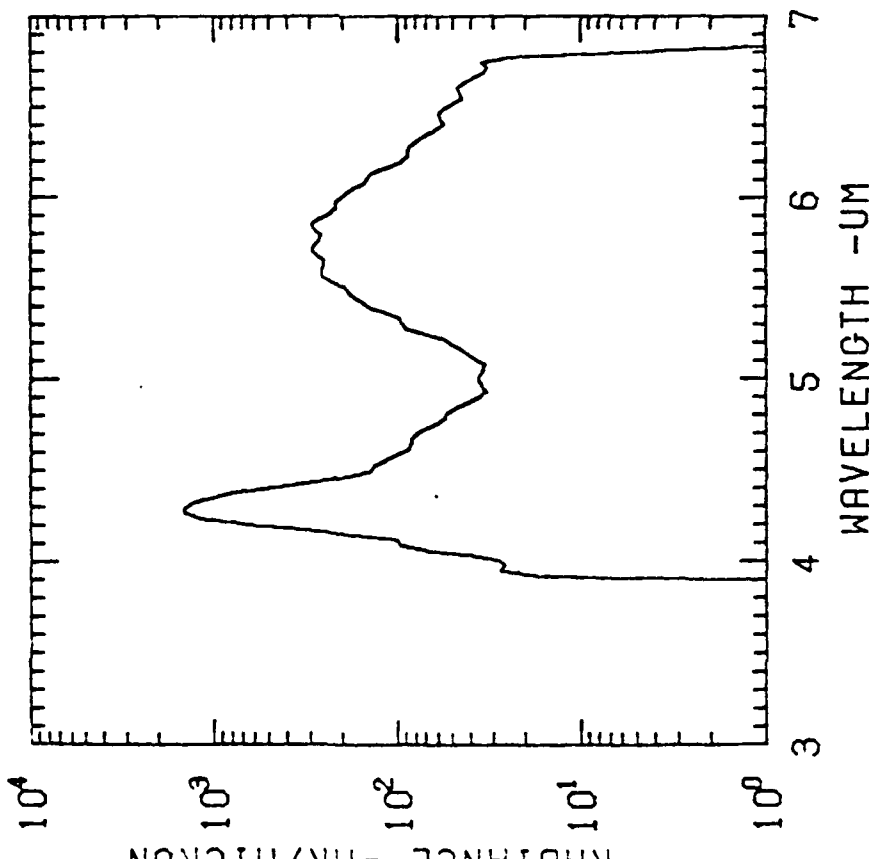
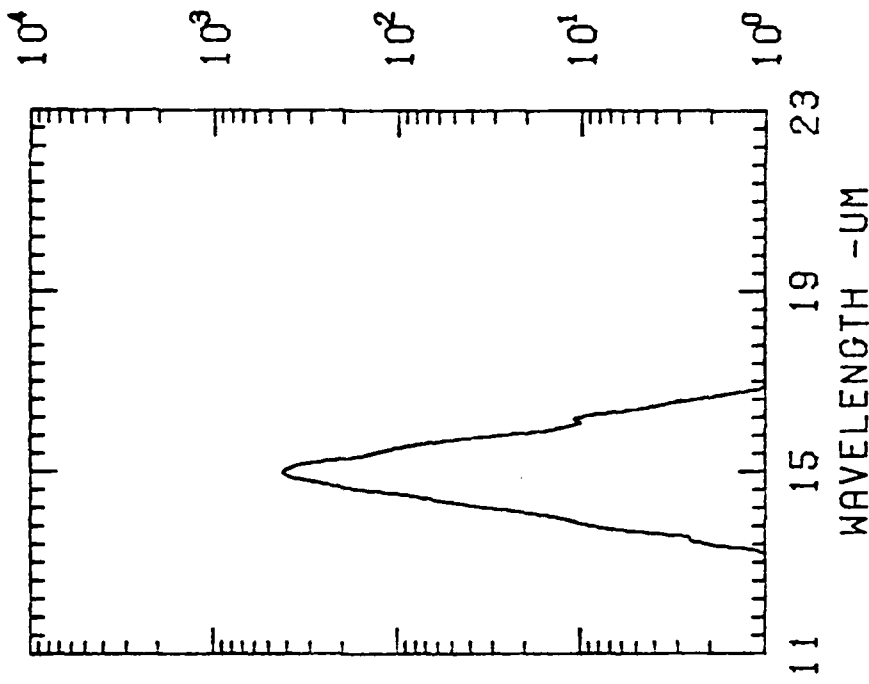
ALTITUDE (KM) ALTITUDE (KM)
 86.9 86.7 86.6 86.4 86.3 86.3 86.1 85.9 85.7



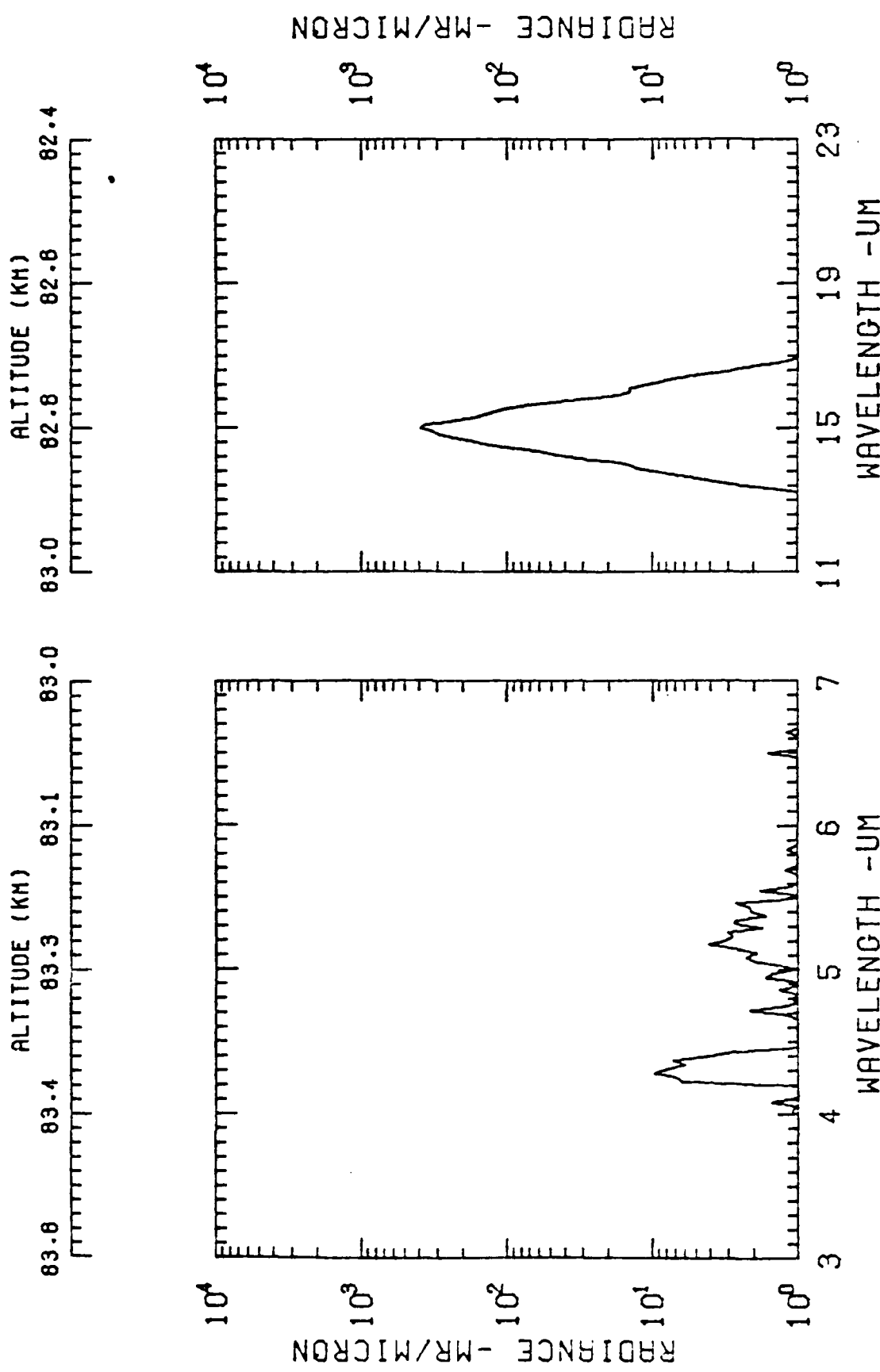
EXCITE SPECTRAL SCAN 1200 TAL= 282.0 ALT= 86.8 ALL GAIN CAL. 53

84.7 84.5 84.4 84.3 84.1 84.1 83.9 83.7 83.5

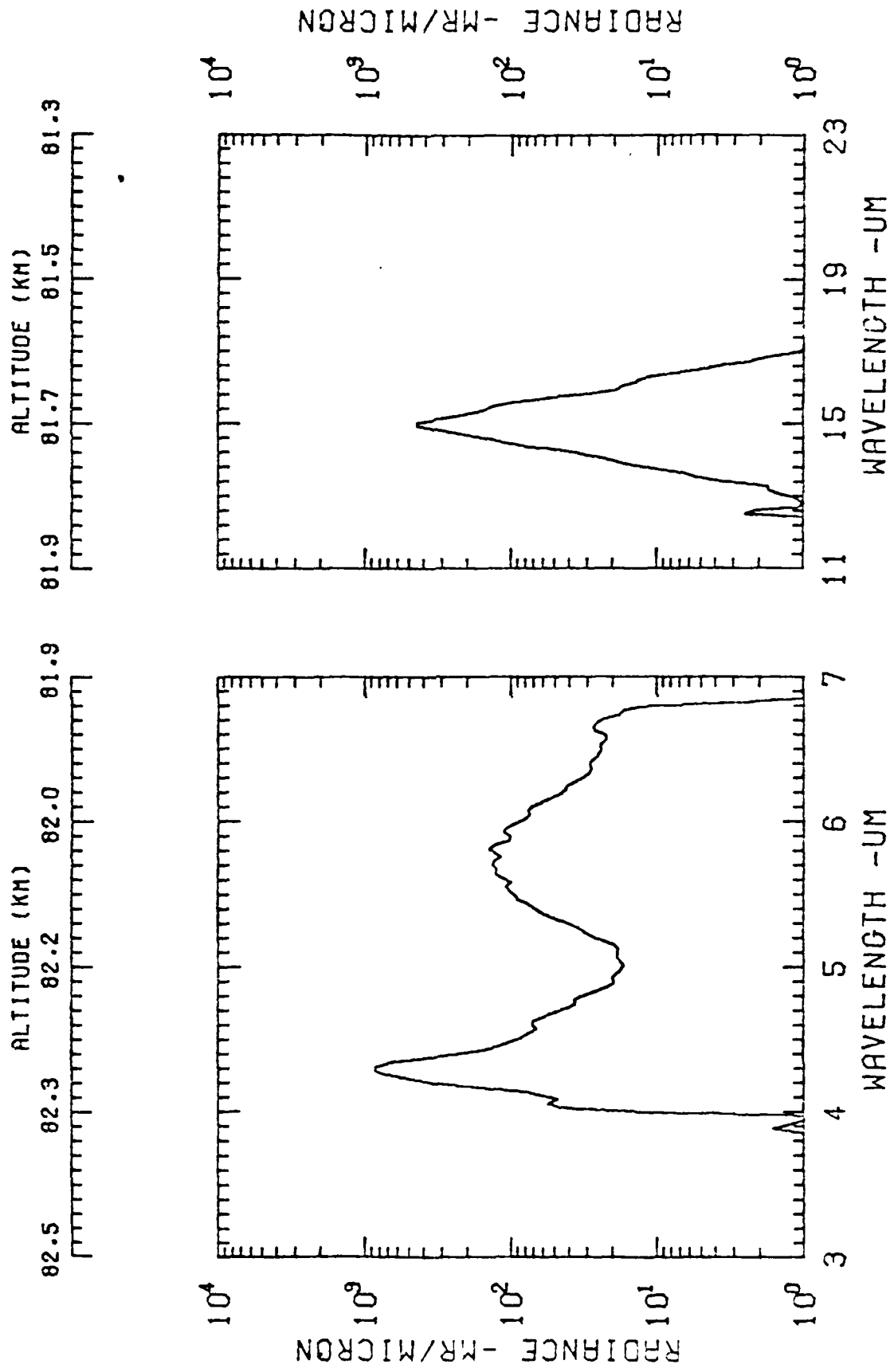
RADIANCE - MR/MICRON



EXCÉDE SPECTRAL SCAN 1202 TAL= 284.4 ALT = 84.6 ALL GAIN CAL. 53

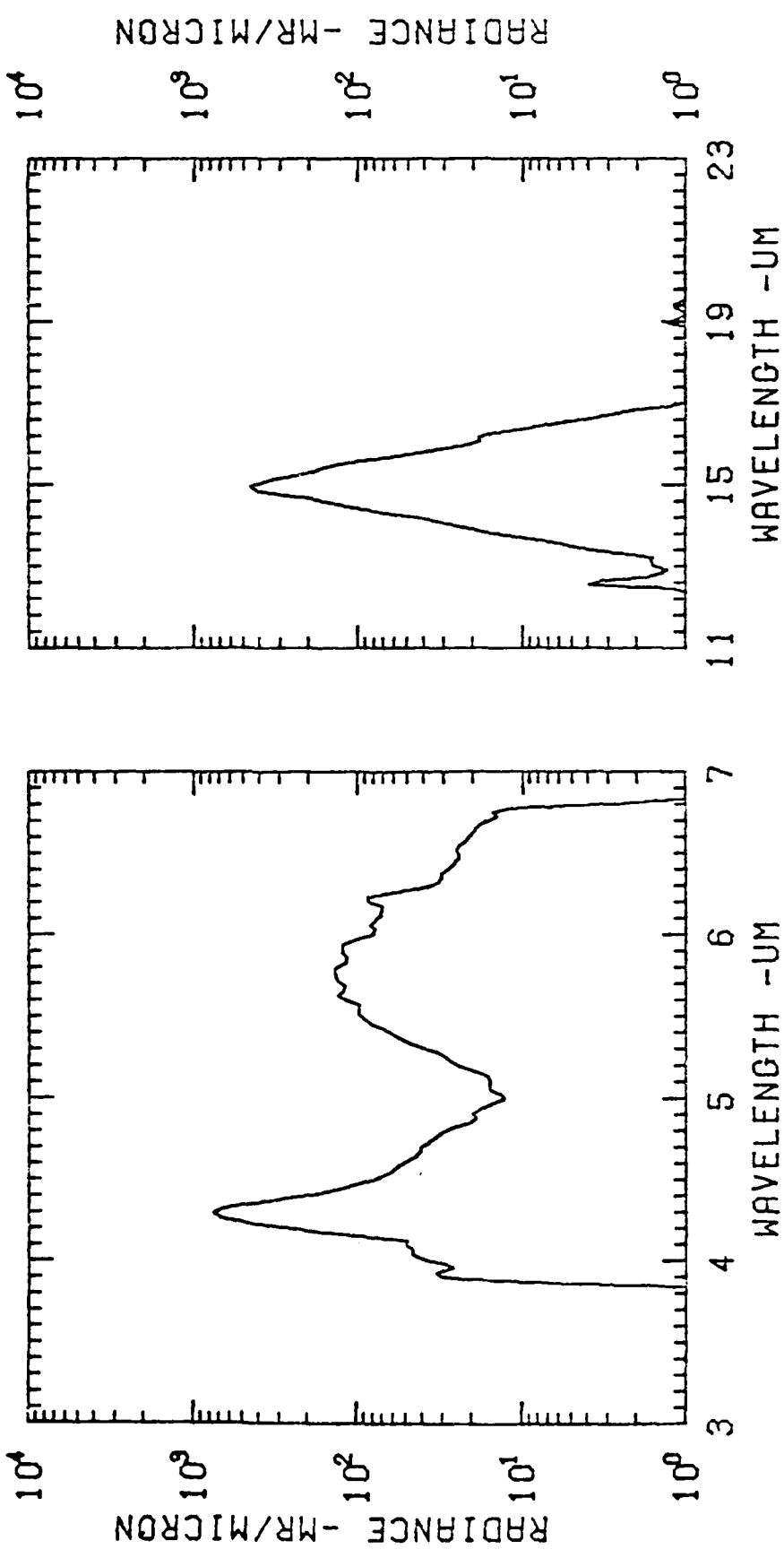


EXCERDE SPECTRAL SCAN 1203 TAL= 285.6 ALT= 83.5 ALL GAIN CAL. 53

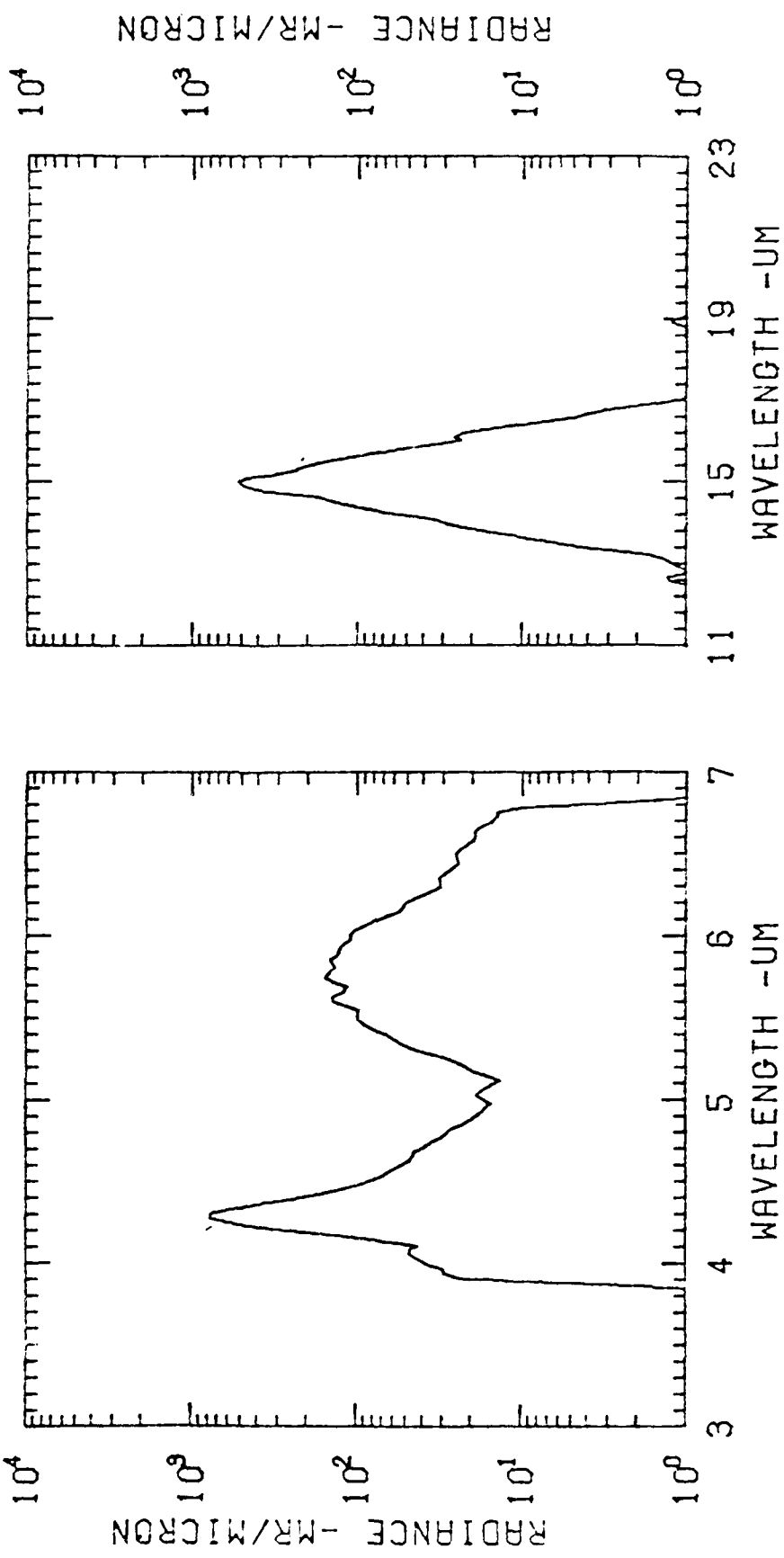


EXCITE SPECTRAL SCAN 1204 TAL= 286.8 ALT= 82.4 ALL GAIN CAL. 53

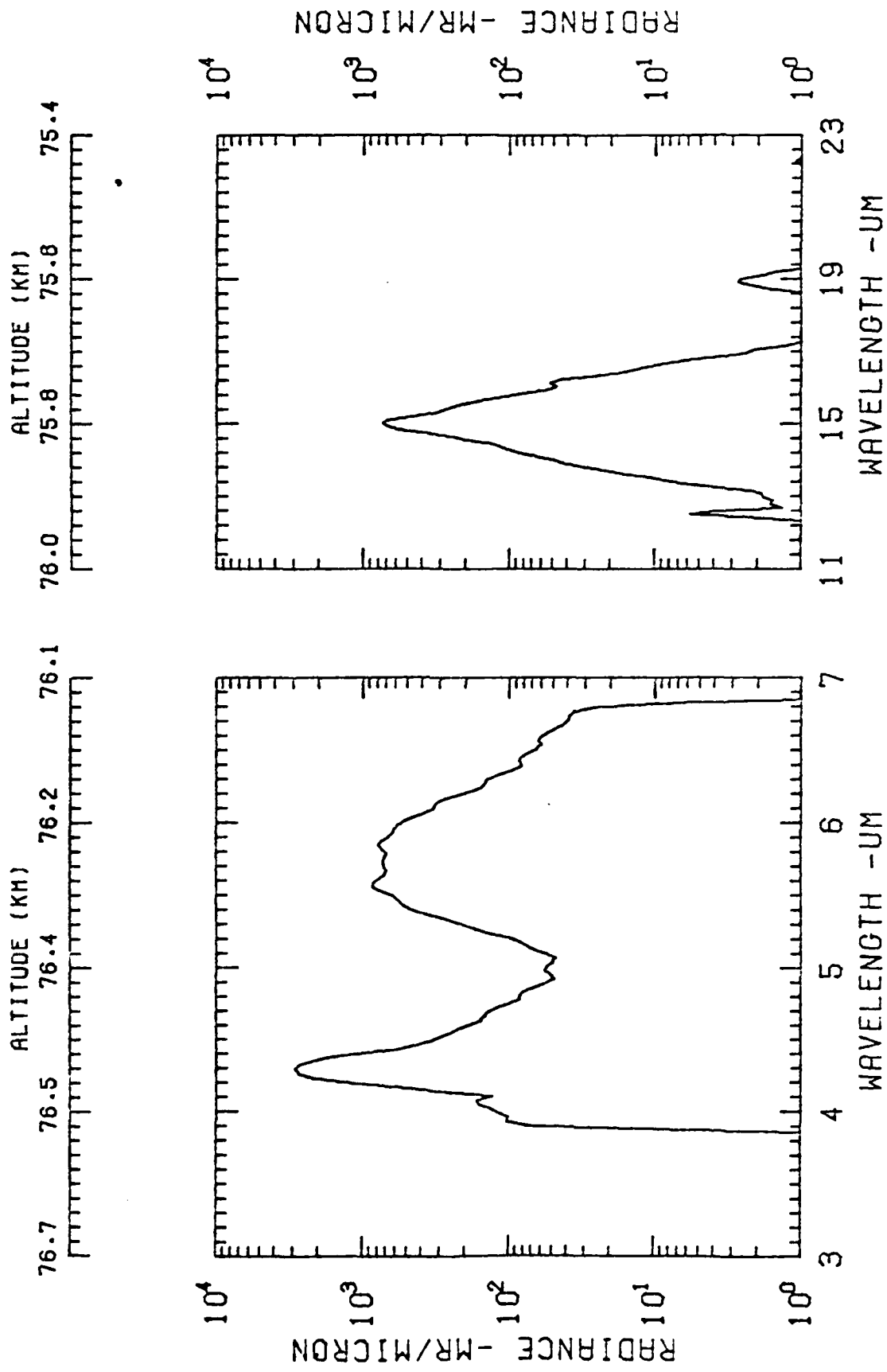
EXCDE SPECTRAL SCAN 1205 TAL= 288.0 ALT= 81.3 ALL GAIN CAL. 53



EXC EDE SPECTRAL SCAN 1206 TAL= 209.2 ALT= 80.2 ALL GAIN CAL. 53

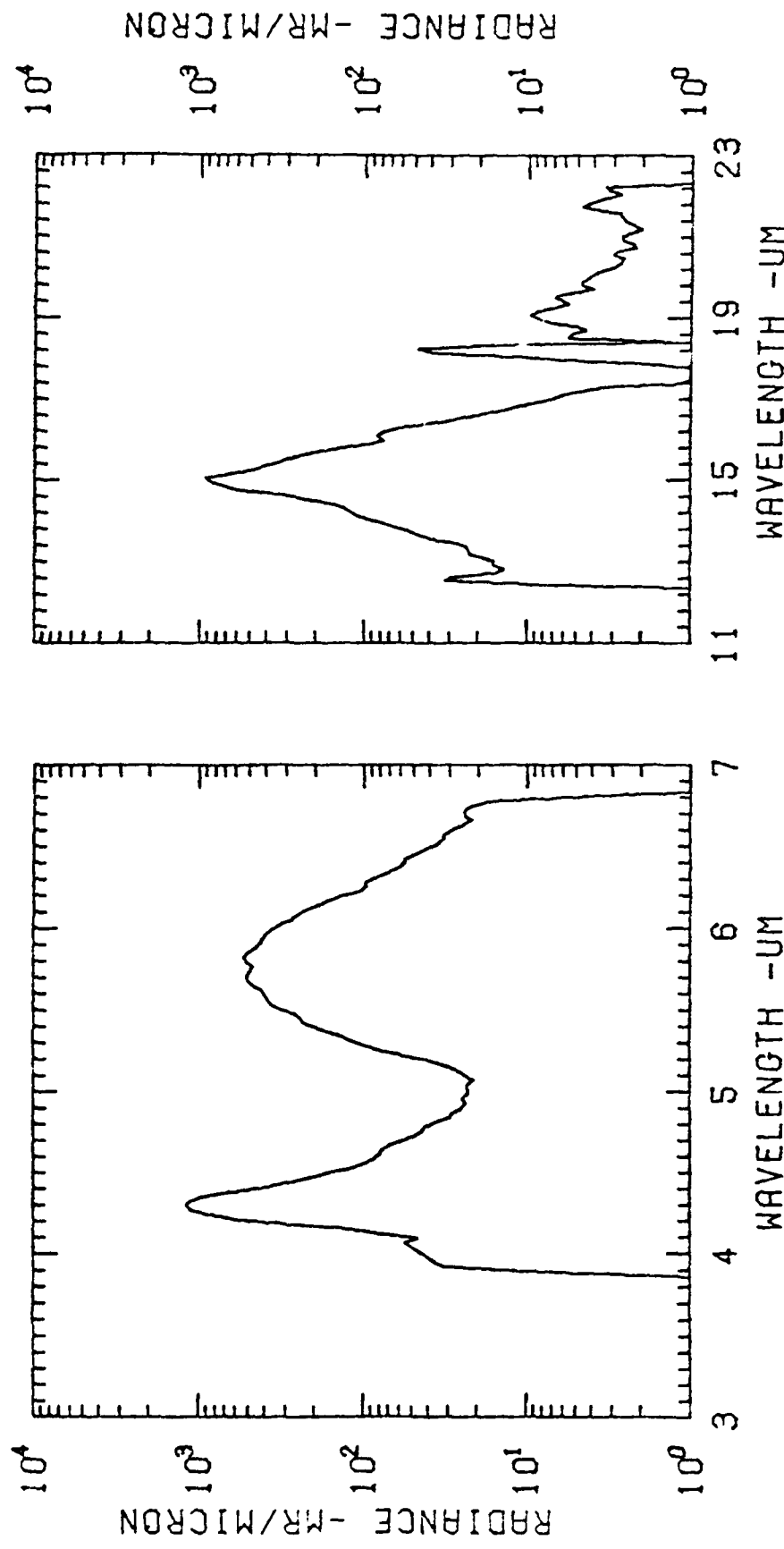


Y
ALTITUDE (KM)
80.2 80.1 79.9 79.7 79.6 79.4 79.2 79.0



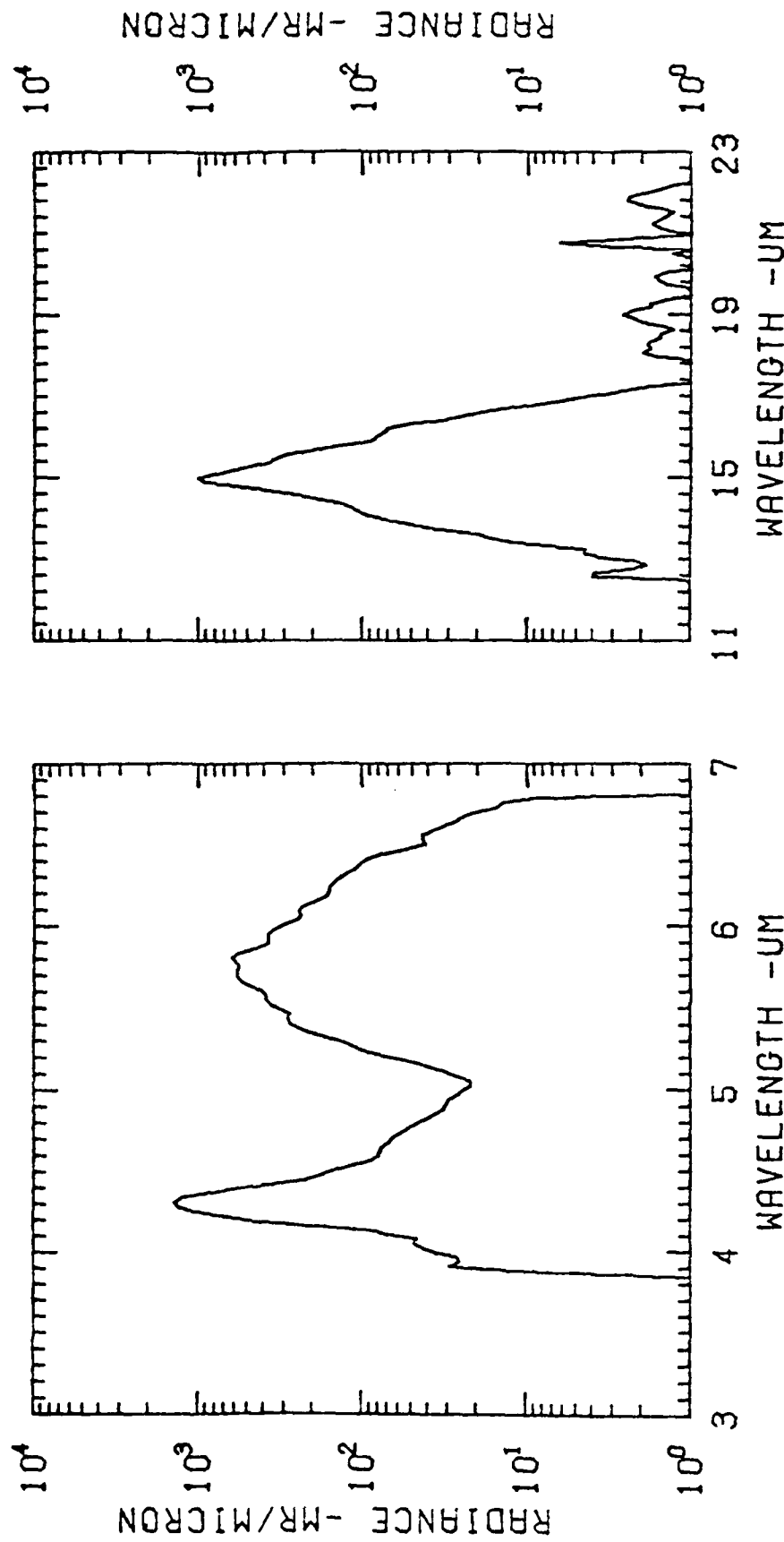
EXCDE SPECTRAL SCAN 1209 TAL= 292.0 ALT= 76.6 ALL GAIN CAL. 53

ALTITUDE (KM) 75.3 75.2 75.0 74.8 74.6 74.4 74.2



EXCDE SPECTRAL SCAN 1210 TAL= 294.0 ALT= 75.4 ALL GAIN CAL. 53

74.3 74.1 74.0 73.8 73.6 73.4 73.2 73.0
 ALTITUDE (KM)



EXCDE SPECTRAL SCAN 1211 TAL= 295.3 ALT= 74.2 ALL GAIN CAL. 53

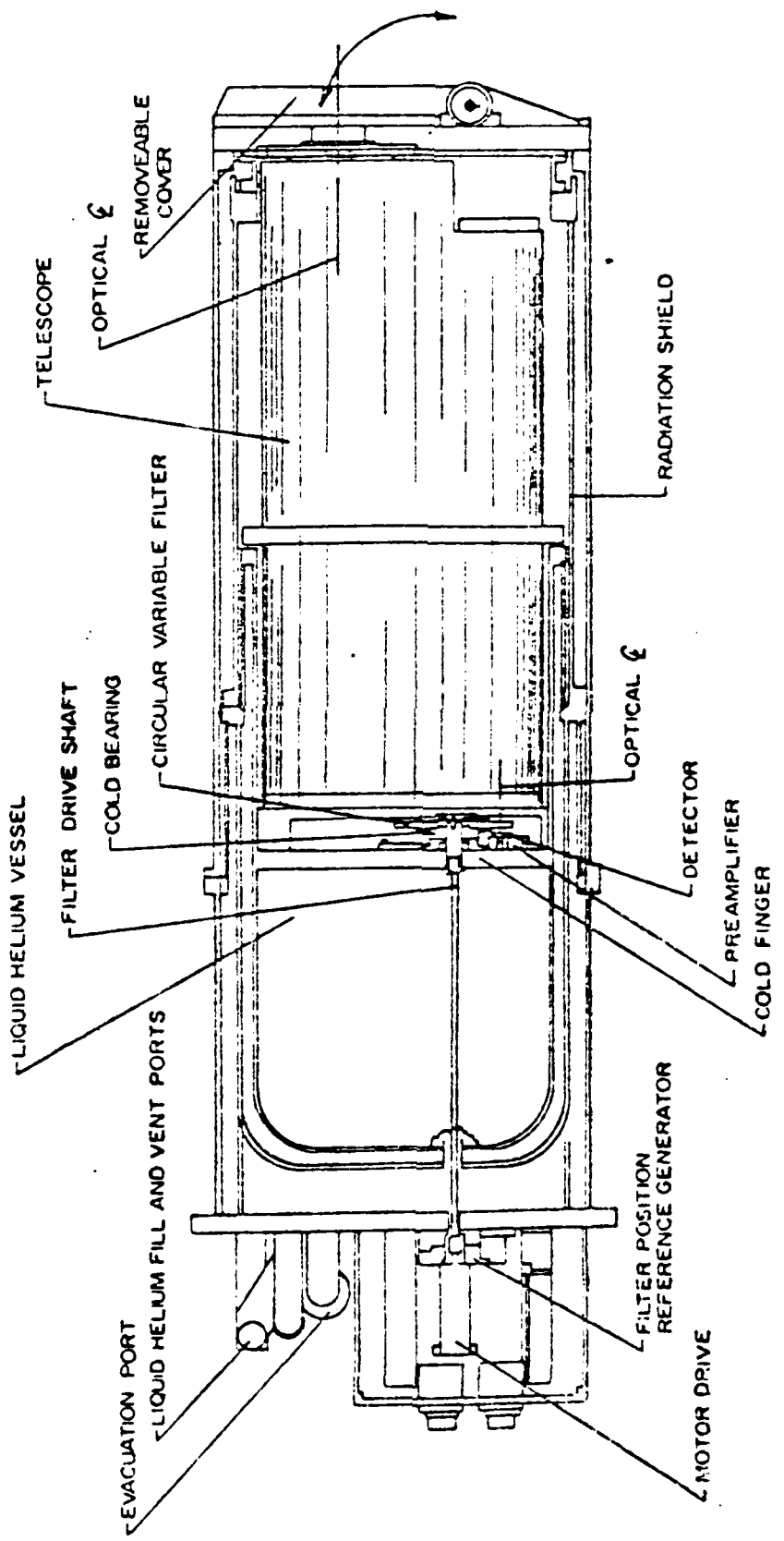


Figure: 2.0-1 Schematic of a typical circular variable filter (CVF) spectrometer.

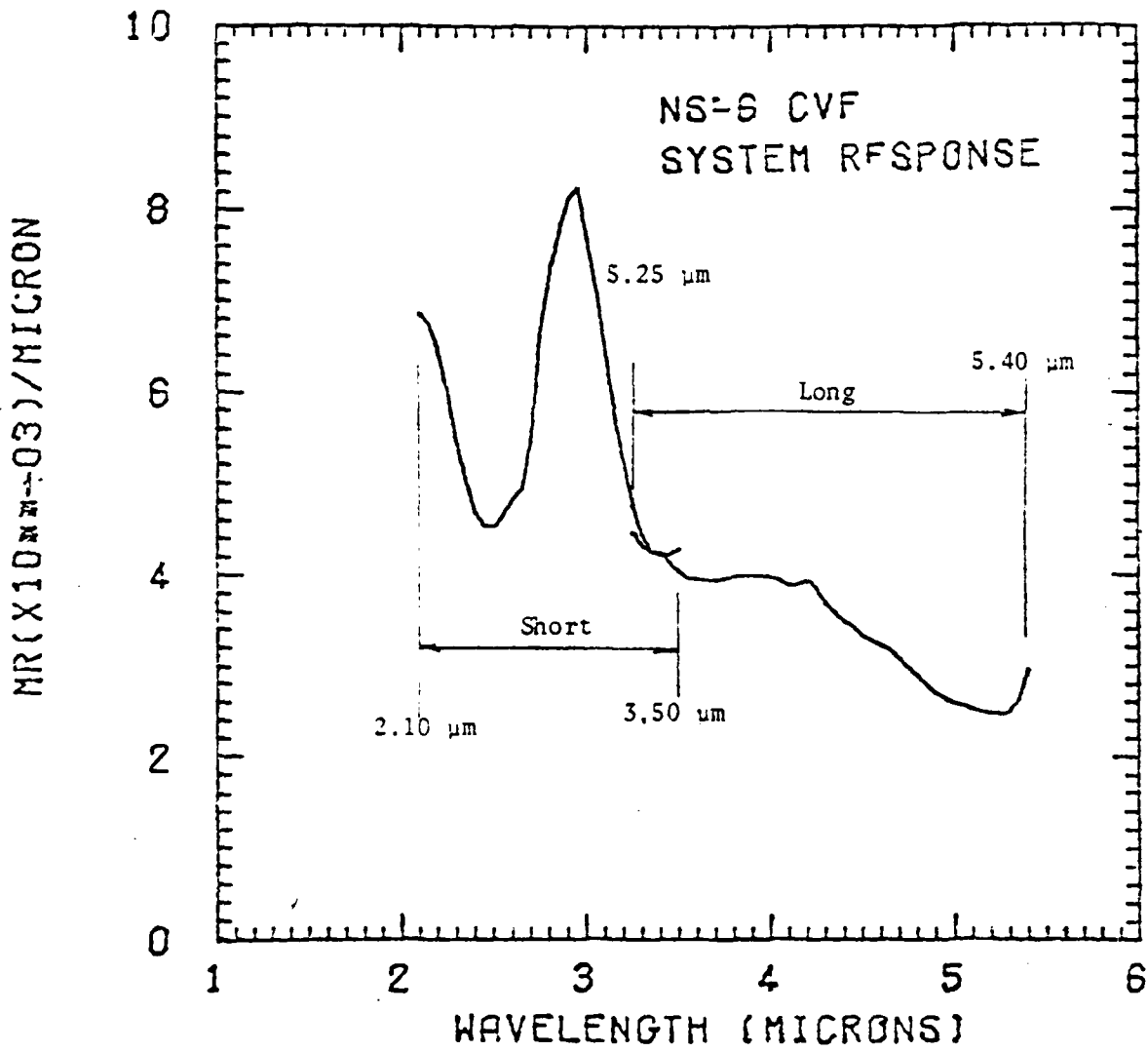


Figure 2.1-1. CVF brightness calibration (NS-6-4)

82.0 82.0 81.9 81.7 81.7 81.7 81.6
ALTITUDE (KM)

EXCIDE SPECTRAL SCAN DATA $\text{Fl}_1 = 287.2$ $\text{Fl}_2 = 82.1$ GMU

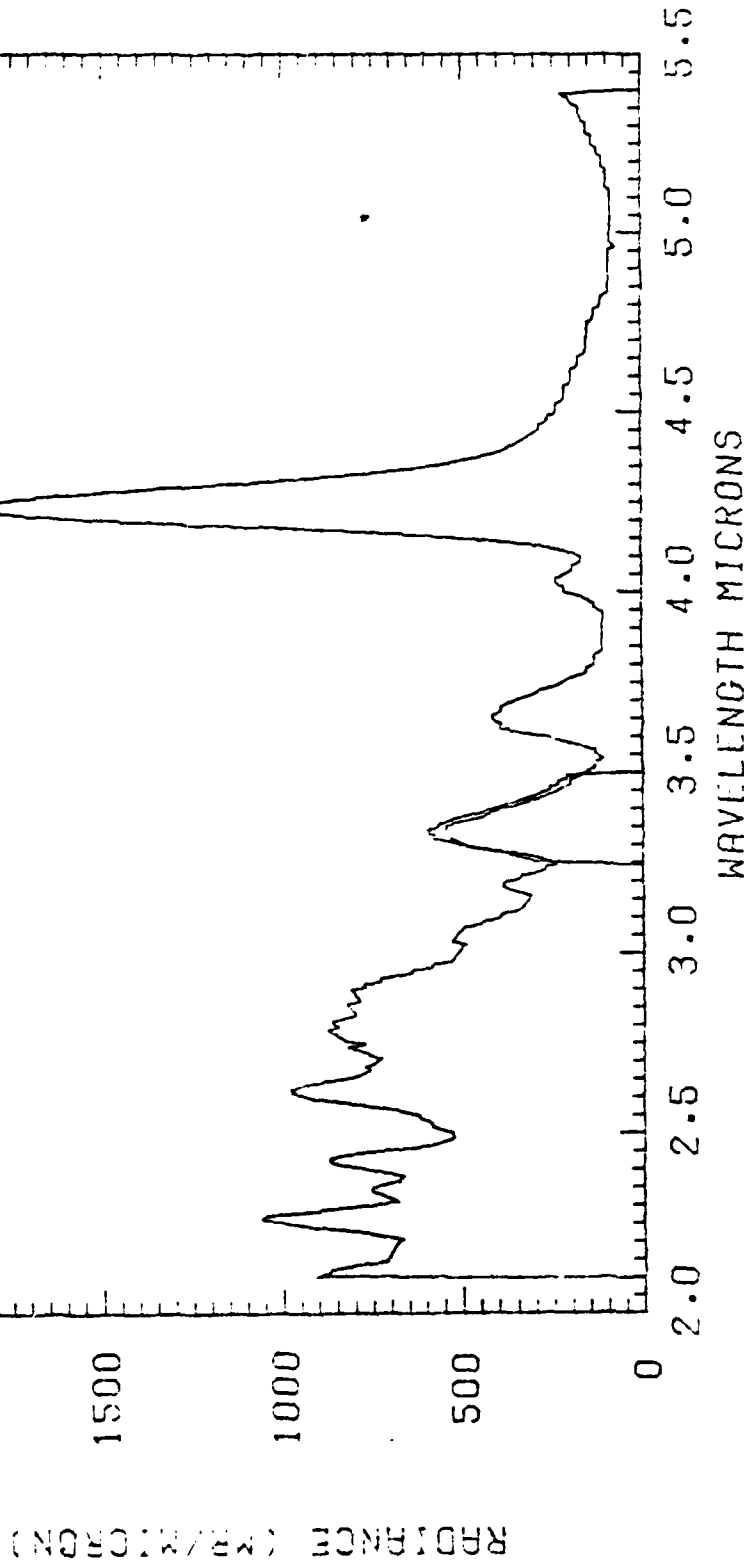


Figure 2.3-1. Sample spectra from EXCIDE short wavelength CVF spectrometer during electron gun operation.

MR/UM-V011

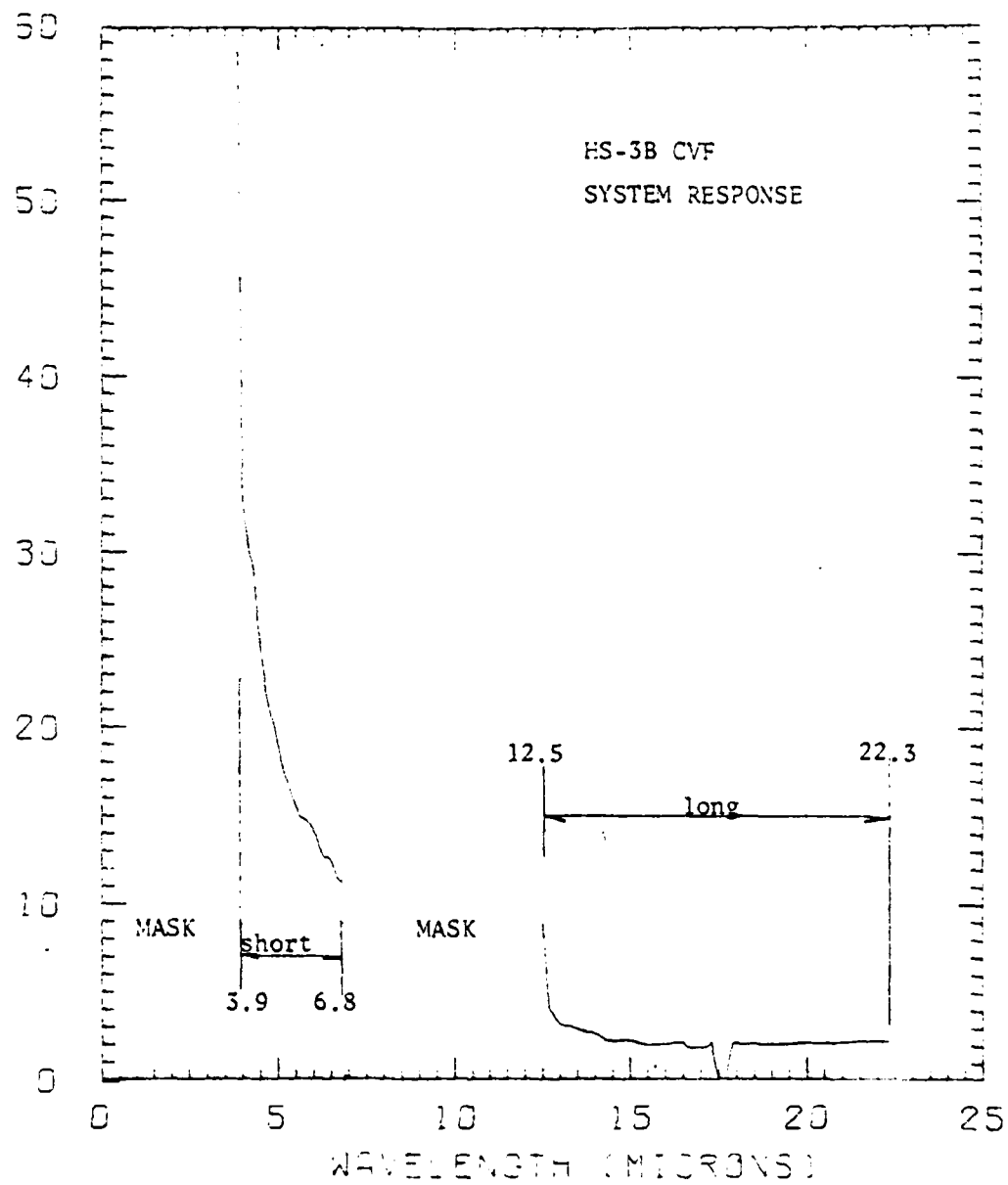


Figure 3.1-1 CVF Brightness Calibration (HS-3B-1)

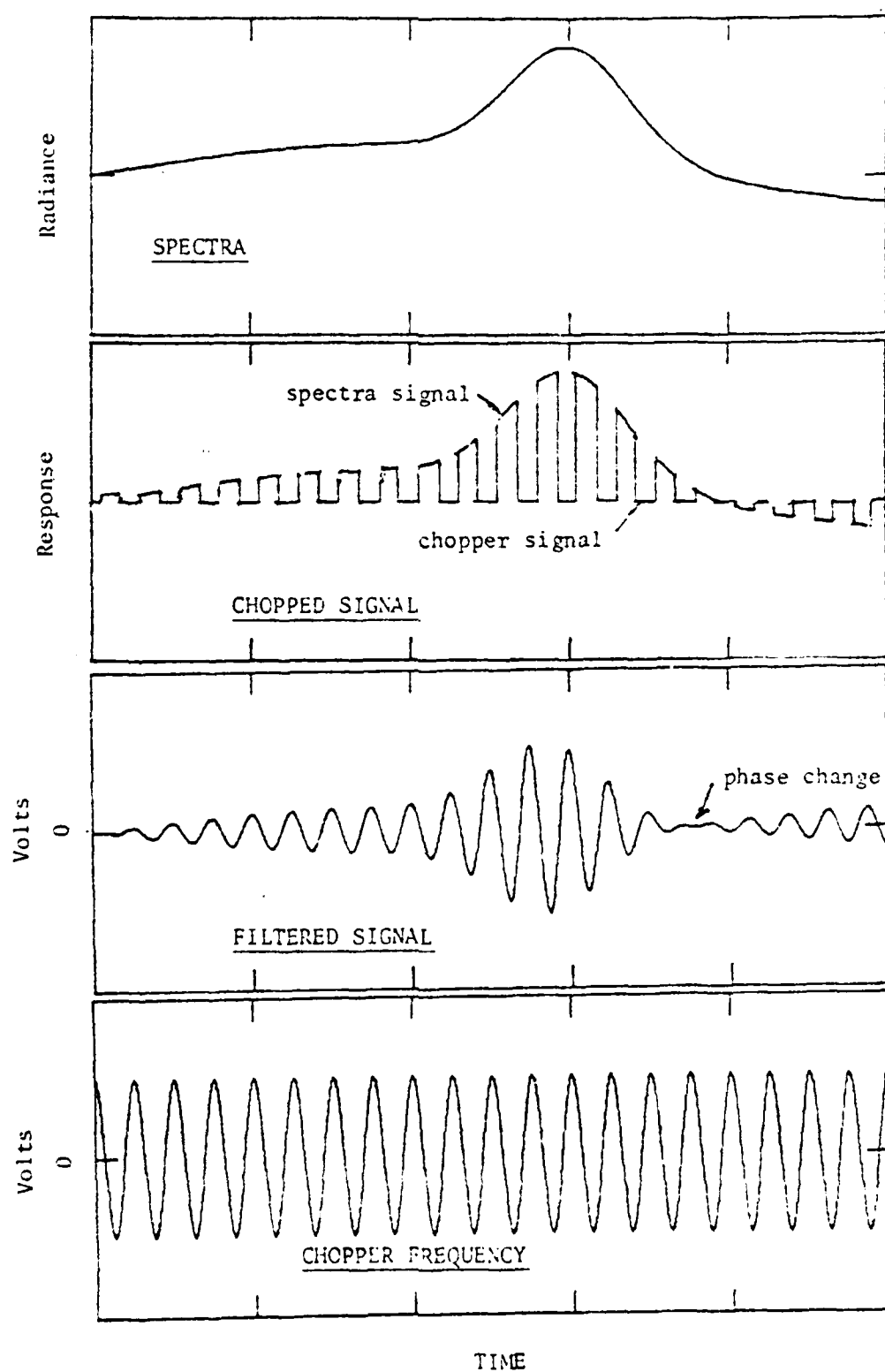


Figure 3.3-1. Principle of optically chopped CVF observation showing phase reversal when source radiance is less than copper radiance.

CHOPPER FIT

B= 194.0954
C= -144.2404
FREQ 106.555

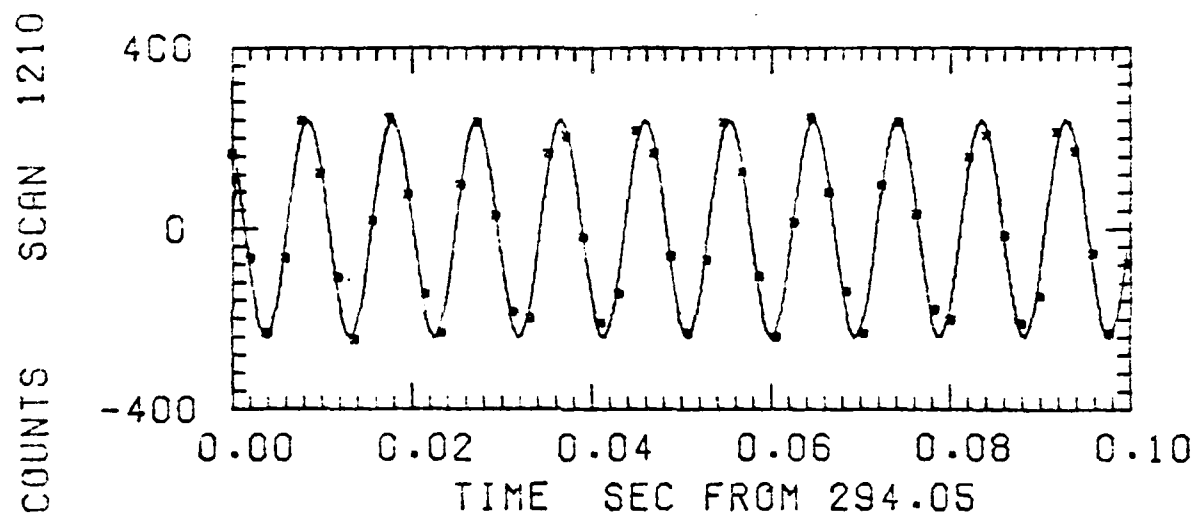
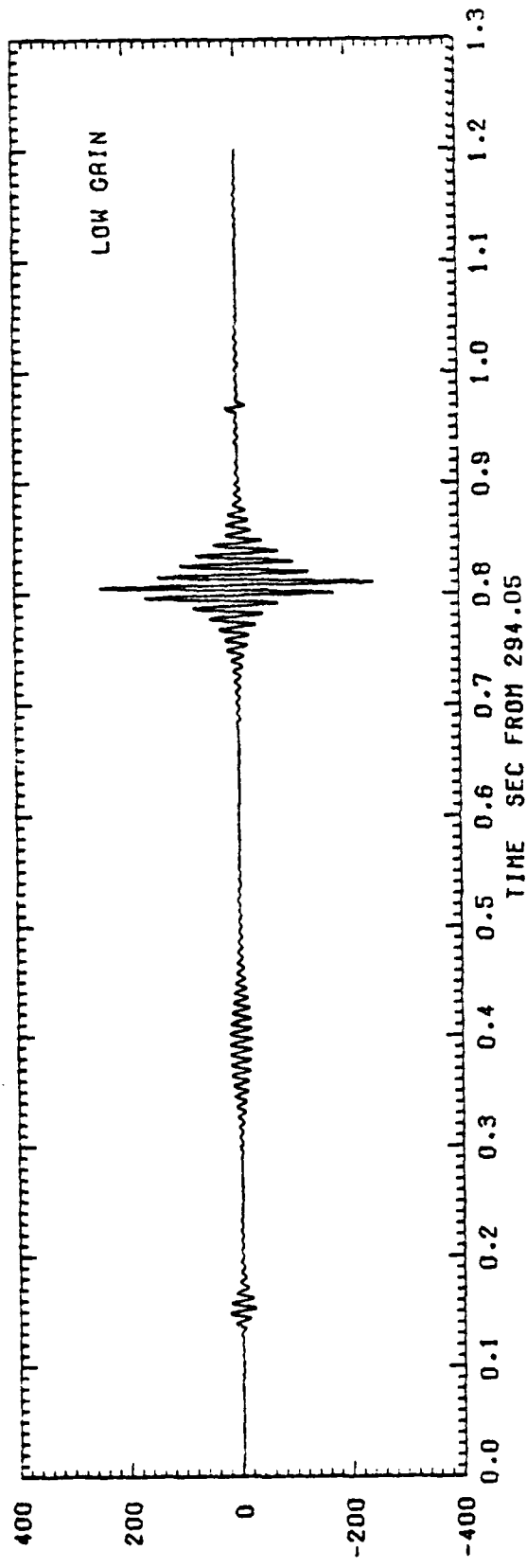


Figure 3.3-2. Example of least squares fit (sinusoid) to chopper signal (solid squares, for spectral scan 1210. Also shown are frequency and constants determined as a result of the best fit.



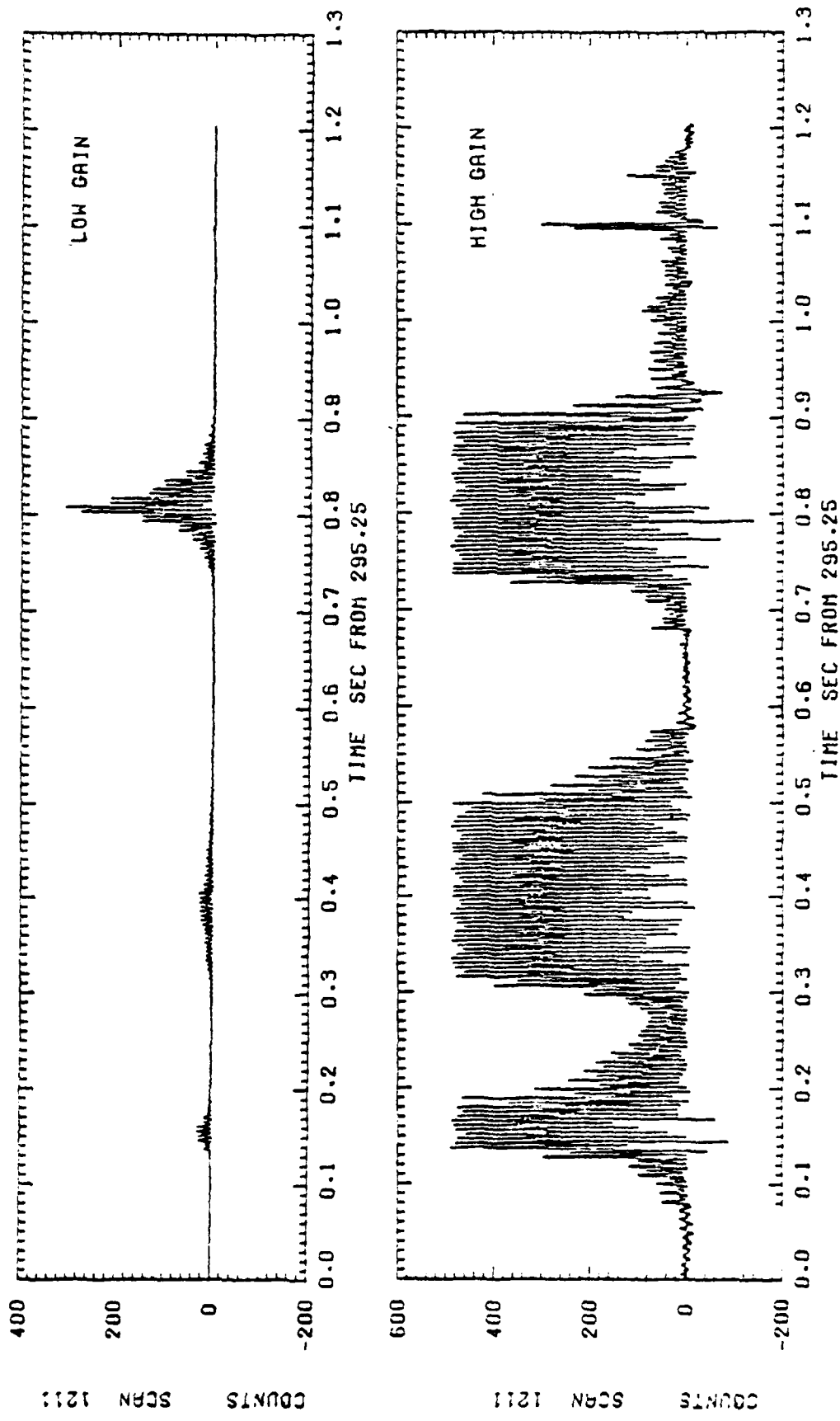


Figure 3, 3-3

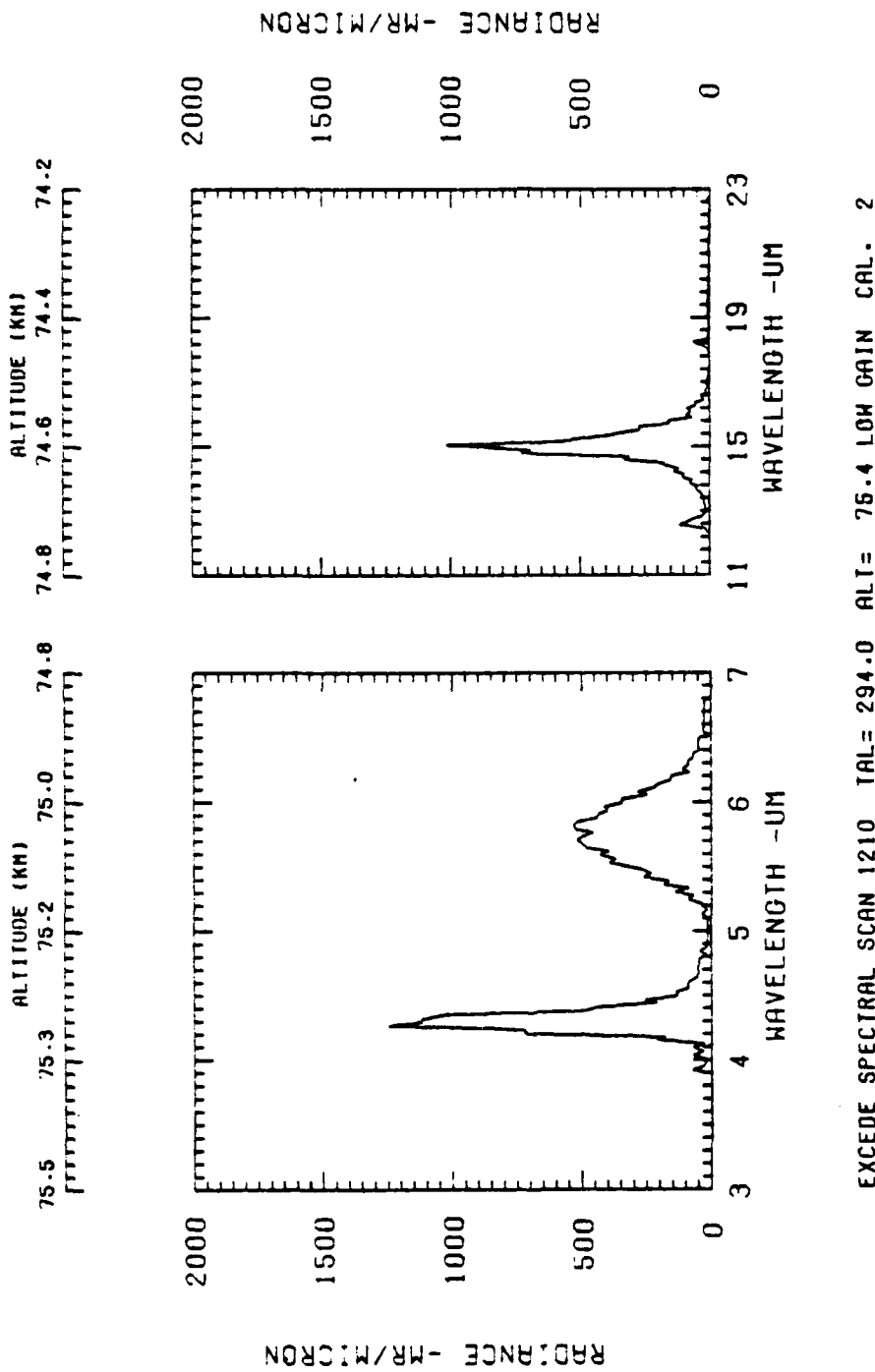


Figure 3.3-4 Example of unfiltered spectrum obtained with the EXCITE chopped CVF.

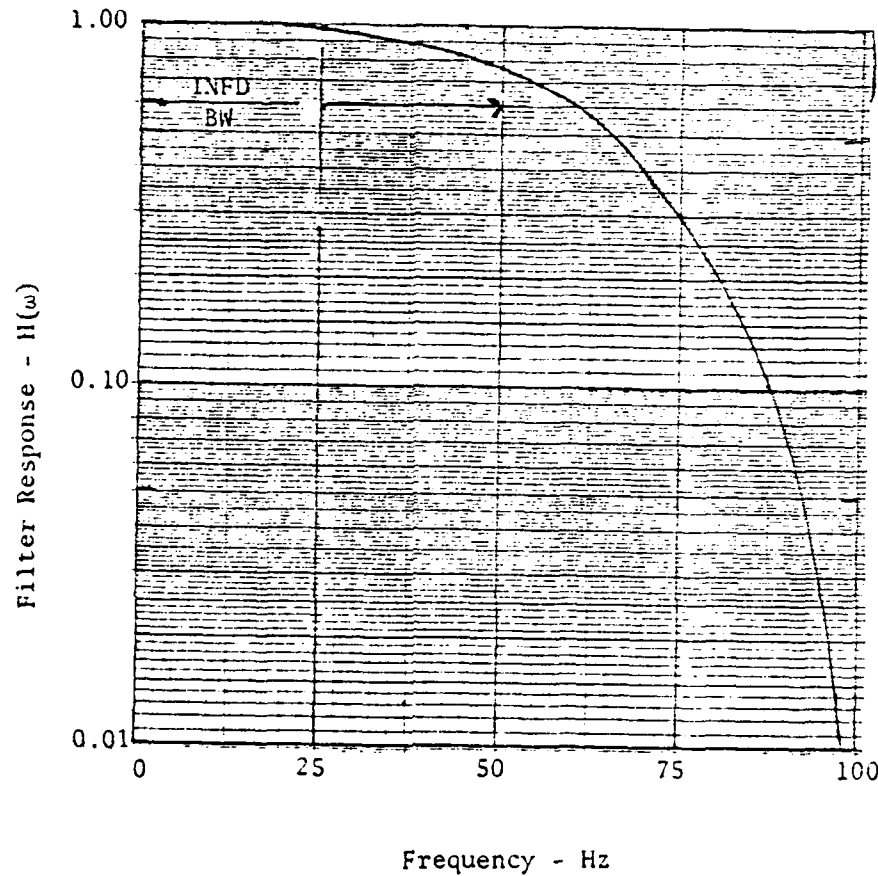


Figure 3.3-5. Frequency response of smoothing filter used after decimating data base to a sampling frequency of 205 Hz EXCEDE information bandwidth is 50 Hz.

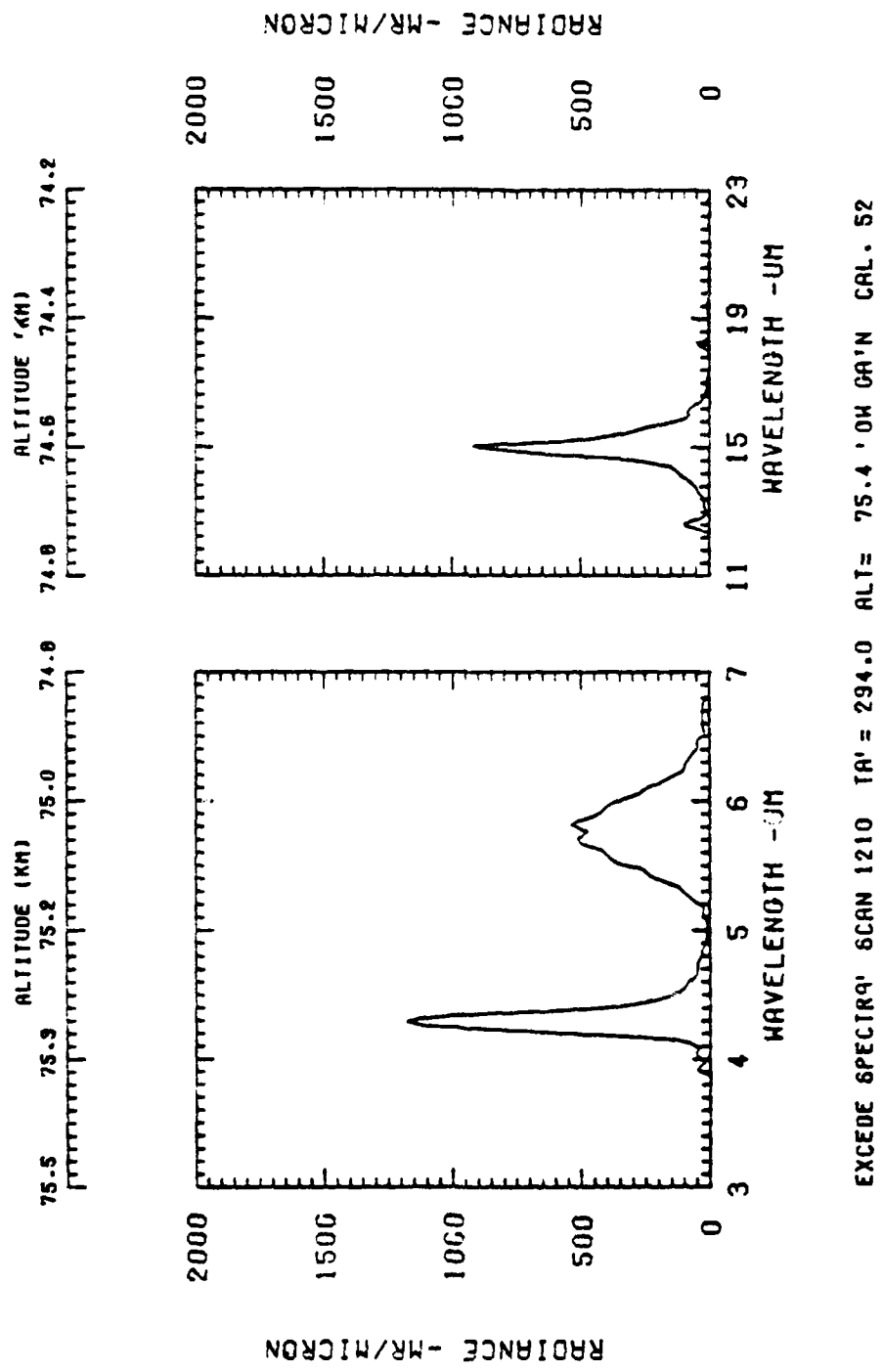


Figure 3.3-6 Example of smoothed spectrum using a 5 point smoothing filter.